Gene therapy with phosphodiesterases 2A and 4B in a murine model of pressure overload-induced cardiac hypertrophy

Doctoral thesis of

Nikoleta Pavlaki

University of Hamburg
Faculty of Mathematics, Informatics and Natural Sciences
Department of Chemistry

Hamburg 2021

Supervisor - Reviewer

Prof. Dr. rer. nat. Viacheslav O. Nikolaev

Institute of Experimental Cardiovascular Research
Center for Experimental Medicine
University Medical Center Hamburg-Eppendorf

Co-supervisor - Reviewer

Prof. Dr. med. Elke Oetjen

Institute of Clinical Pharmacology and Toxicology
Center for Experimental Medicine
University Medical Center Hamburg-Eppendorf

Date of Disputation: 25th June 2021

Die vorliegende Arbeit „Gene therapy with phosphodiesterases 2A and 4B in a murine model of pressure overload-induced cardiac hypertrophy“ wurde am Institut für Experimentelle Herz-Kreislaufforschung des Universitätsklinikums Hamburg-Eppendorf im Zeitraum 1. Juli 2017 - 30. April 2021 angefertigt.

List of publications

Pavlaki, N., De Jong, K. A., Geertz, B., Nikolaev, V. O., Froese, A., (2021). Cardiac hypertrophy changes compartmentation of cAMP in non-raft membrane microdomains. *Cells*, *10*(3), 535.

Ramuz, M., Hasan, A., Gruscheski, L., Diakonov, I., **Pavlaki, N.**, Nikolaev, V. O., Harding, S., Dunsby, C., & Gorelik, J. (2019). A Software Tool for High-Throughput Real-Time Measurement of Intensity-Based Ratio-Metric FRET. *Cells*, *8*(12), 1541.

Pavlaki, N., & Nikolaev, V. O. (2018). Imaging of PDE2-and PDE3-mediated cGMP-to-cAMP cross-talk in cardiomyocytes. *Journal of cardiovascular development and disease*, *5*(1), 4.

Contents

List of abbreviations

5'-AMP	adenosine-5'-monophosphate
8-Br-cAMP-AM	8-Bromoadenosine-3',5'-cyclic monophosphate, acetoxyl-methyl ester acetylcholine
AAV9	Adeno-associated virus serotype 9
ACh	acetylcholine
AC	adenylyl cyclase
β-AR	β-adrenergic receptor
β_1-AR	β_1-adrenergic receptor
β_2-AR	β_2-adrenergic receptor
β_3-AR	β_3-adrenergic receptor
β-Arr	beta-arrestin
ATP	adenosine triphosphate
BAY	BAY 60-7550, PDE2A specific inhibitor
BCA	Bicinchoninic Acid
BDM	2,3-butanedione monoxime
BSA	Bovine serum albumin
CaM	calmodulin
CaMKII	Ca^{2+}/calmodulin-dependent kinase II
cAMP	3',5'-cyclic adenosine monophosphate
CFP	(enhanced) cyan fluorescent protein
cGMP	3',5'-cyclic guanosine monophosphate
CGP	CGP-20712A
CICR	calcium-induced calcium release
CILO	cilostamide, PDE3 inhibitor
CNG	cyclic nucleotide-gated ion channel
CNBD	cyclic nucleotide binding domain
Da	Dalton
EF	ejection fraction
Epac	exchange protein directly activated by cAMP

Epac1-camps	Epac1-camp biosensor
FCS	Fetal calf serum
FS	fraction shortening
(e)GFP	(enhanced) green fluorescent protein
Forsk	Forskolin
FRET	Förster Resonance Energy Transfer
GC	guanylyl cyclase
GPCR	G-protein coupled receptor
HEK cell	Human embryonic kidney 293A cell
HR	heart rate
HW/BW	heart weight to body weight ratio
HW/TL	heart weight to tibia length ratio
IBMX	3-isobutyl-1-methylxanthine
ICI	ICI 118,551
ICER	inducible cAMP early repressor
ISO	isoproterenol
IVDd	intraventricular septum thickness in diastole
LUC	control Renilla Luciferase
LTCC	L-type Ca^{2+} channel
LV mass/BW	ratio of left ventricular mass to body weight
LVIDd	left ventricular internal diameter in diastole
LVPWd	left ventricular posterior wall thickness in diastole
LW/BW	lung weight to body weight ratio
LW/TL	lung weight to tibia length ratio
mAKAP	muscle A kinase-anchoring protein
min	minute(s)
NCX	Na^{+}/Ca^{2+} exchanger
PCR	Polymerase chain reaction
PDE	phosphodiesterase
PKA	protein kinase A

PLB	phospholamban
PP1	phosphatase 1
PP2A	phosphatase 2a
ROLI	rolipram, PDE4 inhibitor
ROS	reactive oxygen species
RyR2	cardiac ryanodine receptor
s	second(s)
SHAM	placebo surgery, scientific control
SR	sarcoplasmic reticulum
SEM	standard error of the mean
SERCA2a	sarco-/endoplasmic reticulum Ca^{2+}-ATPase 2a
SICM	scanning ion conductance microscopy
TAC	transverse aortic constriction
TnI	Troponin I (inhibitory)
WGA	wheat germ agglutinin
(e)YFP	(enhanced) yellow fluorescent protein

List of figures

List of tables

Zusammenfassung

Herzinsuffizienz (HF) ist eine chronische Herz-Kreislauf-Erkrankung mit extrem schlechter Prognose, die trotz umfangreicher Medikamente immer noch bei einer 5-Jahres-Sterblichkeitsrate von ~ 50% bleibt. Die Unfähigkeit des Herzens, den Stoffwechselbedarf des Körpers durch ausreichende Blutversorgung zu decken, wird durch genetische Anomalien, Myokardinfarkt oder Bluthochdruck (Drucküberlastung) verursacht. Unabhängig vom pathophysiologischen Mechanismus, der zur HF-Entwicklung führt, ist der Zustand typischerweise durch eine chronische neurohormonelle Hyperaktivierung entweder des sympathischen oder des Renin-Angiotensin-Systems gekennzeichnet, um die verringerte Herzkontraktilität zu kompensieren. Im gesunden Herzen reguliert der sympathische Antrieb, hauptsächlich durch β-adrenerge Signale, Herzfunktionen wie Kontraktionskraft, Herzrelaxation und Schlagfrequenz, indem die Produktion des zweiten Botenstoffs 3',5'-cyclischen Adenosinmonophosphats (cAMP)erhöht wird. Weitere parakrine Faktoren und Hormone wie Stickoxid (NO) und natriuretische Peptide (NPs) wirken den cAMP-induzierten Effekten durch die Produktion von 3',5'-cyclishcem Guanosinmonophosphat (cGMP) entgegen. In Kardiomyozyten spielen cAMP und cGMP sowohl physiologisch als auch pathophysiologisch zahlreiche und manchmal antagonistische Rollen. Diese cyclischen Nukleotide (CNs) werden durch hydrolysierende Enzyme, sogenannte Phosphodiesterasen (PDEs), streng reguliert. Von den 11 PDE-Familien sind PDE1-5 und PDE8-9 in Kardiomyozyten exprimiert. Bei Herzinsuffizienz ist jedoch die Herzfunktion reduziert und das Zusammenspiel zwischen CNs und PDEs beeinträchtigt. Die Proteinspiegel dieser spezifischen hydrolysierenden Enzyme ändern sich dramatisch und ihre Aktivität zur Erzeugung funktionell relevanter cAMP-Mikrodomänen in Kardiomyozyten wird herunterreguliert. In der Vergangenheit wurden PDE-Hemmer wie z.B. Milrinon entwickelt, um die Kontraktilität des Herzens zu erhöhen. Obwohl sie bei Patienten mit Herzinsuffizienz im Endstadium zur kurzfristigen Linderung wirksam sind, erhöhen sie bei einer Langzeitbehandlung Herzrhythmusstörungen und die Mortalität.

In dieser Arbeit wurde eine entgegengesetzte Hypothese getestet, ob eine Überexpression von PDEs mittels Adeno-Assoziierten-Virus (AAV) basierten Vectoren übermäßige Mengen an lokalem cAMP in verschiedenen Mikrodomänen von Kardiomyozyten reduzieren und dem Fortschreiten der Herzinsuffizienz entgegenwirken kann. Durch die Überexpression von PDE2A und PDE4B in einem Mausmodell der durch eine transversale Aortenkonstriktion (TAC) induzierten Drucküberlastungs-Herzinsuffizienz konnte das veränderte Zusammenspiel von CN-PDEs in subzellulären Mikrodomänen wiederherstellt und HF Verlauf untersucht werden. Tiere, die Förster-Resonanz-Energie Kardiomyozyten-Transfer (FRET)-basierte cAMP-Biosensoren für membran- und sarkoplasmatische Retikulum-assoziierte Mikrodomänen exprimierten, wurden in eine Sham ad drei TAC operierte Gruppen randomisiert und drei Tage nach der TAC-Operation entweder Kontrollvektor-, PDE2A- oder PDE4B-AAV injiziert. Um die Wirksamkeit des Ansatzes zu beurteilen, wurde nach 4 und 8 Wochen eine Echokardiographie durchgeführt, und danach wurden die Tiere zur experimentellen Analyse der PDE-

Expression und -Funktion getötet. Frisch isolierte ventrikuläre Myozyten wurden für die Bildgebung lebender Zellen mittels FRET-Imaging verwendet, um den Einfluss der Gentherapie auf die cAMP-Dynamik in membran- und sarkoplasmatischen Retikulum-assoziierten Mikrodomänen zu untersuchen. Die Auswirkungen der PDE2-, PDE3- und PDE4-Hemmung auf die β-adrenerge Vorstimulation wurden unter allen experimentellen Bedingungen gemessen. Zusätzlich zu FRET-Studien, die die Wirkung der Gentherapie auf die cAMP-Kompartimentierung in funktionell relevanten und krankheitsveränderten subzellulären Mikrodomänen mechanistisch untersuchten, wurden Einzelzellkontraktilitätsmessungen durchgeführt, um mikrodomänenspezifische Veränderungen bei PDE-Überexpression mit Arrhythmieentstehung zu verknüpfen.

Diese Strategie lieferte tiefe Einblicke in die PDE-abhängige Regulation der Kardiomyozytenfunktion und testete die Wirksamkeit der AAV-vermittelten Überexpression verschiedener PDE-Familien auf das Fortschreiten der Herzinsuffizienz. Die Ergebnisse legen nahe, dass eine kardiale Gentherapie mit den Phosphodiesterasen PDE2A und PDE4B eine milde, aber vorteilhafte Wirkung gegen durch Drucküberlastung induzierte Hypertrophie und Arrhythmien hatte. Das Hauptenzym PDE4B3, das am cAMP-Abbau im Mausherz beteiligt ist, wurde erfolgreich überexprimiert, hat teilweise gegen Hypertrophie und fast komplett gegen Verlust der kontraktilen Funktion geschützt, trug signifikant zur Hydrolyse und Kompartimentierung von cAMP bei und reduzierte die Initiierung von Arrhythmien nach β-adrenerger-Stimulation erheblich. Die Überexpression von PDE2A3 hat dagegen weder gegen Hypertrophie noch gegen den Verlust der kontraktilen Funktion nach TAC geschützt, hob jedoch effektiv die β-adrenerg stimulierte Arrhythmien auf.

Abstract

Heart failure (HF) is a chronic cardiovascular disease with extremely bad prognosis which remains still at ~ 50% 5- year mortality rate despite extensive medication. The inability of the heart to meet the metabolic demands of the body by providing sufficient blood supply is caused by genetic abnormalities, myocardial infarction or hypertension (pressure overload). Regardless of the pathophysiological mechanism leading to HF development, the condition is typically characterized by chronic neurohormonal hyperactivation, either of the sympathetic or of the renin-angiotensin-aldosterone system, aiming to compensate the reduced cardiac contractility. In a healthy heart, the sympathetic drive, mainly through β-adrenergic signaling, regulates cardiac functions such as force of contraction, heart relaxation and beating frequency by increasing the production of a second messenger 3',5'-cyclic adenosine monophosphate (cAMP). Further paracrine factors and hormones such as nitric oxide (NO) and natriuretic peptides (NPs) counteract the cAMP-induced effects by producing 3',5'-cyclic guanosine monophosphate (cGMP). In cardiomyocytes, cAMP and cGMP play numerous, and sometimes antagonistic roles, both physiologically and pathophysiologically. These cyclic nucleotides (CNs) are tightly regulated by hydrolyzing enzymes called phosphodiesterases (PDEs). Of the 11 PDE families, PDE1-5 and PDE8-9 have been reported to be expressed in cardiomyocytes. However, in heart failure, the cardiac function is reduced and the interplay between CNs and PDEs is compromised. The protein levels of these specific hydrolyzing enzymes alter dramatically, and their activity to generate functionally relevant cAMP microdomains in the cardiomyocyte is downregulated. Historically, PDE inhibitors such as milrinone have been developed to increase cardiac contractility. However, while efficacious for short-term relief in end-stage heart failure patients, they increase cardiac arrhythmias and mortality when used in long-term treatment schemes.

In this work, an opposite hypothesis was tested, i.e., whether overexpression of PDEs via adeno-associated viral (AAV) vectors can reduce excessive amounts of local cAMP in different cardiomyocyte microdomains and counteract heart failure progression. By cardiomyocyte overexpression of PDE2A and PDE4B in a mouse model of pressure-overload heart failure induced by Transverse Aortic Constriction (TAC) was studied if the restored CN-PDEs interplay in subcellular microdomains can ameliorate HF. Animals expressing Förster resonance energy transfer (FRET)-based cAMP biosensors for membrane- and sarcoplasmic reticulum-associated microdomains were randomized into one sham and 3 TAC operated groups and injected with either control vector, PDE2A or PDE4B AAVs three days after TAC surgery (therapy study). To assess the efficacy of the approach, echocardiography was performed at 4 and 8 weeks, and thereafter, experimental analysis of the PDE expression and function. Freshly isolated ventricular myocytes were used for live cell imaging by FRET to evaluate the impact of gene therapy on cAMP dynamics in membrane- and sarcoplasmic reticulum-associated microdomains eight weeks after TAC. The effects of PDE2, PDE3 and PDE4 inhibition upon β-adrenergic prestimulation, were measured under all experimental conditions. In addition to FRET studies that mechanistically dissected the effect of gene

therapy on cAMP compartmentation in functionally relevant and disease-altered subcellular microdomains, single-cell contractility measurements were performed to link microdomain-specific changes upon PDE overexpression to arrhythmia susceptibility.

This strategy provided deep insights into PDE-dependent regulation of cardiomyocyte function and tested the efficacy of AAV-mediated overexpression of various PDE families on heart failure progression. The results suggest that cardiac-targeted gene therapy with phosphodiesterases PDE2A and PDE4B had a mild but beneficial effect against pressure overload-induced hypertrophy and arrhythmias. The major enzyme, PDE4B3, involved in cAMP degradation in mouse heart was successfully overexpressed, partially protected against hypertrophy and almost completely prevented from the loss of contractile function, significantly contributed in cAMP hydrolysis and compartmentation and substantially minimized arrhythmia initiation after β-adrenergic stimulation. In contrast, PDE2A3 overexpression, neither protected against hypertrophy nor preserved contractile function after TAC, but definitely abrogated arrhythmias induced by β-adrenergic signaling.

1. Introduction

Shortly after the discovery of its molecular mechanism of action by Sutherland in the late 50s (*Beavo and Brunton, 2002*), 3',5'-cyclic adenosine monophosphate (cAMP) research paved the way for interesting scientific findings and established the important role of cAMP as an integral component of multiple physiological functions (*Altarejos and Montminy, 2011; Bodor et al., 2012; Brudvik and Tasken, 2012; Holz, 2004; Kandel et al, 2001; Leech et al., 2010; Morozov et al., 2003; Tengholm and Gylfe, 2009; Torgersen et al., 2002; Zagotta et al., 2003*) in a plethora of tissues. cAMP signaling still attracts a lot of scientific attention and remains a key element to unmet pathological conditions. This ubiquitously expressed, intracellular second messenger (the other one is 3',5'-cyclic guanosine monophosphate, cGMP) is involved in signaling cascades that require an extracellular stimulus to activate its production. Ligand binding to the G-protein coupled receptors (GPCRs) recruits stimulatory (G_s) or inhibitory (G_i) proteins that regulate cAMP synthesis within seconds (*Hein et al., 2006*) via cAMP-forming enzymes, namely adenylyl cyclases (ACs) which convert ATP into cAMP and pyrophosphate.

1.1. cAMP and its downstream effectors in the mammalian heart

In healthy mammalian cardiomyocytes, the sympathetic activation mainly via β-adrenergic receptor (β-AR) signaling stimulates cAMP production and mediates its excitatory effects by increasing contractile force (inotropy), heart rate (chronotropy), and cell relaxation (lusitropy) (*Bers 2008; Zagotta et al., 2003*). When a ligand binds to a G protein-coupled receptor (GPCR) located on the plasma membrane, a conformational change occurs, cAMP is formed by adenylyl cyclases (ACs) which, then, acts in cells via one or more of its downstream effector proteins, such as:

(a) cAMP-dependent protein kinase (PKA); as the main effector protein in the cAMP signaling cascade, PKA is responsible for the phosphorylation of several calcium handling proteins involved in cardiac excitation-contraction coupling (ECC) including L-type Ca^{2+} channel (LTCC) at the plasmalemma, phospholamban, and ryanodine receptors at the sarcoplasmic reticulum (SR), myosin-binding protein C, and troponin I at the myofilaments *(Bers 2002, 2008*), while Ca^{2+}-inhibited AC5 and AC6 are the predominant cAMP generating adenylyl cyclases in adult (AC5 and AC6) and fetal (AC6) ventricular cardiac tissue (*Defer et al., 2000*);

(b) exchange proteins directly activated by cAMP (Epac1 and Epac2) (*De Rooij et al., 1998*); they are implicated in pathological cardiomyocyte growth (*Morel et al., 2005; Métrich et al., 2008*);

(c) cyclic nucleotide gated ion channels (CNGCs) including HCN channels located in the sinus node; CNGCs regulate the capacity of cardiac cells to initiate spontaneous action potentials (automaticity) (*Wit and Rosen 1983; Larsson 2010; Zoccarato and Zaccolo, 2017*);

(d) the recently discovered Popeye-domain-containing proteins which affect cardiac pacemaking (*Froese et al., 2012; Schindler et al., 2016*).

In parallel, non-canonical second messengers (e.g., 3',5'-cyclic uridine monophosphate cUMP) generated by ACs and guanylyl cyclases (GCs) have been recently introduced (*Seifert 2015; Seifert et al., 2015*), but the available published data provide only limited information regarding their effector proteins and physiological significance in the cardiovascular system.

1.2 The concept of cAMP compartmentation in cardiac cells

The fact that multiple receptor stimuli can trigger diverse intracellular effects (*Buxton and Brunton, 1983; Steinberg and Brunton, 2001*) generated via the production of just a few intracellular second messengers such as cAMP or cGMP led to a currently accepted theory of cyclic nucleotide compartmentation. Compartmentation refers to the mechanisms by which multiple spatially segregated cAMP/PKA and/or cGMP/PKG signaling pathways exert different or even opposing functional effects in distinct subcellular microdomains of the same cell (*Zaccolo 2011; Zoccarato and Zaccolo 2017*). It appears to be of critical importance for cardiovascular system, since local cyclic nucleotide actions and the interplay of the cAMP signaling pathways are involved in both physiological functions and pathological conditions.

Several proteins (*Fischmeister et al., 2006; Mika et al., 2012; Saucerman et al., 2014; Vandecasteele et al., 2006; Ziolo et al., 2008*) contribute to cyclic nucleotide compartmentation, which spatially, temporally, and functionally controls their downstream effects, extensively studied for cAMP in the cardiovascular system (*Bender and Beavo, 2006; Francis et al., 2011; Keravis et al., 2012; Tsai and Kass, 2009*). They include:

(a) GPCRs located in lipid rafts (*Balijepalli et al., 2006; Pani et al., 2009*), at transverse tubules *(Kamp and Hell, 2000*) and in non-caveolar membrane domains (*Agarwal et al., 2017; Pavlaki et al., 2021*),

(b) ACs and GCs (*Guellich et al., 2014; Timofeyev et al., 2013*),

(c) Scaffold proteins (*Ghigo et al., 2017; Redden et al., 2017; Schrade et al., 2017*) such as A-kinase anchoring proteins (AKAPs) (*Francis et al., 2011; Dodge-Kafka et al., 2006; Maurice et al., 2014*) and Calveolin-3 (*Balijepalli et al., 2006; Balijepalli et al., 2008; Carnegie et al., 2009; Nichols et al., 2010*),

(d) physical barriers - e.g., mitochondria, cAMP buffering by PKA, cAMP export (*Cheepala et al., 2013; Sassi et al., 2012*) are some of the mechanisms that create locally confined intracellular domains regulating signaling, and

(e) the most prominent and extensively studied of all, the phosphodiesterase (PDE)-mediated hydrolysis of cyclic nucleotides, which is of high pharmacological and clinical interest (*Conti et al., 2014; Houslay et al., 2010; Maurice et al., 2014*). PDEs can control cyclic nucleotide compartmentation by creating spatial second messenger gradients via local hydrolysis/degradation (*Zaccolo and Movsesian, 2007*).

1.3 Major myocardial PDE isoforms - expression and activity in health and disease

PDEs are enzymes categorized as phosphohydrolases that selectively catalyze the hydrolysis of 3'-cyclic phosphate bonds of adenosine and/or guanosine 3',5' cyclic monophosphate and fine-tune the signaling of the intracellular second messengers (*Bender and Beavo, 2006*). These degrading enzymes constitute one of the most important mechanisms, by which cyclic nucleotides are spatially, temporally, and functionally compartmentalized in cardiomyocytes and other cells under physiological conditions, as their activities modulate the intensity, duration and localization of the signals transmitted by cyclic nucleotides, thus being crucially involved in their compartmentation (*Castro et al., 2006; Jurevicius and Fischmeister, 1996; Mika et al., 2012; Moltzau et al., 2013; Moltzau et al., 2014; Nikolaev et al., 2006;*). In pathological conditions, though, such as heart failure (HF), cyclic nucleotide pathways undergo profound alterations such as β-AR desensitization and redistribution (*Lohse et al., 2003; Nikolaev et al., 2010*), G_i alteration (*Melsom et al., 2014*) or even dramatic changes in PDE expression and/or localization to distinct microdomains (*Abi-Gerges et al., 2009; Berisha et al., 2019; Pavlaki et al., 2021; Perera et al., 2015; Sprenger et al., 2015*).

By briefly overviewing the 11 PDE families (*Conti et al., 2007; Wood et al., 2015*), there are seven, namely PDE1 (activated by Ca^{2+}/calmodulin) (*Vandeput et la., 2007*), PDE2 (cGMP-activated) (*Mongillo et al., 2006*), PDE3 (cGMP-inhibited) (*Ahmad et al., 2015*), PDE4 (activated by PKA) (*Leroy et al., 2008; Mika et al., 2013; Richter et al., 2011*), PDE5 (*Gamanuma et al., 2003*), PDE8 (*Houslay et al., 2007*), and PDE9 (*Lee et al., 2015*) being expressed and functional in mammalian cardiomyocytes (*Mika et al., 2012; Lee et al., 2015*) as an integral part of the multimolecular signaling/regulatory complexes, i.e., signalosomes (*Ahmad et al., 2015; Francis et al., 2011; Houslay et al., 2007; Maurice et al., 2014*) (**Figure 1**).

Out of these seven, only five PDEs (PDE1, PDE2, PDE3, PDE4 and PDE8) catalyze the cAMP hydrolysis generating functionally and spatially confined microdomains (*Conti and Beavo, 2007; Fischmeister et al., 2006; Houslay et al., 2007; Zaccolo and*

Movsesian, 2007) with PDE2, PDE3 and PDE4 being the key phosphodiesterases expressed in the myocardium (*Bender and Beavo, 2006; Mika et al., 2012*).

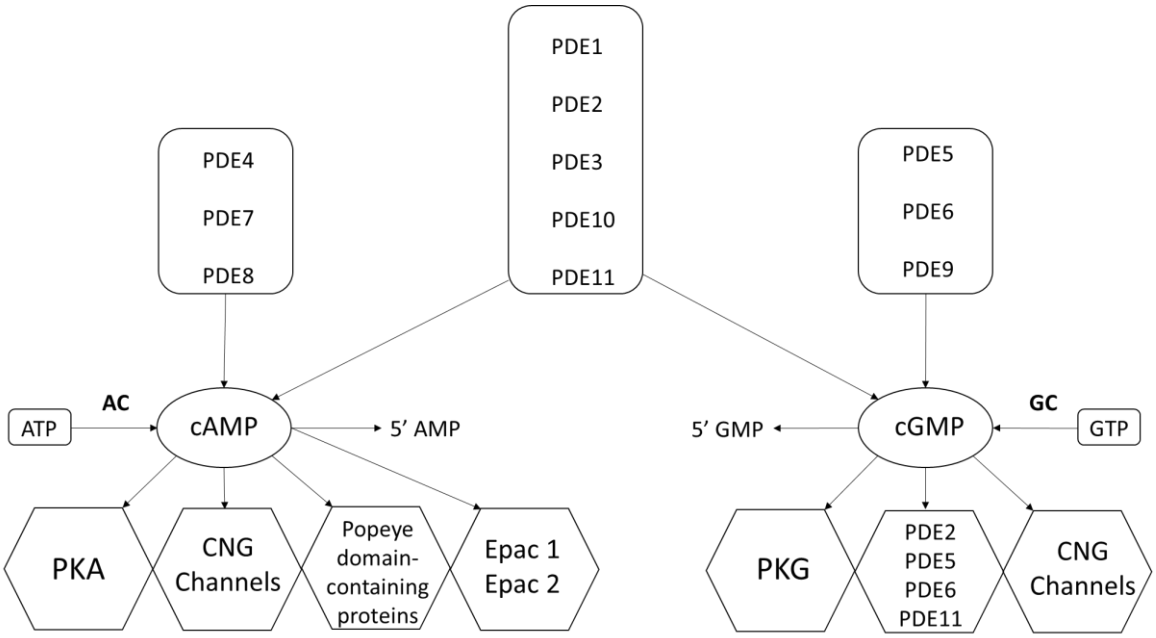

Figure 1. Phosphodiesterase-mediated cyclic nucleotide catalytic hydrolysis; PDE specificity and downstream effector proteins. cAMP degradation catalyzed by PDE4, PDE7 and PDE8. cGMP degradation catalyzed by PDE5, PDE6 and PDE9. Both cAMP and cGMP degradation catalyzed by PDE1, PDE2, PDE3, PDE10, PDE11. PKA, PKG, CNG channels, Epac1, Epac2 and Popeye domain-containing proteins are downstream effectors of cyclic nucleotide cascade. Adapted from *Ahmad et al. 2015; Pavlaki and Nikolaev, 2018*.

1.3.1. PDE2

PDE2 is a dual-substrate enzyme, which hydrolyzes both cAMP and cGMP with similar maximal rates in bovine adrenal and heart tissues (*Martins et al., 1982*). Only one gene (*pde2a*) gives rise to three known PDE2A isoforms (PDE2A1, PDE2A2, PDE2A3), which are differentially located in the cytosol, mitochondria, and cellular membranes (*Guellich et al., 2014; Mongillo et al., 2006*). PDE2A1 resides in the cytosol in contrast to mitochondria-membrane-localized PDE2A2 and plasma membrane-localized PDE2A3 (*Castro et al., 2006*). It is characteristic of this PDE family that the cGMP-mediated control of cAMP hydrolysis arises, when cGMP binds allosterically to the GAF-B domain of PDE2A, so that cAMP hydrolysis occurs with a 10-fold higher rate (*Martinez et al., 2002; Mumby et al, 1982; Rosman et al., 1997*). In this manner, cGMP via PDE2A is able to negatively regulate cAMP levels (*Bender and Beavo, 2006*) and therefore to initiate a negative cGMP-to-cAMP cross-talk (*Lugnier, 2006*). Initially cloned from rat brain (*Yang et al., 1994*) and purified from bovine or calf tissues (heart, liver adrenal gland, and platelets) (*Martins et al., 1982; Yamamoto et al., 1983*), the PDE2A protein is also found in endothelial cells, macrophages, and brain (*Bender and Beavo, 2004; Juilf et al.,1999*). Platelet aggregation (*Dickinson et al., 1997*), aldosterone secretion (*MacFarland et al., 1991*), and regulation of calcium channels (*Simmons and Hartzell, 1988*) require PDE2A-mediated hydrolysis of cAMP. Recently,

a PDE2A isoform regulating the mitochondrial respiratory chain has been detected, discovering a possible new pathway for the drug-induced control of mitochondrial function (*Acin-Perez et al., 2011*). Of particular importance are those studies referring to PDE2A expression in isolated cardiomyocytes and myocardium, where PDE2A together with PDE5 is also involved in the degradation of soluble GC-synthesized cGMP, whereas particulate GC-synthesized cGMP is preferentially hydrolyzed by PDE2A (*Castro et al., 2006; Zaccolo and Movsesian, 2007*). In terms of cGMP and cAMP pathway interactions, cGMP binding to PDE2 enhances the hydrolytic activity of the enzyme and enables the negative cGMP-to-cAMP cross-talk (*Brescia and Zaccolo, 2016; Weber et al., 2017*).

Although PDE2 is modestly expressed in cardiomyocytes under physiological conditions, it coordinates the cAMP pools associated with β-AR signaling, contractility, Ca^{2+} homeostasis and mitochondrial function (*Sadek et al., 2020*). In human and animal models of HF, it has been found that its expression is upregulated, as an important defense mechanism against cardiac stress induced by excessive β-AR drive (*Mehel et al., 2013*). In the very same study, PDE2 overexpression in cultured rat myocytes significantly attenuated norepinephrine- or phenylephrine-mediated hypertrophy and paved the way for the generation of a cardiac-specific PDE2A3 transgenic (TG) mouse line (*Vettel et al., 2016*). This latter animal model showed a marked reduction in resting as well as in maximal heart rate, while cardiac output was completely preserved due to greater cardiac contraction (*Vettel et al., 2016*). This well tolerated phenotype persisted also in elderly TGs with no indications of cardiac pathology and, more importantly, TG animals were resistant to triggered ventricular arrhythmias after catecholamine injection (*Vettel et al., 2016*). Molecular studies on the cardiomyocyte level showed lower basal phosphorylation levels of Ca^{2+}-cycling proteins including ryanodine receptor type 2 (RyR2) in TG hearts and improved contractility, Ca^{2+} transients and $I_{Ca,L}$, in addition to remarkably reduced Ca^{2+}-leakage after Ca^{2+}-spark analysis of isolated TG cardiomyocytes (*Vettel et al., 2016*). Obviously, the activation of myocardial PDE2 may represent a novel intracellular anti-adrenergic and anti-arrhythmic therapeutic strategy despite the opposite contradictory findings that rather PDE2 inhibition might be also cardioprotective in some cases *(Baliga et al, 2018; Zoccarato et al., 2015).*

1.3.2. PDE3

Another important cGMP-regulated PDE is PDE3 that hydrolyzes both cAMP and cGMP. Often referred to as cGMP-inhibited PDE (*Abi-Gerges et al., 2009; Yang et al., 2009*), PDE3 shows higher catalytic rates for cAMP but relatively high affinity for cGMP, which competitively inhibits cAMP hydrolysis (*Degerman et al., 1997; Shakur et al., 2001*). This creates the so-called positive cGMP-to-cAMP cross-talk. PDE3A and PDE3B are the two PDE3 subfamilies, with the former being abundant in cardiomyocytes, oocytes, vascular smooth muscle and platelets and the latter being expressed in the pancreas, liver, and adipose tissue (*Shakur et al., 2001*). PDE3A controls myocardial contractility by interacting with the sarco-/endoplasmic reticulum Ca^{2+} ATPase (SERCA2a) (*Beca et al., 2013*). By utilizing their direct positive inotropic effects, PDE3 inhibitors had been used for acute treatment of end-stage heart failure (HF) (*McMurray et al., 2012*), albeit presenting increased mortality as well as incidence

of arrhythmias and sudden death after chronic use (*Landry et al., 2008; Packer et al., 1991*). PDE3A is considered the predominant phosphohydrolase for cAMP catabolism in human cardiomyocytes (*Hambleton et al., 2005*), while it plays a secondary role in that of rodent ones (*Abi-Gerges et al., 2009; Molina et al., 2012; Weishaar et al., 1987*). In contrast, PDE3B seems to be more actively engaged in energy metabolism (*Choi et al., 2006; Degerman et al., 2011*), but it can also protect the heart from ischemia/reperfusion injury (*Chung et al., 2015*). Knockout models have revealed that PDE3A, but not PDE3B, exerts inotropic and chronotropic effects after treatment with PDE3 inhibitors (*Sun et al., 2007*) because PDE3A regulates SERCA2a activity and subsequent SR Ca^{2+} uptake (*Beca et al, 2013*). By chronically suppressing its expression or action, myocyte apoptosis *in vitro* (*Ding et al., 2005*) or deterioration of ischemia/reperfusion-induced apoptosis and cardiac injury *in vivo* (*Oikawa et al., 2013*) have been observed. Similarly, disruption of PDE3B interaction with phosphoinositide 3-kinase γ, which can serve as an AKAP, had deleterious effects (*Ghigo et al., 2012; Patrucco et al., 2004; Perino et al., 2011*) such as arrhythmias (*Ghigo et al., 2012*), necrotic cardiac tissue damage, and fibrosis (*Patrucco et al., 2004*). PDE3 along with other PDEs constitutes an integral part of cAMP degradation. Evidence suggests that it may also control cGMP levels (*Chung et al., 2015; Götz et al., 2014)*, atrial dynamics, and myocyte ANP release, depending on the involved induction mechanism (*Wen et al., 2004; Zaccolo and Movsesian, 2007*). In terms of cGMP and cAMP pathway interactions, cGMP binding to the catalytic domains of PDE3 reduces the rate of cAMP degradation, thereby mediating the positive cGMP-to-cAMP cross-talk (*Stangherlin et al., 2011*).

In pathological conditions, it has been revealed that PDE3A is decreased, particularly in hypertrophy and HF (*Abi-Gerges et al., 2009*). Apart from regulating PLB phosphorylation and thus SERCA2a activity in humans and mice (*Ahmad et al., 2015; Beca et al., 2013*), PDE3A1 also acts as a negative regulator of cardiomyocyte apoptosis, by controlling the expression of the transcriptional repressor and pro-apoptotic factor, ICER (inducible cAMP early repressor) (*Yan et al., 2007*). Inhibition of this mechanism in mice with cardiac-specific overexpression of PDE3A1 was associated with protection during ischemia-reperfusion (*Oikawa et al., 2013*). Recently, elegantly performed studies at the onset of cardiac hypertrophy were able to show that both PDE2A and PDE3A undergo a disease-driven redistribution between various subcellular microdomains such as β-AR-associated membrane compartments and the SR (*Perera et al., 2015; Sprenger et al., 2015*), a mechanism by which changes in cAMP compartmentation can drastically impact on contractile function, but also lead to the development of better HF therapeutics.

1.3.3. PDE4

This cAMP-specific phosphohydrolase is encoded by four genes, among which three expressed in the mammalian heart (*pde4a, pde4b, pde4d*) (*Kostic et al., 1997; Richter et al., 2011*). There are more than 20 isoforms that reside in distinct cAMP compartments owing to their N-terminus specificity (*Houslay and Adams, 2003*), important for organization and signal transduction within cardiomyocytes. PDE4 is reportedly the predominant phosphohydrolase for cAMP catabolism in murine cardiomyocytes (*Leroy et al., 2008*), its activity dependents on PKA phosphorylation

via feedback loop after cAMP degradation (*MacKenzie et al., 2002*), and its major isoforms mainly regulate the subcellular organization and compartmentation. The most important one is PDE4B that mediates the β-AR induced PKA-phosphorylation of the LTCC channels in the plasma membrane of adult murine cardiomyocytes (*Leroy et al., 2011*), while the other one, PDE4D, is linked to the RyR2 and SERCA2a complexes. Specifically, PDE4D3 is part of the RyR2 microdomain (*Lehnart et al., 2005*), while PDE4D5 and PDE4D8 participate in the formation of those initiated by either β_1- or β_2-ARs ligand binding (*Bailllie et al., 2007; Richter et al., 2008*). Upon β_2-AR stimulation, PDE4D5 enhances PDE-mediated cAMP hydrolysis and facilitates the switch from G_s to G_i coupled signaling (*Daaka et al. 1997*) via β-arrestin *(Baillie et al., 2003; Bailllie et al., 2007; Lynch et al., 2005; Perry et al., 2002; Richter et al., 2008*). An unidentified 4D isoform has been implicated into SERCA2a microdomain, regulating PLB phosphorylation and hence SERCA2a activity in murine hearts under basal conditions (*Beca et al., 2011; Kerfant et al., 2007*). Last but not least, PDE4A and PDE4B (no D-isoforms) constitute integral components of the PI3K -cAMP compartment (*Ghigo et al., 2012*). Although not directly involved in cardiac contractility, heart rate or blood pressure (*Zhao et al., 2015*), PDE4 enzymes tightly regulate PKA phosphorylation and modify the localized signaling into tight compartments (*Fertig and Bailllie, 2018*).

Pharmacologically, PDE4 inhibition has beneficial effects on cardiomyocyte function (*Lehnart and Marks, 2006*); however, many unfavorable cardiac effects occur from sustained inhibition of this enzyme, increasing the incidence of mortality (*Packer et al., 1991*). Moreover, in pathological cardiac hypertrophy induced by sympathetic overdrive, there was dramatic reduction in enzyme expression (~ 50% for PDE4B) (*Abi-Gerges et al., 2009; Karam et al. 2020*) and subsequently increased susceptibility to arrhythmias and heart failure (*Bobin et al., 2016; Lehnart et al., 2005; Leroy et al., 2011; Molina et al, 2012*). Cardiac-targeted overexpression of PDE4B3 (*Karam et al., 2020*) in diseased animal and human cell models presented cardioprotective effects against sympathetic overdrive without depressing basal function.

1.4. cAMP compartmentation at the sarcolemma and RyR2 microdomains

As already emphasized, the generation of cAMP microdomains in cardiomyocytes is crucial for signal transduction, and cAMP consistently abides to the norm of subcellular organization.

This highly organized form of signal transduction was initially discovered in rabbits (*Buxton and Brunton, 1983*), when the β-adrenergic and prostaglandin receptor-mediated responses revealed diverse cAMP amounts and PKA activity in distinct fractions of homogenized cardiomyocytes. While both receptors led to comparable cAMP increase in the cells, only the downstream effects of β-adrenergic signaling reached both cytosolic and particulate fractions *(Buxton and Brunton, 1983*). Thereafter, a considerable number of research studies has unraveled and verified the wide spectra of cAMP nano- or microdomains occurring by orchestrated (i.e., spatial and temporal) confinement (*Castro et al, 2006; Jurevicius and Fischmeister. 1996; Perera and Nikolaev, 2013*).

In sarcolemma, specifically, there is a multitude of machineries by which membrane proteins remain restricted (*Bethani et al. 2010*), and segregated into distinct

microdomains (*Agarwal et al., 2017*). One such relevant to our study mechanism involves the concentration of cholesterol and sphingolipids, accompanied by certain phospholipids, to shape domains in a gel-like, liquid-ordered form, namely lipid rafts (*Allen et al. 2007; Brown 2006; Jacobson et al. 2007*). Although, it still remains unclear how the proteins of interest are restricted to or excluded from the subcellular compartments organized by lipid rafts in the plasma membrane (*Agarwal et al., 2017)*, biochemically and functionally related approaches introduced caveolae, a specific subset of lipid rafts linked to the scaffolding protein caveolin, to shed light on cAMP-mediated signal compartmentation in cardiac myocytes (*Rybin et al., 2000; Head et al., 2005; Harvey and Calaghan, 2012; Perera et al., 2015*). Caveola are generated mainly by the polymerization of caveolins, small proteins with three palmitoylation sites near their C-terminus (*Agarwal et al., 2017; Williams and Lisanti 2004*). Closely associated with lipid rafts, these proteins segregate and facilitate the caveola generation by shaping distinct invaginations in the sarcolemma (*Agarwal et al., 2017*). Three caveolin isoforms Cav1, Cav2 and Cav3 are reportedly expressed in cardiac myocytes (*Head et al. 2005*). But Cav3, the muscle-specific one for cardiac, skeletal, and smooth muscle cells (*Balijepalli et al., 2006; Balijepalli et al., 2008; Carnegie et al., 2009; Nichols et al., 2010*), is thought to be the predominant one that tightly organizes membrane microdomain cAMP-signaling proteins (*Agarwal et al., 2017*) such as β_1-AR and β_2-AR (*Agarwal et al. 2011; Balijepalli et al. 2006; Head et al. 2005, 2006; Nichols et al. 2010; Ostrom et al. 2000, 2001, 2004; Rybin et al. 2000; Xiang and Kobilka, 2003*), AC5 and AC6 (*Balijepalli et al. 2006; Head et al. 2005, 2006; Ostrom et al. 2000, 2001, 2004; Rybin et al. 2000*) and G proteins (*Balijepalli et al. 2006; Head et al. 2005; Rybin et al. 2000*). To demonstrate the important role of caveola in cAMP compartmentation, membrane detubulation studies investigated the different cAMP signals initiated by the same receptors residing in caveolar lipid rafts upon cholesterol depletion (*Rybin, et al. 2000; Head et al., 2005; Agarwal et al., 2011*).

Before we swift our interest to the other microdomains, it's worth mentioning that the major focus in cAMP compartmentation so far lies on the different responses occurring between the plasma membrane and the cytoplasm, but not within the plasma membrane itself, where cAMP signaling is not homogenous either. In addition to the caveolar cAMP microdomain of the plasma membrane, there is at least one non-caveolar compartment (*Harvey et al., 2012; Head et al., 2005; Insel et al., 2005; Pavlaki et al., 2021*), in which β-AR signaling leads to more localized cAMP responses due to differences in basal levels, adenylyl cyclase and PDE activity (*Agarwal et al., 2017*), and yields in clearly distinct changes in cAMP compartmentation upon health and disease (*Pavlaki et al., 2021*). Though quite exciting, the exploration of the signaling cascades in cholesterol-depleted parts of the plasma membrane remains still in its infancy.

Another cAMP compartment of increasing interest due to the PKA-mediated Ca^{2+} leak hypothesis is the RyR2 microdomain, within which the ion channel attracts plenty of regulatory proteins and orchestrates the downstream effects of cAMP cascade (*Berisha et al. 2019; Dodge-Kafka et al., 2001; Lehnart et al., 2005; Marx et al., 2000*). The composition of this gargantuan Ca^{2+} channel (~2 mega Da) relies on the formation of a pore region by four identical subunits (*Kushnir and Marks, 2010; Lehnart, 2007*), each

one consisting of a transmembrane C-terminus and a cytosolic, N-terminal domain in distinct foot-form that enables anchoring of enzymes and proteins (*Kushnir and Marks, 2010; Zalk et al., 2007*). The transmembrane C-terminus is located in the SR lumen and is in charge of the homotetramer (ie., RyR2) function (Bhat et al., 1997; Meissner, 2017). This C- terminal region has been particularly linked to triadin and junctin, which facilitate calsequestrin scaffolding to the RyR2 for the "Ca^{2+} release unit" formation (*Fan et al.,2008; Gyorke et al., 2008; Kushnir and Marks, 2010*). The other region, namely the N-terminal cytoplasmic part of the RyR2, aids PKA, CaMKII, phosphatases and other protein scaffolding at specific phosphorylation or ligand-binding sites (*Yano et al., 2006; Zhu et al., 2013*). It was demonstrated that calstabin2 (*Timerman et al., 1994*), PKA (*Marx et al., 2000*), Ca^{2+}/calmodulin-dependent kinase II (CaMKII) (*Wehrens et al., 2004*), phosphodiesterase 4D3 (PDE4D3) (*Lehnart et al., 2005*), calmodulin, sorcin and phosphatases 1 and 2a (PP1 and PP2A) are related to the cytosolic region of RyR2 subunit (*Kushnir and Marks, 2010*). Among all, the 12.6kDa polypeptide calstabin2 can stabilize the closed state of RyR2s upon stoichiometric (1:1) ratio binding to the channel subunits (*Lehnart et al., 2007*).

Furthermore, cardiac RyR2s are the paramount mechanism for SR-mediated Ca^{2+} discharge in cytosol, with the main downstream effector of cAMP cascade (i.e., PKA) being actively engaged in two out of its three phosphorylation sites. Under physiological conditions, muscle A kinase-anchoring protein (mAKAP) mediates the PKA participation to the RyR2 macro complex (*Kushnir and Marks, 2010*) by binding to leucine/isoleucine zipper motifs of the cytosolic RyR2 domain and allows PKA-mediated phosphorylation of the cation channel at serine position 2808, and also at serine 2030 (*Camors et al., 2014*). Moreover, PDE4D3 (*Lehnart et al., 2005*) and phosphatases (*Huke and Bers, 2008*) are actively involved into the above-mentioned signaling complex by regulating local cAMP levels and PKA activity, respectively. So, it can be easily understood why phosphorylation and subsequently RyR2-mediated Ca^{2+} release is dramatically affected, when the balance among these proteins is disturbed in pathological conditions. Lehnart and colleagues (*2005*) had actually reported that PDE4D3 was exclusively involved in the RyR2 microdomain, and its levels were significantly reduced in failing human hearts (*Lehnart et al., 2005*). The fact that mAKAP plays a prominent role in engaging PDE4D3 to the RyR2 microdomain (*Dodge et al., 2001*) revealed additional "targeting" of other factors contributing to the macro complex formation. Indeed, mAKAP regulates Ca^{2+} discharge from the SR by molding a signaling unit that anchors PKA and PDE4D3 around RyR2s, and within interaction distance with PP1/PP2 and calstabin2 (*Dodge et al., 2001; Marx et al., 2000*). And, by this complex, it was revealed that Ser-2808 in human and rodents or Ser-2809 in rabbit was a dual-specificity phosphorylation site mediated by both PKA and CaMKII (*Rodriguez et al., 2003; Wichter et al., 1991*). The second site at Ser-2814 (Ser-2815 in rabbit) is exclusively CaMKII-phosphorylated (*Wehrens et al., 2004*), while the third and last one at Ser-2030 (Ser-2031 in rabbit) is PKA-phosphorylated (*Mozaffarian et al., 2007*). All this evidence led to the identification of three phosphorylation sites in the RyR2 microdomain (*Huke and Bers, 2008*), which could possibly be considered as a mechanism affecting the channel sensitivity to Ca^{2+}, but not as direct regulators of channel opening or closure. Finally, calmodulin and sorcin have been recognized as RyR2-dependent Ca^{2+} release inhibitors (*Yamaguchi et al., 2003*)

that mediate channel closure after Ca^{2+} release (*Farrell et al., 2003; Kushnir and Marks, 2010; Xu et al., 2004*).

It's inevitable not to consider diastolic Ca^{2+} leak through dysfunctional RyR2s as a hallmark of heart failure. Marx and colleagues were the first to postulate that chronic PKA-mediated phosphorylation at serine 2808 depleted calstabin2 from RyR2, increased the channel sensitivity to its natural ligand Ca^{2+} and prolonged its open probability (*Marx et al., 2000*). Subsequently, leaky RyR2s may decrease SR Ca^{2+} content and generate arrhythmias during heart failure. These effects might also occur by chronic/pathological catecholaminergic stimulation (*Lohse et al., 2003; Packer, 1988*), with subsequent downregulation of β-adrenergic receptors or/and cAMP depletion (*Bristow et al., 1982; Brodde, 1993*). During heart failure-associated remodeling, the RyR2 microdomain undergoes profound subcellular alteration by PDE4D3 and PP1/PP2 depletion (*Lehnart et al., 2005*), which triggers homotetramer hyperphosphorylation despite the concurrently depleted cAMP levels in the cells. As long as HF continues to increase the number of patients dying due to structural dysfunction or of sustained ventricular arrhythmias (*Mozaffarian et al., 2007*), the necessity to address the alterations occurring at the molecular level will continue to increase as well. As a natural consequence of the abnormalities in SR content and Ca^{2+} homeostasis, the impaired contractile function will remain a sustained manifestation of HF (*Mohamed et al., 2018*). And should be taken into consideration that the problematic SR Ca^{2+} handling characterized by 'leaky' RyR2 channels due to hyperphosphorylation at Ser2808 and subsequent calstabin2 dissociation from the RyR2 (*Lehnart et al., 2006; Lehnart et al. 2008; Marx and Marks, 2013; Shan et al., 2010*) must not constitute a panacea in disease investigation and result interpretation, but rather be observed from a critical point of view by the time this highly controversial approach has been already disputed by other research groups (*Benkusky et al., 2007; MacDonnell et al., 2008; Zhang et al., 2012*).

1.5 Tools for cyclic nucleotide-related live imaging

Apparently, the need to detect potential alterations in subcellular compartments is crucial, and the visualization of these micro- or nano- compartments (*Hayes and Brunton, 1982)* has to be fulfilled beyond classical biochemical methods (*Buxton and Brunton, 1983; Corbin et al., 1977; Hayes et al., 1979, 1980; Keely, 1977*).

Buxton and Brunton (1983) showed for the first time that prostaglandin induces different PKA activity rates in particulate and soluble fractions of cardiac myocytes upon cAMP formation (*Buxton and Brunton, 1983*). Later on, Jurevicius and Fischmeister (1996), by utilizing a combination of two-barrel microperfusion and whole patch clamp techniques, further confirmed the compartmentation theory in frog ventricular cells, where local application of a β-adrenergic agonist preferentially stimulated the LTCCs close to activated receptors (*Jurevicius and Fischmeister, 1996*).

Multiple techniques have been employed for measuring cAMP gradients in different cell types or tissues, including radio- and enzyme-linked immunoassays (*Pierkes et al., 2002; Takimoto et al., 2005*). However, these techniques are of limited capacity, since they require plenty of tissue material and can only detect global concentrations of cyclic nucleotides without spatial resolution in living cells or among subcellular

microdomains within one cell (*Sprenger and Nikolaev, 2013*). To overcome these challenges, novel approaches have been employed for the visualization of cyclic nucleotide signaling and its compartmentation in real time and high spatiotemporal fidelity (*John et al., 1996; Massberg et al., 1999; Sprenger and Nikolaev, 2013; Zoccarato and Zaccolo, 2017*) primarily built on Förster (or also known as Fluorescence) Resonance Energy Transfer (FRET).

In 1948, the German physicist Theodor Förster introduced the concept of FRET by showing how two fluorescent molecules exchange energy in a non-radiative way (*Kuhn, 2003*). FRET biosensors report a non-radiative energy transfer from an excited fluorescent molecule that acts as a donor to a neighboring (located at nm distance) molecule that acts as an acceptor with subsequent fluorescence emission but without the direct excitation of the acceptor (*Förster, 1948*).

Adams and colleagues were also the first among many groups to utilize the potential of live imaging and to create a FRET-based cAMP probe, called FICRnR (*Adams et al., 1991*). Ever since, multiple genetically engineered FRET sensors have been constructed with high spatiotemporal fidelity for cAMP monitoring (*Bers, 2002, 2008; Biel et al., 1999; Kushnir and Marks, 2010; Mongillo et al., 2006*). Typically, they are composed of two fluorophores presenting moderate overlap in donor-emission and acceptor-absorption spectra. Functional FRET pairs occur (i) by different combinations of green fluorescent protein (GFP) mutants (e.g., cyan fluorescent protein CFP and yellow fluorescent protein YFP) sandwiching a single cyclic nucleotide-binding domain (CNBD) (*Nikolaev and Lohse, 2006*), (ii) appropriate orientation upon conformational change and (iii) within Förster radius to fluoresce. The biosensor expression for experimental purposes can be transiently achieved via neonatal cardiomyocyte transfection or adenovirus-mediated transduction of adult cardiomyocytes (*Brandes and Bers, 1997*). Particularly, the adult rat ventricular myocytes, which can also be transfected with adenovirus, represent the best described example of transient biosensor expression thanks to their robustness and stability under cell culture conditions (*Marx et al., 2000; Simmerman and Jones, 1998; Sulakhe and Vo, 1995; Zhao et al., 1994*). On the contrary, mouse or human myocytes cannot yield high quality results under the same transduction 48-hour-protocol for biosensor expression, because the cells start to dedifferentiate and lose their physiological properties (rod shape, physiologically relevant cAMP content, beating) in due time (*Lehnart, 2007*). To overcome these issues and be able to measure cAMP gradients in robust and healthy cardiomyocytes, transgenic mouse lines were developed for biosensor expression in adult cardiac tissue/myocardium. But still, the problem of spatiotemporal fidelity of cAMP measurements arose, which were rather general and cytosolic-centered instead of specific and localized. Eventually, thanks to appropriate genetic engineering handling even more specific transgenic mouse lines expressing subcellular-targeted biosensors were generated, and were utilized in various genetic and experimental heart disease models allowing credibility of results in subcellular cAMP monitoring (*Berisha et al., 2019; Götz et al., 2014; Pavlaki et al., 2021; Perera et al., 2015; Sprenger et al., 2015*).

Apart from the wide spectrum of FRET-based biosensors that visualize cGMP (*Götz et al., 2014; Honda et al, 2001; Niino et al., 2009; Nikolaev et al. 2006; Nikolaev and Lohse, 2009; Sato et al., 2000*) and cAMP (*Berisha et al., 2019; Mongillo et al., 2006;*

Pavlaki et al., 2021; Perera et al., 2015; Sprenger et al., 2015), or detect the activity of the downstream effector proteins such as PKA (*Adams et al., 1991; Backsai et al., 1993; Lehnart et al., 2005; Mongillo et al., 2004; Nikolaev et al., 2004; Zaccolo et al., 2000; Zaccolo and Pozzan, 2002*), Epac (*Börner et al, 2011; Calebiro et al., 2009; DiPilato et al., 2004; Klarenbeek et al., 2015; Nikolaev et al., 2004; Ponsioen et al., 2004*), or CNG channels (*Nikolaev et al., 2006; Rich et al., 2000, 2001*), new potential has been revealed, as FRET can be further combined with other techniques for more accurate exploration of cyclic nucleotide compartments. One such technique is scanning ion conductance microscopy (SICM), which can be used to deliver receptor ligands onto defined membrane structures to targeted distinct cAMP or cGMP pools and to study receptor–microdomain interactions. SICM is a non-optical imaging technique that uses a small glass nanopipette to obtain a highly resolved morphological profile of a living cell membrane based on ion current measurement (*Hansma et al., 1989; Korchev et al., 1997; Miragoli et al., 2011; Nikolaev et al., 2010*) and, when combined with FRET, accurately detects microdomain alterations in health and disease *(Froese and Nikolaev, 2015; Nikolaev et al., 2010; Subramanian et al., 2018).*

1.6 Gene therapy as an alternative therapeutic approach for heart failure

HF is still a poorly therapeutically addressed pathology, which represents the final common stage of many cardiac diseases and describes the structural or functional defect of the heart to meet the metabolic needs of the body by delivering oxygen whenever required (*Waagstein et al., 1976; McMurray et al., 2012*). Regardless of the underlying HF cause, patients show a neurohumoral hyperactivation, i.e., of renin-angiotensin and sympathetic systems, in response to reduced systolic function, causing further detrimental cardiac injuries. This creates a pathological "vicious circle" where chronic activation of β-adrenergic receptor (β-AR) signalling plays a central role as attested by the beneficial effect of β-blockers in HF (*Waagstein et al., 1976; Packer et al., 1996*). The β-adrenergic pathway results in an increase in cAMP levels to augment cardiac contractility and function. PDEs that degrade these second messengers (*Mika at el., 2012*) and ensure the specificity of their signaling into compartments under physiological conditions, undergo dramatic loss of expression or function, the tight organization in compartments is strongly remodeled in HF and is thought to participate in further deterioration of the heart. To date, PDE inhibition proved either detrimental in HF with reduced ejection fraction (*Packer et al., 1991*) or inefficient in patients with preserved ejection fraction (*Redfield et al., 2013*), as the increase in intracellular cAMP content is one of the best described features in the molecular and cellular pathophysiology of heart failure (*Movsesian, 2000*).

And since the currently available pharmacological interventions have been proven to be either insufficient or proarrhythmic, the emergence of gene therapy appears to be a promising strategy against heart failure. Besides, there are also other factors explaining the increasing interest in unconventional approaches. First of all, there is still an unmet need to develop effective treatments decreasing the morbidity and mortality of heart failure. Second, this highly prevalent problem is associated with a grim prognosis despite continuous therapeutic progress (*Lipskaia et al., 2010; Sadek e al, 2020).* And third, many attractive therapeutic targets, such as the sarco-endoplasmic reticulum calcium ATPase (SERCA2a) (*Lipskaia et al., 2010)* remain without available or

effective pharmacological modulators. Thus, gene therapy, particularly of heart failure (**Figure 2, Table 1**), is gaining momentum and appears as a promising alternative to currently available therapeutic schemes.

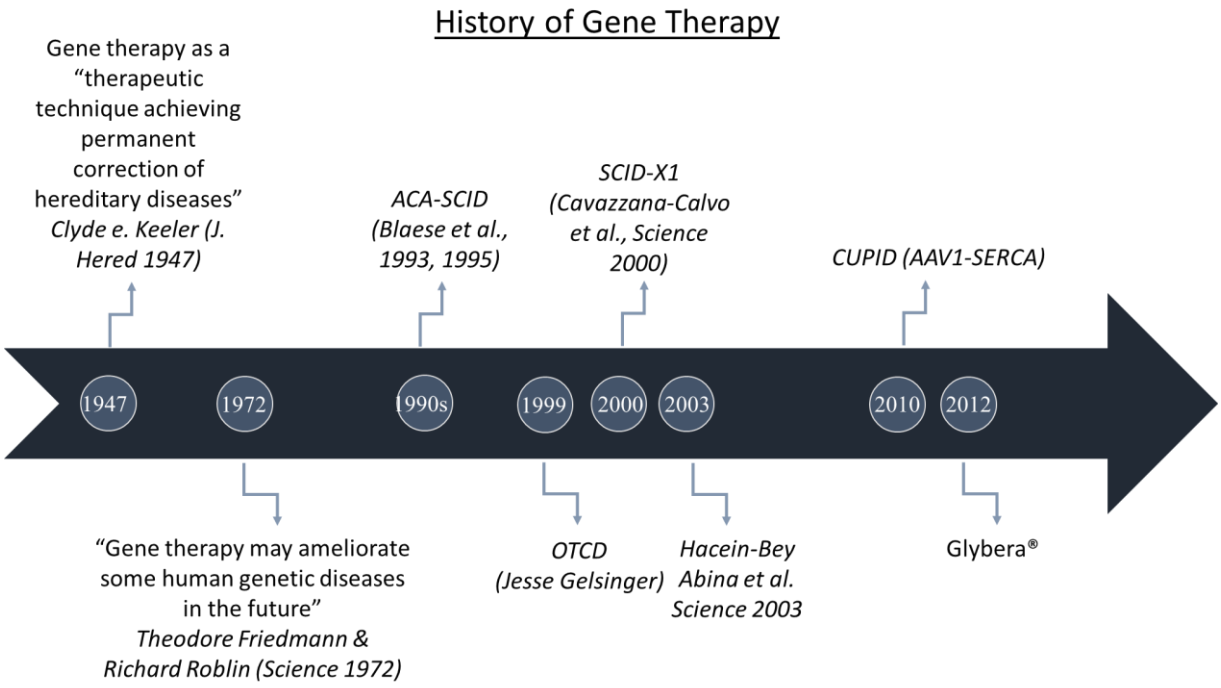

Figure 2. History of gene therapy. Milestones that paved the way to modern therapeutic approaches.

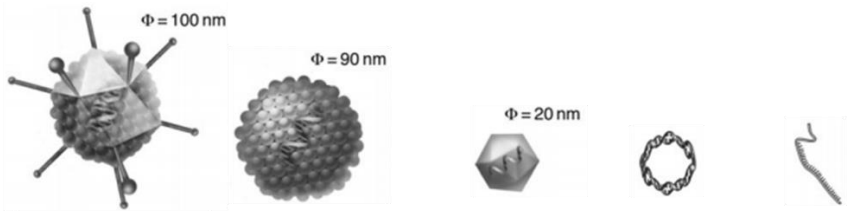

Vector Characteristics	Adenovirus	Lentivirus	Adeno-associated virus	Plasmid	Modified RNA
Expression:	Short-term	Long-term	Long-term	Short-term	Short-term
Information capacity:	Double-stranded DNA	Single-stranded RNA	Single-stranded DNA	DNA	Single-stranded RNA
Immune response:	Strong	Mild	Low	Moderate	Low

Table 1. Vector characteristics for cardiac-targeted gene therapy. Viral and non-viral vectors are utilized for short- or long-term expression of the encoded information in the heart with the least possible immune response and maximum cardiac tropism. Adapted from *Hulot et al., 2016.*

So far, the majority of the molecular targets of HF gene therapy with translational potential are related to calcium handling in cardiomyocytes such as SERCA2a, phospholamban, the S100A1 protein, the ryanodine receptor and the inhibitor of the protein phosphatase 1 (*Hulot et al., 2016)*, or other targets, related to cAMP signaling

such as adenylyl cyclase and very recently downstream effectors such as PDEs that have an integral role in cardiac physiology and/or disease.

1.6.1 Therapeutic targets related to the cAMP signaling cascade for enhancing contractility

1.6.1.1. Beta-adrenergic receptor signaling

Chronic HF is associated with increased sympathetic drive which may be compensated early in disease, but the long-term neurohormonal activation induces the desensitization of β-adrenergic signal transduction, including β-adrenergic receptor (β-AR) down-regulation, up-regulation of β-ARK (β-AR kinase) and increased inhibitory G-protein alpha-subunit ($G_{\alpha i}$) function (*Feldman et al., 2005; Lipskaia et al., 2007*).

Decreases in cAMP levels and production were reported in heart failure, although conflicting reports exist between rodent models and humans (*Gao et al., 1999; Regitz-Zagrosek et al., 1994*). Increasing cAMP through the administration of β-AR agonists or through the inhibition of phosphodiesterases has proven detrimental in clinical heart failure (*Hasenfuss et al., 2011*). On the other hand, genetic manipulation of the β-AR signaling cascade, including β_1/β_2-AR, $G_{\alpha s}$ overexpression or inhibition of β-AR kinase, resulted in transient improvements in contractile function, but also led to progressive cardiac hypertrophy and HF in aging animals (*Vinge et al., 2008; Lohse et al., 2003*).

1.6.1.2. Calcium cycling proteins

The maintenance of stable intracellular calcium levels during systole and diastole is governed by numerous channels and exchangers that regulate the flow of calcium ions between the extracellular space, cytoplasm and intracellular stores.

Sarcoplasmic reticulum (SR) plays an important role in Ca^{2+} movement during excitation-contraction (EC)-coupling. The sarcoplasmic reticulum is an intracellular membranous network, which can store calcium. It initiates muscle contraction by calcium release through ryanodine receptors (RyR2s) into the cytosol and facilitates muscle relaxation by active calcium re-uptake by the sarco-endoplasmic reticulum Ca^{2+} ATPase, SERCA2a (*Bers, 2002; 2008*).

During excitation, depolarization leads to opening of voltage-gated L-type Ca^{2+} channels (LTCCs), allows the entry of a small amount of Ca^{2+}, which further stimulates the release of much larger amount of Ca^{2+} from SR via RyR2s (calcium-induced calcium release - CICR) and leads ultimately to contraction (*Bers, 2002; 2008*).

During relaxation, Ca^{2+} is re-accumulated into SR by SERCA2a and extruded by Na^+ Ca^{2+} exchanger, which results in restoration of diastolic Ca^{2+} concentration (*Bers, 2002; 2008*).

Defects in Ca^{2+}-handling, however, are typical in HF, and Gwathmey et al. (*1987*) was the first to report calcium cycling abnormalities in human HF, partially due to decreased SERCA2a activity and regardless of the HF etiology (*Gwathmey et al., 1987*). SERCA2a gene therapy in experimental models of HF have clearly contributed to improved cardiac contractility (*Kawase et al., 2008*), compensation of energy supply and utilization (*Sakata et al., 2007*), reduction in ventricular arrhythmias (*Prunier et*

al., 2008) and improved coronary flow by eNOS activation in endothelial cells (*Hadri et al., 2010*). Lately, another mediator of SERCA2a activity has been recognized as a major player of calcium homeostasis in cardiomyocytes, the small ubiquitin-like modifier type 1 (SUMO1) (*Kho et al., 2011*). In failing human ventricles, SUMO1 levels were reduced, but AAV9-mediated gene therapy increased its levels, improved SERCA2a activity and hemodynamic performance, and reduced mortality in small and large experimental models of HF (*Kho et al., 2011*).

Phospholamban (PLB) is a reversible endogenous inhibitor of SERCA2a found in the SR or ER of mainly muscle cells, interacts with SERCA2a when being in its unphosphorylated form and decreases ligand affinity and pump activity. PLB phosphorylation by cAMP or Ca^{2+}/calmodulin-dependent protein kinase relieves SERCA2a inhibition and results in enhanced contractility (*Lompre et al., 2010*). PLB inhibition could be reasonably considered as another approach to improve Ca^{2+} handling in the heart. In human HF, protein phosphatase-1 (PP1) activity increases, and this results in PLB dephosphorylation. Ablation of the endogenous phosphatase inhibitor (inhibitor-1) or PP1 overexpression in murine hearts has been linked to decreased β-AR-mediated contractility or cardiac function, and premature death similar to HF (*Pathak et al., 2005*). In contrast, when the constitutively active inhibitor-1 (I1c) suppressed PP1 in transgenic mice, PLB phosphorylation increased and cardiac contractility improved (*Pathak et al., 2005*), a finding that was recently validated via I1c gene therapy in a model of ischemic HF (*Ishikawa et al., 2014*).

Last but not least, a protein, S100A1, that promotes cardiac contractility and relaxation by improving both RyR2 and SERCA2a activities. Gene therapy with AAV6-S100A1 reversed LV dysfunction and remodeling in a rat model of HF (*Pleger et al., 2007*), while preclinical studies in ischemic cardiomyopathy revealed significant improvements in contractile function by AAV9-mediated S100A1 gene transfer (*Pleger et al, 2011*).

1.6.1.3 Myofilaments

When energy from ATP hydrolysis fuels myosin to move along actin filaments, their interaction initiates contraction in cardiomyocytes. Nowakowski et al. (*2013*) showed that the contractility in striated muscles can be further improved by increasing myosin binding to actin and enhancing cycling kinetics after replacement of ATP with 2-deoxyATP (*Nowakowski et al., 2013*). This substrate is naturally limited but its production can be increased by overexpressing ribonucleotide reductase (R1R2). In human and animal models of HF, RIR2 overexpression enhanced contractility (*Moussavi-Harami et al., 2015*) and LV systolic function (*Nowakowski et al., 2013*).

1.6.2. Other molecular targets of cAMP signaling cascade

Apart from compensating the dysfunctional β-AR signaling or depressed myocardial contractility in HF, gene therapy could be also successfully utilized in restoring the reduced intracellular cAMP content of failing hearts, which constitutes one of the best described features in the molecular and cellular pathophysiology of heart failure (*Movsesian, 2000*).

1.6.2.1 Adenylyl Cyclase

To increase cAMP bioavailability, adenylyl cyclase (AC) could be overexpressed via cardiac gene therapy (*Feldman et al.., 2005*), since it is the enzyme responsible for cAMP synthesis and acts as a rate-limiting factor in signal transduction (3 AC molecules for 100 molecules of $G_{\alpha s}$ and 1 molecule of β-AR) (*Ostrom et al., 2000*).
There are two major cardiac isoforms, AC5 and AC6, activated by $G_{\alpha s}$ and phosphorylated and subsequently inhibited by the protein kinase A (PKA) (feedback regulation of signaling cascade) (*Defer et al., 2000; Hanoune et al., 2001*). Each isoform is differentially regulated by membrane receptors: purinergic receptors activate AC5 (*Puceat et al., 1998*), whereas AC6 is specifically activated by β1-AR, but not by β2-AR (*Stark et al., 2004*). AC5 protein is mostly abundant in fetal hearts, declines with development and increases with pressure-overload hypertrophy (*Hu et al., 2009*). By contrast, AC6 expression declines in experimental HF models induced by chronic pressure overload or myocardial infarction, as part of the desensitization of the β-AR signaling cascade (*Espinasse et al., 1999; Hu et al., 2009*).
Overexpression of AC5, despite an increase in basal and forskolin-stimulated cAMP production, did not constrain β-AR signaling in cardiomyocytes or contractile function in young mice (*Tepe et al., 1999*), but led to the development of a dilated cardiomyopathy with aging (*Mougenot et al., 2019*). Moreover, targeted disruption of AC5 in mice prolonged longevity and protected the heart against aging, pressure overload and catecholamine-induced stress (*Vatner et al., 2009; Okumura et al., 2003*). By contrast, overexpression of AC6 increased β-AR-stimulated contractility, and improved cardiac function and survival in numerous animal models of cardiac dysfunction, including one of cardiac aging (*Tang et al., 2011*).
The apparent contradiction between the cardiotoxic effects of β_1-AR signaling cascade stimulation and beneficial effect of AC6 overexpression was explained partially by the cytosolic localization of the AC6 molecule, which directly affects phospholamban phosphorylation and increases SR calcium transient (*Gao et al., 2008; 2010*). However, this hypothesis was disputed using mouse models overexpressing AC8 (*Lipskaia et al., 2000; Lipskaia et al., 2011*), which is not coupled to the β-AR signaling cascade and is stimulated by calcium-calmodulin. Young transgenic mice overexpressing cardiac AC8 showed an improved β-adrenergic reactivity that enhanced cAMP synthesis, PKA activity, SR calcium cycling and contractile function (*Lipskaia et al., 2000; Georget et al., 2002; Georget et al., 2003*). However, increasing cAMP/PKA signaling by AC8 overexpression eventually led to dilated and hyperkinetic cardiomyopathy in aged mice (*Lipskaia et al., 2011*). Moreover, a recent report suggested that the beneficial effects of AC6 gene transfer on calcium cycling and contractile function might not be mediated by an increase in cAMP production and can be observed after gene transfer of an inactive AC6 mutant (*Levin et al., 2011*).
The potential benefit of AC enhancement in heart failure cannot be clearly predicted as the obtained results from several animal studies are not consistent and a clear understanding of the cardiac AC/cAMP signaling pathway, especially of its subcellular compartmentation is still lacking (*Kairouz et al., 2012; Lyon et al., 2008; Mougenot et al., 2019*).

1.6.2.2 PDE4B3

All this information led to the next reasonable step in bypassing defective β-AR signaling and reducing the excessive amounts of local cAMP by overexpression of PDEs, the enzymes implicated in cAMP catabolism. Mostly inspired by the above-mentioned phenotype of the PDE transgenic mice, there has been so far only one report using the cAMP hydrolysing PDE isoform PDE4B3 for gene therapy in human and animal heart failure models. Its initial results showed that PDE4B3 enzyme overexpression had beneficial effects against sympathetic overdrive, hypertrophy and arrhythmia initiation, but not against HF induced decline in cardiac contractility in male C57BL/6J mice (*Karam et al., 2020*).

1.7 Rationale of the study

Taking into consideration the excessive amounts of local cAMP in different cardiomyocyte microdomains, as well as the increasing number of animal and human studies clearly demonstrating the equally important decrease in PDE expression and activity during HF, mainly due to sympathetic overdrive, we decided to utilize a gene therapy approach and investigate the potential of overexpressing key PDEs of the myocardium against cardiac remodelling, hypertrophy and arrhythmias.
In particular, as outlined above, it is known that, PDE2 which is upregulated in diseased cardiomyocytes, under physiological conditions coordinates the cAMP pools associated with β-AR signaling, contractility, Ca^{2+} homeostasis and mitochondrial function (*Sadek et al., 2020*). In human and animal models of HF, it has been found that its expression is upregulated, as an important defense mechanism against cardiac stress induced by excessive β-AR drive (*Mehel et al., 2013*). Moreover, PDE2 overexpression in cultured rat myocytes significantly attenuated norepinephrine- or phenylephrine-mediated hypertrophy and paved the way for the generation of a cardiac-specific PDE2A3 transgenic (TG) mouse line (*Vettel et al., 2016*), which demonstrated marked reduction in resting as well as in maximal heart rate with preserved cardiac output due to greater cardiac contraction (*Vettel et al., 2016*). This well tolerated phenotype persisted also in elderly TG mice with no indications of cardiac pathology and, more importantly, TG animals remained resistant to triggered ventricular arrhythmias after catecholamine injection (*Vettel et al., 2016*). Molecular investigation on the TG cardiomyocyte level revealed lower basal phosphorylation levels of Ca^{2+}-cycling proteins including RyR2, and improved contractility, lower Ca^{2+} transients and $I_{Ca,L}$, as well as remarkably reduced Ca^{2+}-leakage after Ca^{2+}-spark analysis (*Vettel et al., 2016*). Obviously, the activation of myocardial PDE2 may represent a novel intracellular anti-adrenergic and anti-arrhythmic therapeutic strategy.

In pathological conditions, it has also been revealed that PDE3A is decreased, particularly in hypertrophy and HF (*Abi-Gerges et al., 2009*). Apart from regulating PLB phosphorylation and thus SERCA2a activity in humans and mice (*Ahmad et al., 2015; Beca et al., 2013*), PDE3A1 also acts as a negative regulator of cardiomyocyte apoptosis, by controlling the expression of the transcriptional repressor and pro-apoptotic factor, ICER (inducible cAMP early repressor) (*Yan et al., 2007*). Inhibition

of this mechanism in mice with cardiac-specific overexpression of PDE3A1 was associated with protection during ischemia-reperfusion (*Oikawa et al., 2013*). Recently, elegantly performed studies at the onset of cardiac hypertrophy were able to show that both PDE2A and PDE3A undergo a disease-driven redistribution between various subcellular microdomains such as β-AR-associated membrane compartments and the SR (*Perera et al., 2015; Sprenger et al., 2015*), a mechanism by which changes in cAMP compartmentation can drastically impact on contractile function, but also lead to the development of better HF therapeutics.

And also, albeit pharmacological PDE4 inhibition has beneficial effects on cardiomyocyte function (*Lehnart and Marks, 2006*), many unfavorable cardiac effects occur from sustained inhibition of this enzyme, increasing the incidence of mortality (*Packer et al., 1991*). A variety of studies concerning pathological cardiac hypertrophy induced by sympathetic overdrive revealed dramatic reduction in enzyme expression (~ 50% for PDE4B) (*Abi-Gerges et al., 2009; Karam et al. 2020*) and subsequently increased susceptibility to arrhythmias and heart failure in animals and humans (*Bobin et al., 2016; Lehnart et al., 2005; Leroy et al., 2011; Molina et al, 2012*).

1.8 Objective/Aim of the study

As prior evidence suggests that HF will continue to remain an elusive therapeutic target with a rather grim prognosis for the next years, we decided to utilize the potential of gene therapy and overexpress PDE2A3 and PDE4B3 in a murine Transverse Aortic Constriction (TAC) model that reproduces human hypertension or aortic valve stenosis with the aim to develop and characterize a new cardiac-targeted gene delivery approach that could reduce the excessive amounts of local cAMP in different cardiomyocyte microdomains and reverse or protect against heart failure progression.

By overexpressing PDE2A3 and PDE4B3 in failing mouse hearts, we investigated the β-AR-mediated signaling together with PDE-mediated hydrolytic activity in distinct cardiomyocyte microdomains and assessed its effectiveness against pressure overload-induced hypertrophy and arrhythmias.

Major goals of the thesis were:

- Cardiac-targeted PDE overexpression by AAV9 expressing PDE2A3 or PDE4B3 *in vivo*.
- Real-time monitoring of cAMP and unravelling of individual PDE contribution in the RyR2 microdomain of mouse ventricular cardiomyocytes.
- Real-time monitoring of cAMP and analysis of PDE effects in the caveolin-rich membrane microdomain of mouse ventricular cardiomyocytes.
- Analysis of PDE overexpression effect on cardiac hypertrophy and β-AR induced arrhythmias.

2. Materials and Methods

2.1 Materials

2.1.1 Mouse lines

αMHC-Epac1-camps-JNC	Berisha et al. 2019
αMHC-pmEpac1-camps	Perera et al. 2015

2.1.2 Antibodies

Primary antibodies:

α-Tubulin, mouse monoclonal antibody	Sigma
Calsequestrin, rabbit polyclonal antibody	Thermo Fischer Scientific
Cav3, mouse monoclonal antibody	BD #610421
GAPDH, mouse monoclonal antibody	HyTest Ltd, #5G4
PDE2A, rabbit monoclonal antibody	FabGennix, #PDE2A-101AP
PDE3A, rabbit monoclonal antibody	Yan lab, *Ding et al., 2005*
PDE4B, rabbit monoclonal antibody	abcam, #ab170939
PDE4D, rabbit monoclonal antibody	abcam, #ab171750
RyR2, rabbit monoclonal antibody	Sigma Aldrich, #HPA020028
RyR2 (Ser2808), rabbit monoclonal antibody	Badrilla, #A0-10-30

Secondary antibodies:

Alexa Fluor 568, goat anti-rabbit	Thermo Fisher, #A-11011
Alexa Fluor 594, donkey anti-sheep	abcam, #ab150180
Alexa Fluor 633, donkey anti-sheep	Thermo Fisher, #A-21100

2.1.3 Chemicals

Acrylamide (Rotiphoreses Gel 30)	ROTH
Agarose	peqlab
Ammonium persulfate (APS)	Sigma

BAY 60-7550	Cayman
Bovine serum albumin (BSA)	Sigma
2,3-butanedione monoxime (BDM)	Sigma
Bromphenol blue	Applichem
8-Br-2'-*O*-Me-cAMP-AM	BioLog Life Science Inst.
$CaCl_2$	Merck Millipore
CGP-20712A	Sigma
Cilostamide	Sigma
Complete protease inhibitor cocktail tablets	Roche
Dimethylsulfoxide (DMSO)	AppliChem
Ethylene glycol tetraacetic acid (EGTA)	AppliChem
Ethylenediaminetetraacetic acid (EDTA)	AppliChem
Ethidium bromide solution	ROTH
Forane (Isolflurane)	Abbott
Forskolin	Sigma
Glycine	Sigma
HEPES	Sigma
ICI 118,551	Sigma
Isoproterenol (ISO)	Sigma
3-Isobutyl-1-methylxanthine (IBMX)	Sigma
KCl	Merck Millipore
$KHCO_3$	Sigma
KH_2PO_4	Merck Millipore
MDL-12,330A	Sigma
2-Mercaptoethanol	Sigma
Methanol	ROTH
$MgCl_2$	Sigma
$MgSO_4$ x $7H_2O$	Sigma
Milk powder	ROTH
NaCl	Merck Millipore

NaOH	ROTH
Na_2HPO_4 x $2H_2O$	Merck Millipore
$NaHCO_3$	Sigma
N,N,N',N'-Tetramethylenediamine (TEMED)	Sigma
Paraformaldehyde (PFA)	Sigma
PhosphoSTOP phosphatase inhibitor cocktail tablets	Roche
Ponceau S	Sigma
Rolipram	Sigma
Sodium azide	Sigma
20% Sodium dodecyl sulfate solution (20% SDS)	Fluka
Taurine	Sigma
Tris(hydroxymethyl)-aminomethan (TRIS)	ROTH
10% Triton -100 solution, peroxide-free	AppliChem
Tween20	Sigma

2.1.4 Cell culture materials

Minimum Essential Medium (MEM)	Invitrogen
Phosphate Buffer Saline Dulbecco's (PBS)	Biochrom
Fetal Bovine Serum, FBS Superior (FBS)	Biochrom
Penicillin/Streptomycin (10.000 U/mL/10.000µg/mL)	Biochrom
Insulin-Transferrin-Selenium supplement	Invitrogen
L-Glutamine, 200mM	Biochrom

2.1.5 Enzymes

Liberase DH (Collagenase I and II)	Roche, #5401089001
Trypsin, 2.5% solution	Invitrogen

2.1.6 Kits and others

BCA Protein Assay Kit	Thermo Scientific
Direct PCR-Tail	peqLab
Enhanced chemiluminescence reagent	Thermo Scientific

LB-agar powder	AppliChem
LB medium powder	Applichem
Protein ladder (Protein marker V)	peqLab
1kb DANN-ladder	New England Biolabs
100bp DANN-ladder	New England Biolabs
5x loading dye (for agarose gel electrophoresis)	AppliChem
Laminin	Sigma
Roticlear	ROTH
TAE buffer	AppliChem
Vectashield Mounting Medium	Vector Laboratories
Wheat Germ Agglutinin (WGA)	Sigma

2.2 Methods

2.2.1 Generation of transgenic moue lines with strong C57BL/6N background

2.2.1.1 Animal breeding

The animal facility of the University Medical Center Hamburg-Eppendorf accommodated the transgenic and wildtype C57BL/6N mice (from Charles River Laboratories, Göttingen, Germany) and FVB/N1 mice (from Janvier Labs, Saint Berthevin, France) for our experimental purposes.

Transgenic mice initially produced on FVB/N1 background to express the cAMP biosensors Epac1-JNC (also called E1-JNC, represents a fusion of the cytosolic cAMP biosensor Epac1-camps to the N-terminal of the SR protein junctin which forms a stable complex with the ryanodine receptor) for RyR2 (*Berisha et al., 2019*) and pmEpac1-camps (also called pmEpac1, it contains Epac1-camps sequence with N-terminal 10 amino acid peptide from Lyn kinase responsible for palmitoylation and myristoylation and, hence, membrane targeting) for caveolin-rich membrane microdomains (*Perera et al., 2015*) in adult cardiomyocytes under the control of the α-myosin heavy chain (αMHC) promotor were backcrossed 10 times with C57BL/6N mice (*Madissoon et al., 2014*) for the generation of transgenic mouse lines on the C57BL/6N background. Only mice either heterozygous (+/T) for the biosensor or wildtypes (+/+), were used for the experiments.

Female mice aged 8-20 weeks old were registered using Tbase software, while animal technicians were in charge of mouse husbandry. Animal experimental work conformed to institutional rules for reduction, replacement and refinement (3Rs) as well as governmental guidelines and was approved by the local animal welfare authority BGV Hamburg (approved number N109/2018).

2.2.1.2 Genotyping

PCR-based (*Saiki et al., 1988*) genotyping was utilized to distinguish transgenic and wildtype mice. Ear or tail biopsies taken from E1-JNC and pmEpac1 trangenic offspring were subjected to overnight digestion with 200µL Proteinase K-containing lysis solution DirectPCR-Tail Buffer under vigorous shaking (55°C). After sample inactivation at 85°C for 45 minutes (heat inactivation of Proteinase K) and cooling down to 4°C, the supernatants were directly used for PCR amplification. In parallel, a negative (H_2O) and a positive control (plasmid encoding the sensor) were subjected to the same procedure, as follows:

94°C	5 min	
94°C	30 sec	35x
62°C	30 sec	
72°C	50 sec	
72°C	7 min	
4°C	∞	

Final steps for analysis included sample loading on 1% agarose gel, running in TAE buffer and fragment detection at ~340bp for E1-JNC and ~365bp for pmEpac1 mouse lines. All genotyping work and analysis were performed by Ms. Sophie Sprenger, Ms. Annabelle Kühl and Ms. Viktoria Hänel (Institute of Experimental Cardiovascular Research, University Medical Center Hamburg-Eppendorf).

2.2.1.3 Ventricular cardiomyocyte isolation

Ventricular cardiomyocytes from adult female hearts were isolated via retrograde Langendorff perfusion of the aorta with an enzymatic digestion solution (*Börner et al., 2011)* in a perfusion system comprising of a water bath (39°C), a peristaltic pump (adjusted to 3mL/min outflow), plastic tubing and a 20 G cannula (*Louch et al., 2011*).

Necessary steps before isolation required (a) preheating of the water bath at 39°C, (b) thorough rinsing of the tubing system with H_2O and subsequently with perfusion buffer (35mL frozen aliquots: 113 mmol/L NaCl, 4.7 mmol/L KCl, 0.6 mmol/L KH_2PO_4, 0.6 mmol/L Na_2HPO_4 x $2H_2O$, 1.3 mmol/L $MgSO_4$ x $7H_2O$, 12 mmol/L $NaHCO_3$, 10 mmol/L $KHCO_3$, 10 mmol/L HEPES, 30 mmol/L taurine, 10 mmol/L 2,3-butanedione-monoxime, 5.5 mmol/L glucose, pH 7.4), (c) preparation of two stopping buffers (stopping buffer 1: 2.25mL perfusion buffer, 1.25µL of 100mM $CaCl_2$ and 250µL FCS, stopping buffer 2: 9.5mL perfusion buffer, 3.75µL of 100mM $CaCl_2$ and 500µL FCS) and digestion buffer (29.5mL perfusion buffer plus 3.75µL of 100mM $CaCl_2$) with liberase (300µL frozen aliquots - 50mg in 12mL sterile water, mild shaking every 5 minutes (4x) on ice and stored in 300µL aliquots at -20°C) and trypsin (300µL frozen aliquots, 2.5% solution at -20°C), and (d) transfer of 2.5mL of digestion buffer into a beaker for mechanical disruption of the digested ventricles.

Animals were anesthetized by isoflurane and euthanized by cervical dislocation. Immediately the heart was excised, mounted onto the blunted 20 G cannula (constantly

in cold PBS) and perfused for 3 minutes with the perfusion buffer at 37°C. Subsequently, the perfusion continued with the digestion buffer for at least 10 minutes until the heart turned pale pink. The atria were cut and discarded, and the ventricles were transferred and dissected for 30 seconds into the beaker containing the 2.5mL digestion buffer. Extra 2.5mL of stopping buffer 1 were used to prevent further enzymatic digestion, and the suspension was homogenized with a 1mL-syringe for 3 minutes. The homogenate was infiltrated through a 150µm cell-culture mesh and the cells were left to precipitate. After 10 minutes, the supernatant was discarded and resuspension with stopping buffer 2 prepared the ventricular cardiomyocytes for the next step. Calcium concentration was gradually increased to 1mmol/L according to the following recalcification protocol with 4-minute breaks between each step:

- 2x 50µL of 10mmol/L $CaCl_2$,
- 1x 100µL of 10mmol/L $CaCl_2$,
- 1x 30 µL of 100mmol/L $CaCl_2$,
- 1x 50µL of 100mmol/L $CaCl_2$.

75µL of cell suspension were seeded on laminin-coated coverslips and incubated at 37°C and 5% CO_2 for at least 60-75 minutes before FRET experiments or cell culture medium supplementation (22.5mL Minimum essential medium, 250µL of 0.1% BSA, 250µL of 2mM L-glutamine, 500µL of 10mM BDM, 250µL antibiotics - 100U/mL Penicillin and 100µg/mL Streptomycin, and 250µL insulin-transferrin-selenium supplement).

2.2.2 Transverse Aortic Constriction and AAV9 gene therapy

After body weight determination (>20g) and animal randomization, 9 –12-week-old female mice were anesthetized by 1.5–2% isoflurane in 100% oxygen and subjected to suprasternal incision. The aortic arch was either exposed (Sham) or constricted between the first and second trunk using a defined 27-gauge spacer and 6–0 polyviolene suture (TAC) (*Hu et al., 2003*). The operated mice received intraperitoneal analgesic therapy with buprenorphine and carprofen, and 72 hours post-surgery, the pressure gradient was defined across the TAC region by transthoracic echocardiography utilising a 20 MHz Doppler velocity probe (Visual Sonics Vevo 3100, Toronto Canada) (*Pavlaki et al., 2021*). When the pressure gradient was determined above 50mmHg, the constriction was considered sufficiently good and the mice were injected via their tail-vein with adeno-associated virus serotype 9 (AAV9) (*Zacchigna et al., 2014*) expressing either control luciferase (LUC) or PDE2A3 or PDE4B3 (*Karam et al., 2020*). Echocardiography was performed at eight weeks after surgery with subsequent heart excision for cardiomyocyte isolation (*Börner et al., 2011*) or histological analysis. The TAC and Sham surgeries were carried out by Professor Viacheslav Nikolaev (Institute

of Experimental Cardiovascular Research, University Medical Center Hamburg-Eppendorf).

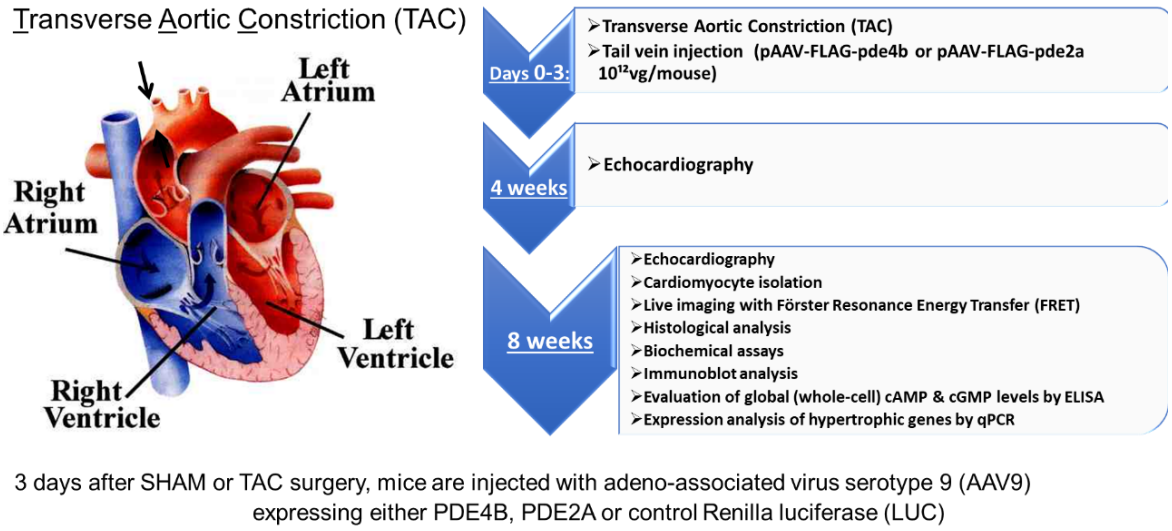

Figure 3. Gene therapy protocol in transgenic TAC C57BL/6N mice. 9-12 weeks old female mice are subjected to transverse aortic constriction (TAC) and injected with adeno-associated virus serotype 9 (AAV9) expressing PDE2A3, PDE4B3 or control Renilla luciferase (LUC) (*Karam et al., 2020*) after pressure gradient measurement. The progress of the disease was monitored by transthoracic echocardiography at eight weeks after TAC before heart collection for experimental analysis.

2.2.3 Characterization of the gene therapy models

2.2.3.1 Echocardiography

Prior to echocardiographic measurements, body weights were determined. *In vivo* analysis of cardiac function and disease progression was performed in a blind-manner by Ms. Birgit Geertz (AG Weinberger, Institute of Experimental Pharmacology and Toxicology, University Medical Center Hamburg-Eppendorf) using transthoracic echocardiography (Visual Sonics Vevo 3100, Toronto Canada) (*Pavlaki et al., 2021*).

Echocardiography analysis was performed in a similarly blind-manner by Dr. Kirstie de Jong (Institute of Experimental Cardiovascular Research, University Medical Center Hamburg-Eppendorf) as previously described (*Simpson et al., 1993; Wagner et al., 2012*). Morphometric and physiological cardiac parameters, i.e., intraventricular septum thickness in systole/diastole (IVDs/d), left ventricular internal diameter in systole/diastole (LVIDs/d), left ventricular posterior wall thickness in systole/diastole (LVPWs/d), stroke volume, cardiac output, heart rate and weight described the disease progression among the animal groups and allowed the determination of physiological parameters such as fractional shortening (FS) or ejection fraction (EF) (*Simpson et al., 1993*).

2.2.3.2 Morphometric analysis

Morphometric parameters of transgenic hearts were analyzed eight weeks after surgery (~20-week-old mice) including body, heart and lung weight and tibia length measurements by an analytical balance (BP300S, Sartorius, Hamburg, Germany) and a sliding caliper, respectively.

2.2.3.3 Histological analysis

Picrosirius red stain or hematoxylin/eosin staining of Sham LUC, TAC LUC, TAC PDE4B and TAC PE2A hearts was performed as described elsewhere (*Wagner et al., 2012; Pavlaki et al., 2021*) by Ms. Kristin Hartmann at the Department of Mouse Pathology, University Medical Center Hamburg-Eppendorf, Medical Center. Moreover, paraffinized transverse sections (5µm) were deparaffinized (3x xylene; each step for 5 minutes) and rehydrated (1x 100% ethanol, 1x 95% ethanol, 1x 80% ethanol, 1x 65% ethanol, 1x 50% ethanol, 1x 25% ethanol and 1x H2O; each step for 5 minutes) for dimension analysis of the cardiomyocytes. The rehydrated sections were stained with wheat germ agglutinin (WGA, 75µg/mL) for 30 minutes in the dark and at room temperature, rinsed thrice for 5 minutes with phosphate-buffered saline, mounted in Vectashield Mounting Medium, and observed under a Keyence Fluorescence microscope Biozero BZ 8100. Images were acquired using Keyence Biozero imaging software (Keyence, Neu-Isenburg, Germany) and analyzed by ImageJ software. The cell area was measured in 50 cardiomyocytes from three individual hearts per group (*Pavlaki et al., 2021*).

2.2.4 Confocal microscopy

Imaging experiments were performed using Zeiss LSM 800 microscope (Carl Zeiss MicroImaging) equipped with a Plan-Apochromat x63/1.40 oil-immersion objective. For biosensor or PDE-overexpression experiments, cells were fixed for 5 min with ROTI Histofix® 4% (Roth), washed and stained overnight with primary mouse monoclonal caveolin 3 (BD #610421) antibody, RyR2 (#HPA020028) antibody, PDE2A3 goat or PDE4B (abcam) antibodies, and subsequently with the respective secondary anti-goat Alexa 457 Fluor® (kindly provided by Florian Weinberger, Institute of Experimental Pharmacology and Toxicology, University Medical Center Hamburg-Eppendorf) or anti-mouse or anti-rabbit Alexa 633 Fluor® antibody (A-21063, Life Technologies). Images were acquired for E1 JNC and pmEpac1 sensors (488 nm diode laser) and for caveolin 3, PDE2A, PDE4B, RyR2 (633 nm diode laser excitation) and automatically analyzed using the ZEN 2019 software (Zeiss).

2.2.5 Western Blot and immunoblot analysis

Heart tissues (i.e., ventricles) were shock frozen and homogenized in a buffer (~300µL) containing: 10 mmol/L HEPES, 300 mmol/L sucrose, 150 mmol/L NaCl, 1 mmol/L EGTA, 2 mmol/L $CaCl_2$ and 1% Triton-X. Proteins were quantified using Pierce BCA protein assay (Thermo Fischer Scientific, Dreieich, Germany) (*Smith et al., 1985)*. Samples were boiled at 95°C for 5 min or 70°C for 10 min depending on the protein of interest, and 10-15 µg of total protein were loaded per lane and subjected to 8-10% SDS-PAGE (*Laemmli, 1970*) and immunoblot analysis (*Towbi et al., 1979)* using PDE2A antibody (1:750, 3% milk) (Fabgennix, Frisco, TX, USA), custom-made rabbit

polyclonal PDE3A antibody (1:1000, 3% milk) (kindly provided by Chen Yan, University of Rochester, Rochester, NY, USA), rabbit monoclonal PDE4B and PDE4D antibodies (1:2000, 5% milk) (Abcam, Berlin, Germany), rabbit polyclonal calsequestrin (1:5000, 3% BSA) (Thermo Fischer Scientific, Dreieich, Germany), and mouse monoclonal α-tubulin antibody (1:5000, 5% milk) (Sigma, Taufkirchen, Germany). For uncalibrated optical density, all scanned blots were analysed by ImageJ software densitometrically (*Pavlaki et al., 2021*).

2.2.6 FRET-based measurements of cAMP

Live cell imaging was performed using a custom-made FRET microscopy system built around a Nikon Eclipse Ti microscope (Nikon, Düsseldorf, Germany) equipped with 63x /1.40 oil-immersion objective (*Pavlaki et al., 2021*). The system recorded cAMP signals generated by donor fluorophore (CFP) excitation at 440 nm every 5 seconds using a CoolLED single-wavelength light emitting diode. Emitted light was detected by an ORCA-03G charge-coupled device camera (Hamamatsu, Herrsching am Ammersee, Germany) after having been split into CFP and YFP channels using a DV2 DualView (Photometrics, Surrey, BC, Canada) (*Sprenger et al., 2012*).

Adult ventricular cardiomyocytes isolated from Sham LUC, TAC LUC, TAC PDE4B3 or TAC PDE2A3 were seeded on laminin-coated coverslips (25mm), incubated at 37ºC and 5% CO_2 for at least 60-75 minutes and supplemented with cell culture medium prior to FRET experiments. For live cell imaging, coverslips with attached cells were first rinsed and then hydrated with 400µL FRET buffer (144 mmol/L NaCl, 5.4 mmol/L KCl, 1 mmol/L $MgCl_2$, 1 mmol/L $CaCl_2$, 10 mmol/L HEPES, pH 7.3) in an Attofluor microscopy chamber.

After reaching a stable baseline, cells were treated according to predefined protocols for cAMP signal stimulation. Offline data analysis was performed using ImageJ, Microsoft Excel, and GraphPad Prism 6 software (*Börner et al., 2011*).

Due to spectra overlap, HEK293A cell were employed for bleed through factor determination by FRET experiments after CFP plasmid transfection.

Raw CFP and YFP intensities were corrected by subtracting the bleed through factor according to the equation:

FRET ratio = (YFP – 0.794 x CFP) / CFP

for the particular FRET microscopy set-up prior to FRET measurements in cardiomyocytes.

The corrected ratiometric FRET traces were normalised to baseline, expressed as a % and plotted against time for spatiotemporal determination of cAMP dynamics.

2.2.7 Single-cell contractility measurements

Adult ventricular cardiomyocytes isolated from Sham LUC, TAC LUC, TAC PDE4B3 or TAC PDE2A3 were seeded on laminin-coated glass-bottomed chambers (35mm), incubated at 37ºC and 5% CO_2 for at least 30 minutes prior to single-cell contractility experiments by the optical sarcomere length measurement method (IonOptix).

The chambers with attached cells were first rinsed and then hydrated with 2mL of freshly prepared IonOptix buffer (3M NaCl, 1M KCl, 500mM KH_2PO_4, 500mM Na_2HPO_4 x 2 H_2O, 500mM $MgSO_4$ x 7 H_2O, 1M HEPES, 500mM Glucose, 100mM $CaCl_2$ x 2 H_2O, Ampuwa H_2O up to desired volume). The cells were paced at 1Hz (*Gorelik et al., 2006)* and stimulated with 100 nM ISO for arrhythmia detection. Offline trace analysis was performed using ION WizardTM and GraphPad Prism 6 software.

2.2.8 Statistical analysis

All data were analyzed by GraphPad Prism 6 software and presented as means ± SE with the indicated number of independent experiments (animals and cells) per condition. Normal distribution was assessed by the Kolmogorov–Smirnov test, and differences among the groups were analyzed using either two-tailed t-test (when two groups were compared), one-way ANOVA for multiple group comparison or the Mann–Whitney test followed by Bonferroni's post-hoc test, as appropriate. FRET imaging data were analyzed by either mixed ANOVA followed by Wald's chi-squared test or by Kruskal-Wallis followed by Dunn's test, as appropriate (*Pavlaki et al., 2021*).

3. Results

3.1 Generation and characterization of TAC gene therapy models

To study how gene therapy affects the disease-driven alterations in the RyR2 and caveolin-rich membrane microdomains respectively, we generated E1-JNC and pmEpac1 mice on the C57NL/6N background, and subjected them to pressure overload-induced cardiac hypertrophy. Eight weeks after TAC, transgenic mice developed a robust compensated cardiac hypertrophy phenotype with reduced contractility (**Tables 2, 3 and 4**), hypertrophy (**Figure 4**), signs of fibrosis (**Figure 4a, 4b**) and clear increase in cell size (**Figure 4c, 4d**). In line with the changes in morphometric and physiological parameters, the protein levels of cardiac PDE2A, PDE3A, PDE4B and PDE4D were largely affected (**Figure 7**) due to TAC and gene therapy treatment. But most importantly, the biosensor expression and localization as well as the PDE overexpression were not affected by the diseased phenotype, as indicated by the FRET experiments, immunofluorescence and immunoblot analysis (**Figures 5, 6 and 7**).

3.1.1 Histological analysis of the TAC gene therapy models

To further validate the diseased phenotype in TAC LUC and TAC PDE2A groups, as well as the partial protection by overexpressing PDE4B, the excised hearts were either enzymatically digested to ventricular cardiomyocytes or paraffinised to cross-sections and subsequently stained with hematoxylin/eosin (H&E), picrosirius red stain (PSR) and wheat germ agglutinin (WGA) for histological analysis.

The results of the PSR staining clearly indicated significant collagen deposition and fibrosis for the TAC LUC and TAC PDE2A cross-sections, while the overexpression of PDE4B protected against hypertrophy and fibrosis (**Figure 4a, 4b**).

The WGA staining of the cells also corobborated to significant increases in cell size after TAC for the diseased and TAC PDE2A groups with similar values for the cardiomyocyte area (**Figure 4d**), while the overexpression of PDE4B in ventricular cardiomyocytes presented clear protection against hypertrophy and more similarities to the control group (**Figure 4c, 4d**).

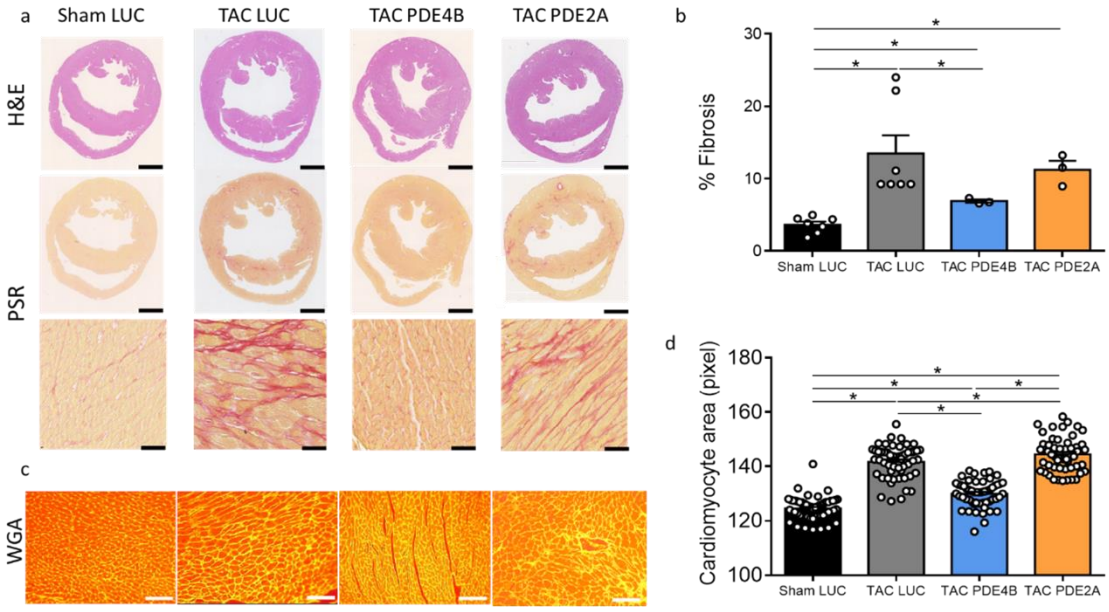

Figure 4. Histological analysis of the TAC gene therapy models. (a) Hematoxylin/eosin and picrosirius red staining of cross-sections from Sham LUC, TAC LUC, TAC PDE4B and TAC PDE2A hearts of transgenic mice. (b) Quantification of fibrosis (%). (c) WGA staining of Sham LUC, TAC LUC, TAC PDE4B and TAC PDE2A cardiomyocytes. Scale bars, 50µm. (d) Quantification of cardiomyocyte area. *$p < 0.005$ by one-way ANOVA.

3.1.2 Immunoblot analysis of TAC gene therapy hearts and isolated cardiomyocytes compared to control group

Another important parameter of the study was to validate the expression and localisation of the cAMP-specific biosensors under all conditions (health, disease and gene therapy), while proving the cardiac-specific overexpression of phosphodiesterases 2A and 4B by confocal imaging and immunoblot analysis.

Since the immunostained E1-JNC and pmEpac1 cardiomyocytes did not differ in terms of biosensor expression and localization after TAC or gene therapy treatment, the next step was to prove that the overexpression of phosphodiesterases occurred only in the gene therapy treated groups. By employing specific antibodies for PDE2A and PDE4B, freshly isolated cardiomyocytes were immunostained and confocal images were acquired (**Figures 5 and 6**). However, the protein expression and quantification of the major cAMP phosphodiesterases by western blot clearly indicated the changes occuring in the respective groups, yielding to 5-fold increase in PDE4B protein levels in the TAC PDE4B groups and 3-fold increase in PDE2A to the TAC PDE2A group respectively. As expected after eight weeks of pressure overload-induced cardiac hypertrophy, the protein levels of PDE3A, PDE4B and PDE4D were significantly decreased in the TAC LUC group with exception to PDE2A (**Figure 7**).

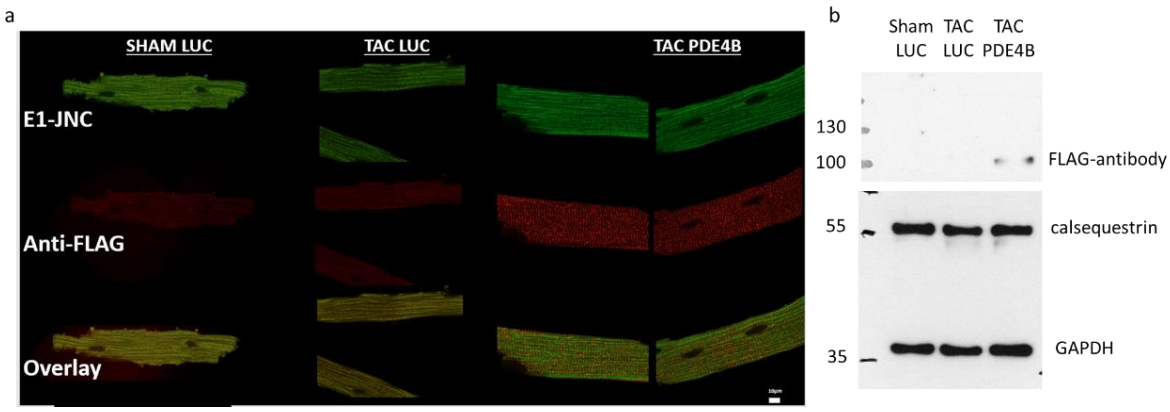

Figure 5. Cardiac-targeted overexpression of phosphodiesterases in ventricular cardiomyocytes. (a) Confocal images of isolated Sham LUC, TAC LUC and TAC PDE4B cardiomyocytes immunostained with the anti-FLAG antibody. Scale bars, 10μm. (b) Representative immunoblots of Sham LUC, TAC LUC and TAC PDE4B cardiomyocytes. Calsequestrin and GAPDH were used as loading controls.

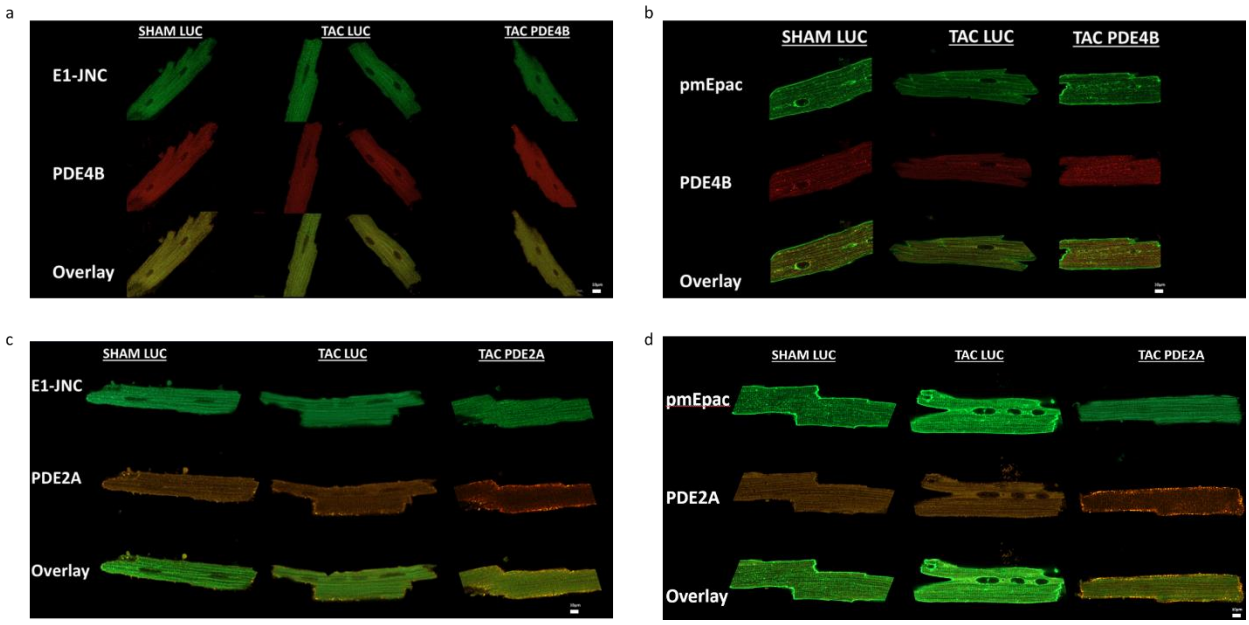

Figure 6. Overexpression of the PDE2A and PDE4B in transgenic hearts 8 weeks after Sham or TAC surgery. (a) Representative confocal images of Sham LUC, TAC LUC and TAC PDE4B expressing the cAMP biosensor for RyR2 microdomain. Scale bars, 10μm. (b) Representative confocal images of Sham LUC, TAC LUC and TAC PDE4B expressing the cAMP biosensor for caveolin-rich membrane microdomain. Scale bars, 10μm. (c) Representative confocal images of Sham LUC, TAC LUC and TAC PDE42A expressing the cAMP biosensor for RyR2 microdomain. Scale bars, 10μm. (d) Representative confocal images of Sham LUC, TAC LUC and TAC PDE42A expressing the cAMP biosensor for the caveolin-rich membrane microdomain. Scale bars, 10μm.

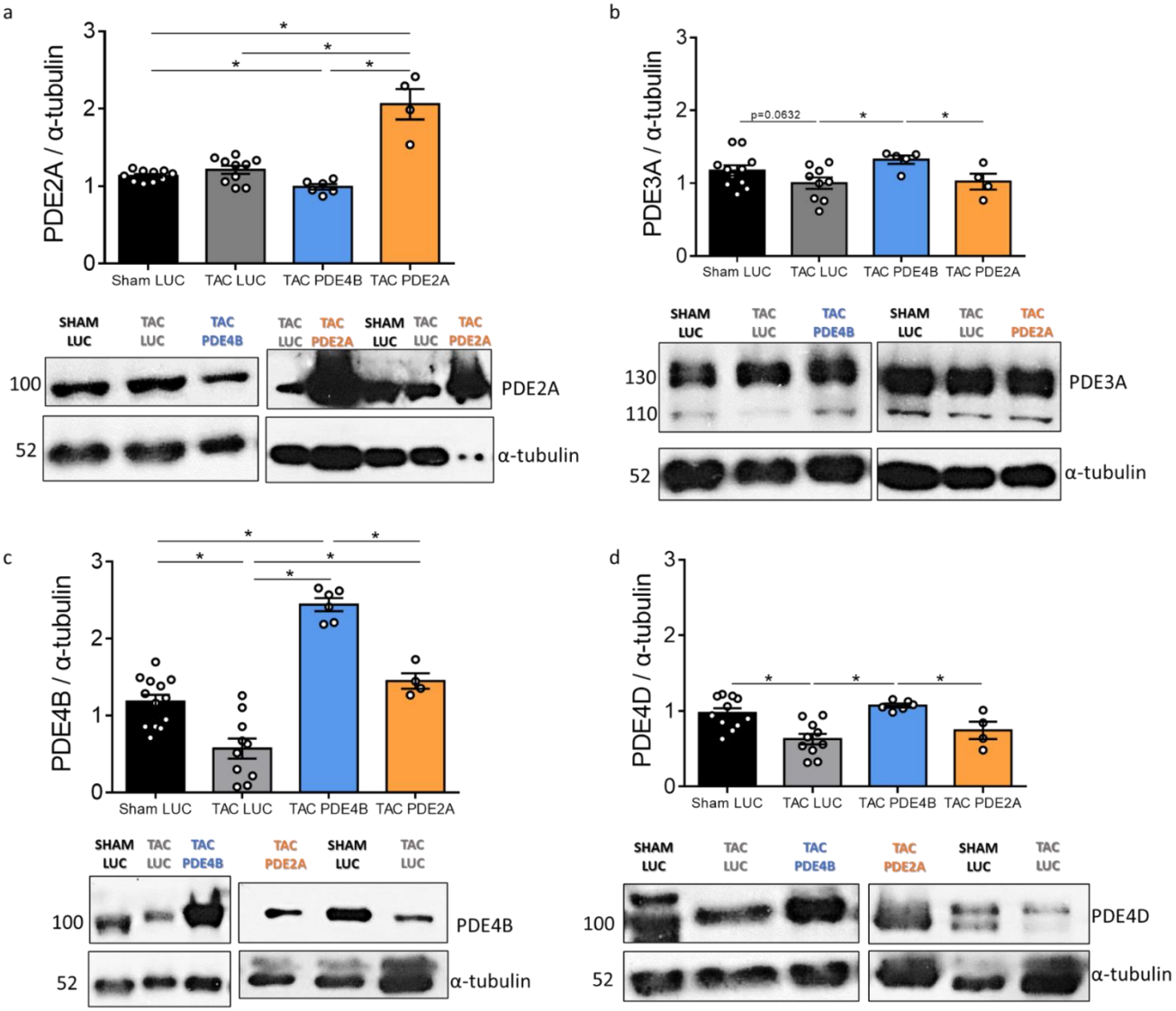

Figure 7. Expression of the major cAMP phosphodiesterases in transgenic hearts 8 weeks after Sham or TAC surgery. Representative immnunoblots and quantification of (a) PDE2A, (b) PDE3A, (c) PDE4B and (d) PDE4D protein expression in Sham LUC, TAC LUC, TAC PDE4B and TAC PDE2A hearts. Means ± SE. *$p < 0.05$ by one-way ANOVA.

3.1.3 Echocardiographic parameters of transgenic TAC LUC, TAC PDE4B and TAC PDE2A mice compared to SHAM LUC littermates

As shown in **Table 2**, the phenotype of the transgenic mice subjected to transverse aortic constriction (TAC) for eight weeks indicated hypertrophy (IVDd, LVIDd, LVPWd) and reduced contractility (EF, FS) compared to their control (Sham LUC) littermates. Only gene therapy with PDE4B appeared to partially protect against hypertrophy (LVPWd) and loss of contractile function (EF) compared to diseased (TAC LUC) and TAC PDE2A groups.

Table 2. Echocardiographic parameters of Sham LUC, TAC LUC, TAC PDE4B and TAC PDE2A mice (C57BL6/N) IVDd: intraventricular septum thickness in diastole, LVIDd: left ventricular internal diameter in diastole, LVPWd: left ventricular posterior wall thickness in diastole, LV mass/BW: ratio of left ventricular mass to body weight, EF: ejection fraction, FS: fractional shortening, HR: heart rate. Means ± SE *$p < 0.05$ by one-way ANOVA.

	Transgenic mice			
Parameters	**Sham LUC**	**TAC LUC**	**TAC PDE4B**	**TAC PDE2A**
Pressure Gradient (mmHg)	2,4 ± 0,08	58,7 ± 3,6*	53,8 ± 3,1*	64,7 ± 4,5*
IVDd (mm)	0,769 ± 0,03	0,964 ± 0,04*	0,875 ± 0,02*	0,947 ± 0,03*
LVIDd (mm)	4,074 ± 0,06	4,567 ± 0,16*	4,124 ± 0,09*	4,241 ± 0,22
LVPWd (mm)	0,606 ± 0,02	0,91 ± 0,05*	0,711 ± 0,04*	0,837 ± 0,03*
LV mass corrected (mm)	79,8 ± 3,8	147,4 ± 11,6*	98,4 ± 5,4*	120,6 ± 7,8*
LV mass/BW (mg/g)	4,2 ± 0,2	7,7 ± 0,6*	5,1 ± 0,3*	6,3 ± 0,4*
EF (%)	50,5 ± 2,7	23,8 ± 2,8*	41,3 ± 3,6*	37,6 ± 6,4*
FS (%)	25,8 ± 1,9	10,2 ± 1,5*	19,2 ± 2*	18,9 ± 3,8*
Stroke volume (µL)	38,4 ± 1,7	24,2 ± 2*	32,1 ± 2,3*	28,9 ± 2,7*
Cardiac Output (mL/min)	18,1 ± 1,1	10,6 ± 1*	15,2 ± 1,2*	13,7 ± 1,2*
HR (bpm)	469 ± 11,9	440,3 ± 19,2	475,6 ± 18,6	478,9 ± 13,6
N	15	13	9	10

3.1.4 Echocardiographic parameters of E1-JNC TAC LUC, TAC PDE4B and TAC PDE2A mice compared to SHAM LUC littermates

The specific echocardiographic analysis of the E1-JNC (**Table 3**) did not differ from the collective results presented in **Table 2**. The diseased phenotype developed in TAC LUC and TAC PDE2A groups, while TAC PDE4B was partially protected against hypertrophy and loss of contractility (**Table 3**).

Table 3. Echocardiographic parameters of Sham LUC, TAC LUC, TAC PDE4B and TAC PDE2A mice (C57BL6/N) expressing the RyR2-targeted biosensor E1-JNC (*Berisha et al., 2019*). IVDd: intraventricular septum thickness in diastole, LVIDd: left ventricular internal diameter in diastole, LVPWd: left ventricular posterior wall thickness in diastole, LV mass/BW: ratio of left ventricular mass to body weight, EF: ejection fraction, FS: fractional shortening, HR: heart rate. Means ± SE. **p* < 0.05 by one-way ANOVA.

	E1-JNC mice			
Parameters	**Sham LUC**	**TAC LUC**	**TAC PDE4B**	**TAC PDE2A**
Pressure Gradient (mmHg)	2,3 ± 0,1	58,2 ± 4,3*	54,8 ± 3,3*	66,2 ± 5*
IVDd (mm)	0,762 ± 0,04	0,901 ± 0,04*	0,881 ± 0,04	0,939 ± 0,03*
LVIDd (mm)	4,003 ± 0,09	4,560 ± 0,19*	4,238 ± 0,1	4,392 ± 0,30
LVPWd (mm)	0,606 ± 0,02	0,919 ± 0,08*	0,717 ± 0,05*	0,847 ± 0,04*
LV mass corrected (mm)	83,05 ± 3,9	125,4 ± 17,4*	114,8 ± 11,2*	127,8 ± 9,3*
LV mass/BW (mg/g)	4,1 ± 0,2	7,3 ± 0,7*	5,4 ± 0,4*	6,5 ± 0,4*
EF (%)	53,3 ± 3,4	22,9 ± 4*	37,8 ± 4,8*	35,9 ± 6,1*
FS (%)	27,6 ± 2,8	9,6 ± 2,4*	17,1 ± 2,5*	17,4 ± 3,1*
Stroke volume (µL)	37,6 ± 1,8	23,9 ± 3,2*	32 ± 3,1	30 ± 4,1
Cardiac Output (mL/min)	17,3 ± 1	10,3 ± 1,6*	14,9 ± 1,7	14 ± 1,8
HR (bpm)	458,6 ± 13,6	437,2 ± 28,5	461,7 ± 26,7	475,7 ± 21,5
N	9	8	6	6

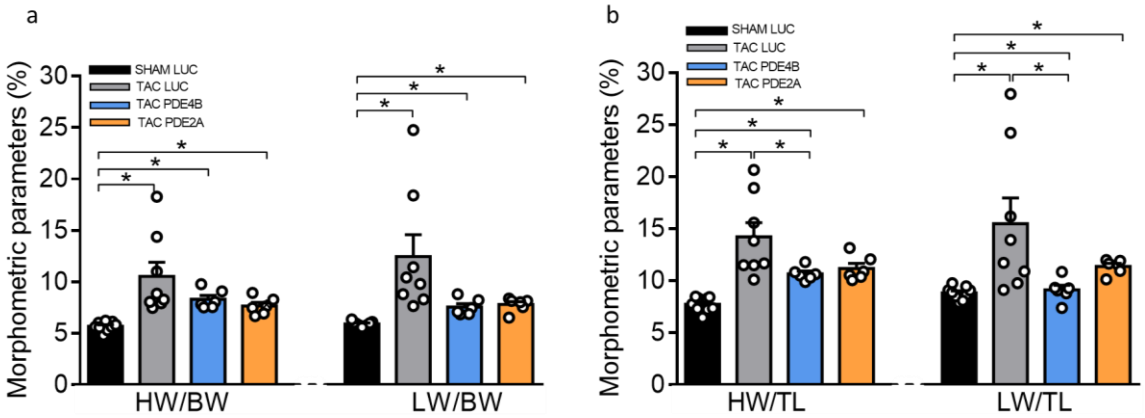

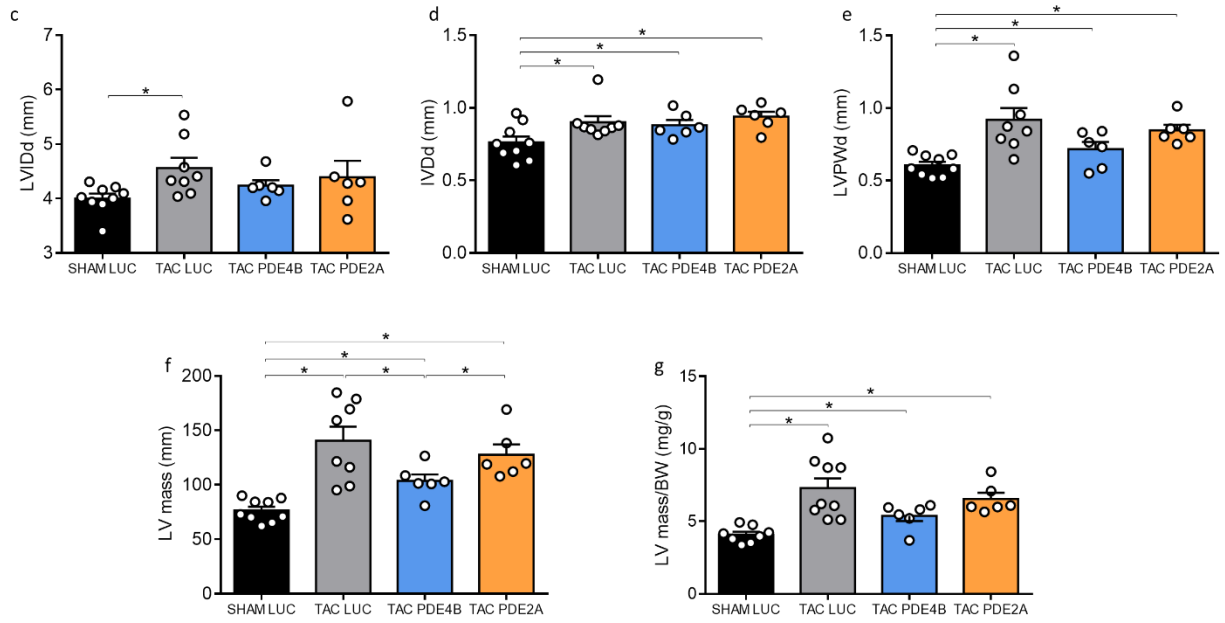

Figure 8. Morphometric parameters of E1-JNC mice expressing the RyR2-targeted biosensor. (a) Heart weight (HW) and lung weight (LW) expressed as ratio to body weight (BW). (b) Heart weight (HW) and lung weight (LW) expressed as ratio to tibia length (TL). (c,d,e) Cardiac dimensions such as intraventricular septum thickness in diastole (IVDd), left ventricular internal diameter in diastole (LVIDd) and left ventricular posterior wall thickness in diastole (LVPWd) expressed in mm. (f) LV mass expressed in mm. (g) Ratio of left ventricular mass to body weight (LV mass/BW) expressed in mg/g. Means ± SE. *$p < 0.05$ by one-way ANOVA.

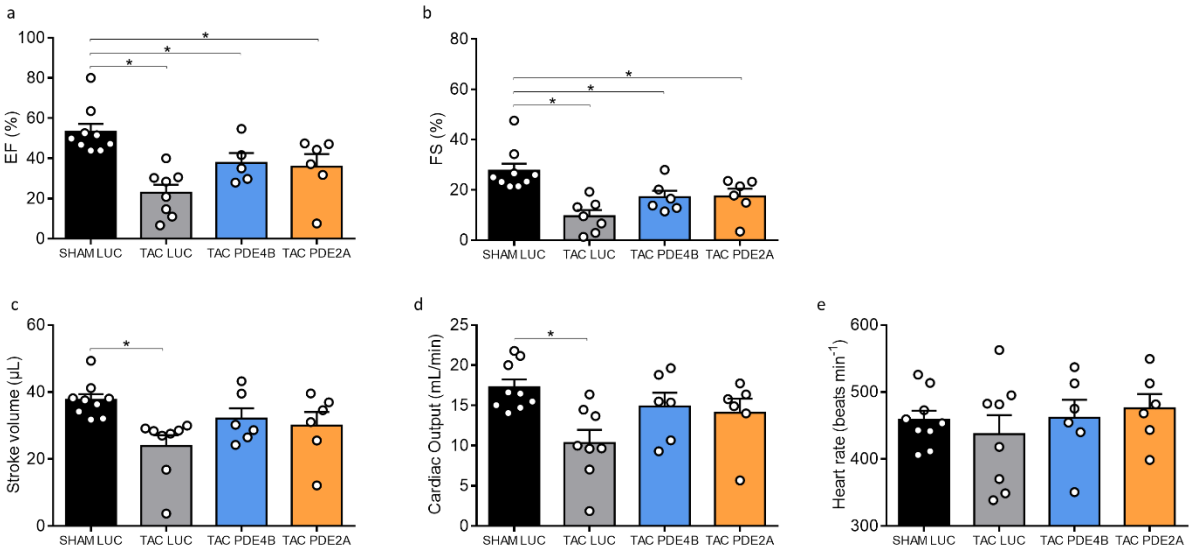

Figure 9. Physiological parameters of E1-JNC mice expressing the RyR2-targeted biosensor. (a) Ejection fraction (EF, %). (b) Fraction shortening (FS, %). (c) Stroke volume (µL). (d) Cardiac output (mL/min). (e) Heart rate (beats per minute). Means ± SE. *$p < 0.05$ by one-way ANOVA.

3.1.5 Echocardiographic parameters of pmEpac1 TAC LUC, TAC PDE4B and TAC PDE2A mice compared to SHAM LUC littermates

Similar to the previous data (**Tables 2, 3**), the pmEpac1 mice showed clear evidence of hypertrophy and loss of contractility in TAC LUC and TAC PDE2A hearts (**Table 4**), while the mice overexpressing PDE4B (TAC PDE4B) were partially protected.

Table 4. Echocardiographic parameters of Sham LUC, TAC LUC, TAC PDE4B and TAC PDE2A mice (C57BL6/N) expressing the pmEpac1 biosensor (*Perera et al., 2015*). IVDd: intraventricular septum thickness in diastole, LVIDd: left ventricular internal diameter in diastole, LVPWd: left ventricular posterior wall thickness in diastole, LV mass/BW: ratio of left ventricular mass to body weight, EF: ejection fraction, FS: fractional shortening, HR: heart rate. Means ± SE. **p* < 0.05 by one-way ANOVA.

Parameters	pmEpac1 mice			
	Sham LUC	TAC LUC	TAC PDE4B	TAC PDE2A
Pressure Gradient (mmHg)	2,5 ± 0,1	59,5 ± 7*	54 ± 11*	55,6 ± 0,5*
IVDd (mm)	0,781 ± 0,0,5	1,066 ± 0,06*	0,862 ± 0,03*	0,959 ± 0,07
LVIDd (mm)	4,180 ± 0,07	4,578 ± 0,32	3,895 ± 0,12	4,016 ± 0,33
LVPWd (mm)	0,606 ± 0,03	0,894 ± 0,05*	0,700 ± 0,07	0,821 ± 0,03*
LV mass corrected (mm)	84,8 ± 7,9	158,3 ± 22,9*	88,1 ± 9,8	110 ± 13,4
LV mass/BW (mg/g)	4,3 ± 0,3	8,5 ± 1,4*	4,4 ± 0,2	5,9 ± 0,9
EF (%)	46,3 ± 2,3	25,3 ± 3,6*	47,1 ± 3,7*	40 ± 14,5
FS (%)	23 ± 1,7	11 ± 1,7*	23,3 ± 2,2*	21,2 ± 9
Stroke volume (µL)	39,7 ± 3,5	24,8 ± 1,7*	32,2 ± 3,9	27,2 ± 3,6*
Cardiac Output (mL/min)	19,3 ± 2	10,9 ± 0,6*	15,8 ± 1,6*	13 ± 1,5*
HR (bpm)	484,7 ± 21,6	445,3 ± 24,4	503,2 ± 4,1	483,7 ± 14,5
N	6	5	3	4

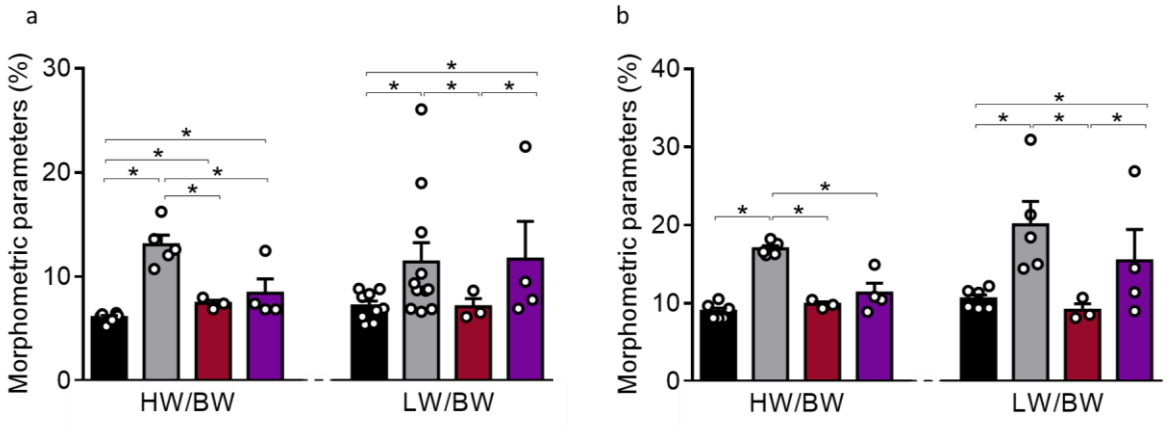

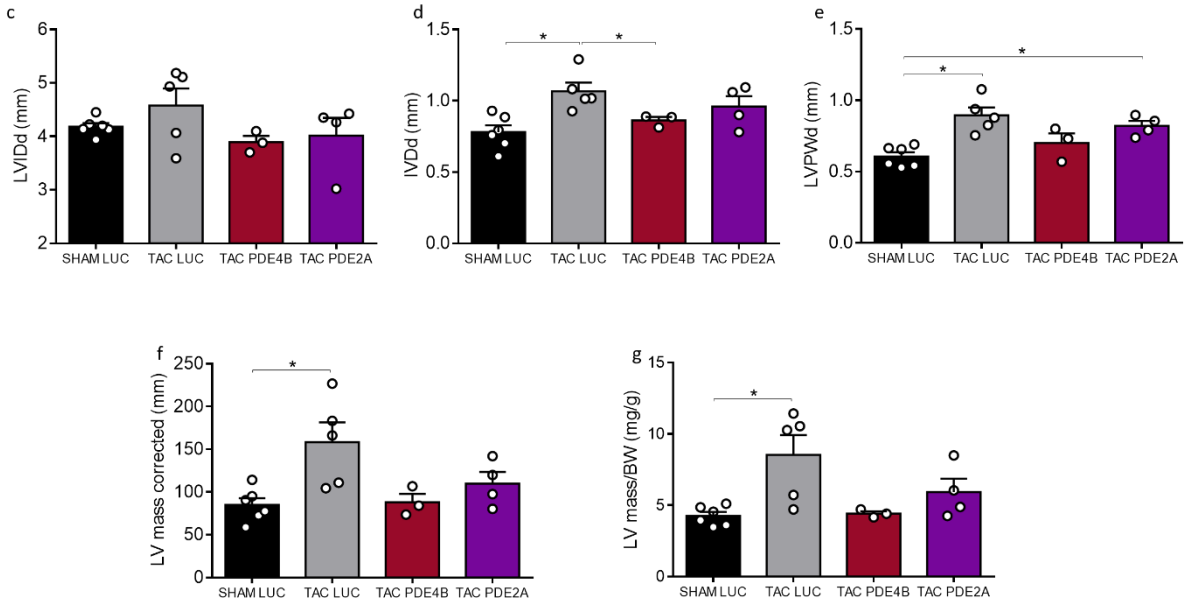

Figure 10. Morphometric parameters of pmEpac1 mice expressing the caveolin-rich membrane-targeted biosensor. (a) Heart weight (HW) and lung weight (LW) expressed as ratio to body weight (BW). (b) Heart weight (HW) and lung weight (LW) expressed as ratio to tibia length (TL). (c,d,e) Cardiac dimensions such as intraventricular septum thickness in diastole (IVDd), left ventricular internal diameter in diastole (LVIDd) and left ventricular posterior wall thickness in diastole (LVPWd) expressed in mm. (f) LV mass expressed in mm. (g) Ratio of left ventricular mass to body weight (LV mass/BW) expressed in mg/g. Means ± SE. *$p < 0.05$ by one-way ANOVA.

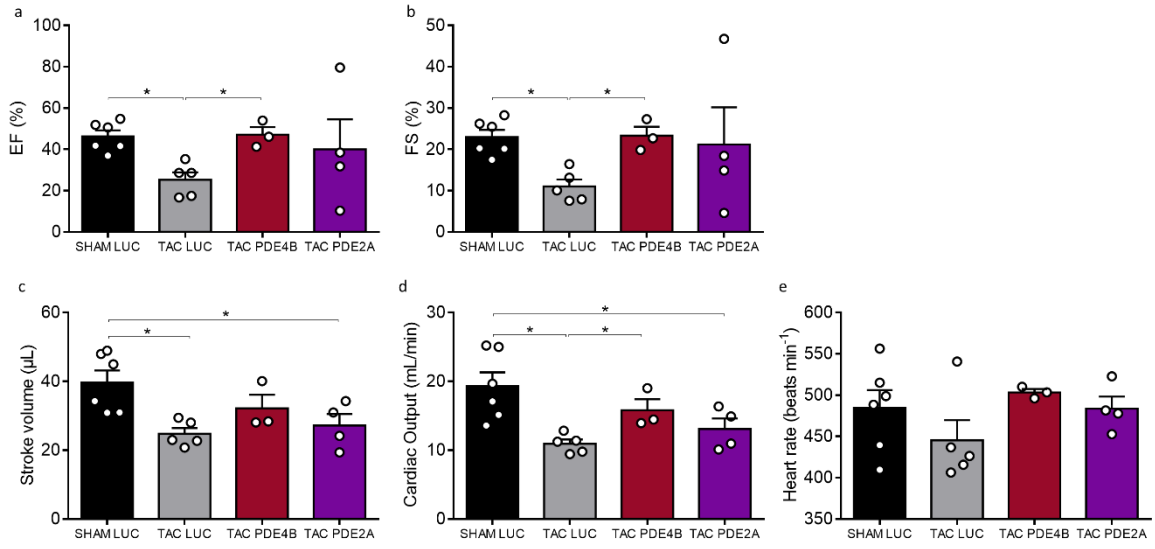

Figure 11. Physiological parameters of pmEpac1 mice expressing the caveolin-rich membrane-targeted biosensor. (a) Ejection fraction (EF, %). (b) Fraction shortening (FS, %). (c) Stroke volume (µL). (d) Cardiac output (mL/min). (e) Heart rate (beats per minute). Means ± SE. *$p < 0.05$ by one-way ANOVA.

3.2 Live imaging of cAMP in the RyR2 microdomain

The heart function is predominantly under the control of the β-adrenergic receptor (β-AR) system upon catecholamine stimulation (*Lohse et al., 2003*), which mediates excitatory effects of the sympathetic nervous system ($\beta_1 >> \beta_2$) by increasing cAMP production (*Bers 2008; Zagotta et al., 2003*) via G_s-protein recruitment and subsequent adenylyl cyclase activation (*Xiang and Kobilka, 2003*). To determine and distinguish the β-AR-mediated contribution to cAMP responses in the RyR2 microdomain, live cell imaging with the targeted E1 JNC biosensor was performed in freshly isolated Sham LUC, TAC LUC, TAC PDE4B and TAC PDE2A ventricular cardiomyocytes.

For selective β-AR subtype stimulation, the non-selective β-AR agonist isoproterenol (ISO), was applied together with one of the two selective inhibitors: ICI118,551 (50 nmol/L) that selectively inhibits β_2-AR or CGP20712A (100 nmol/L) that selectively inhibits β_1-AR. The inhibitors were added into the FRET buffer and all stimulating solutions prior to live imaging. Responses to individual receptor stimulation (**Figure 12**) were calculated from FRET ratio traces as a % of maximal response induced by IBMX (100 μmol/L) plus forskolin (10 μmol/L), which increase cAMP production by non-selective inhibition of PDEs and direct activation of adenylyl cyclases, respectively.

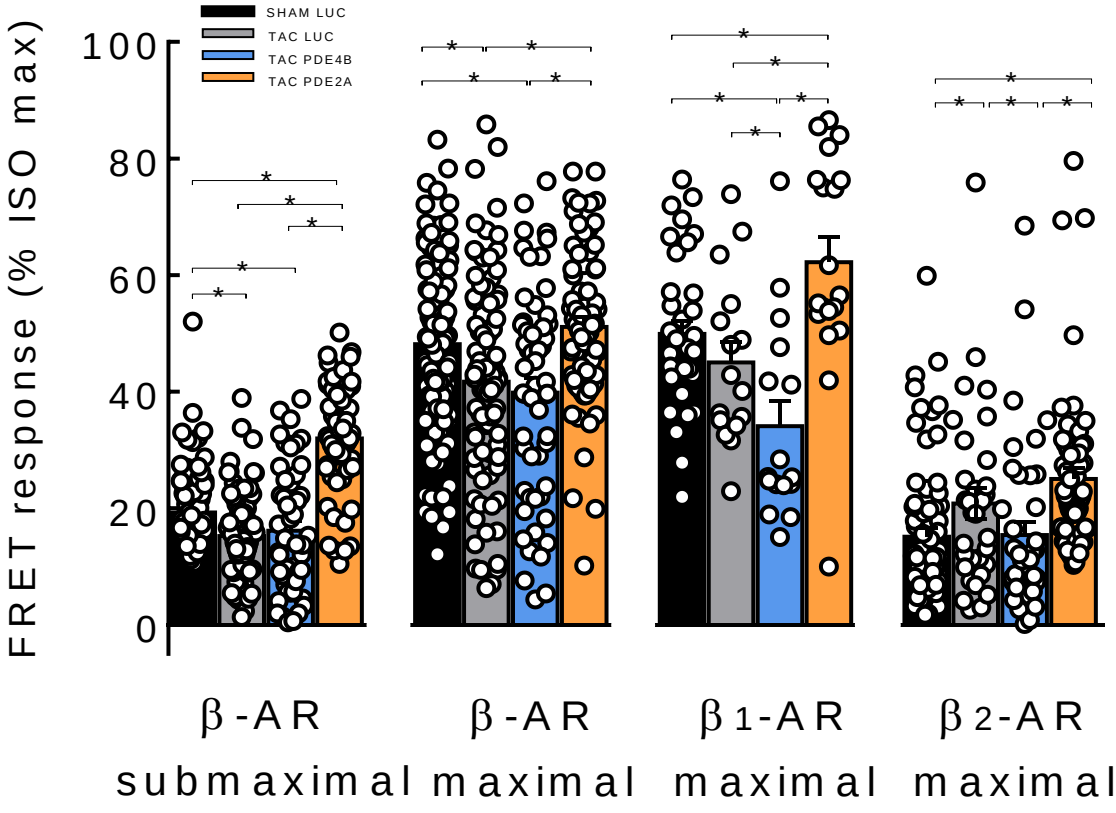

Figure 12. Amplitudes of cAMP response in the RyR2 microdomain upon stimulation of β-ARs (with submaximal 3nmol/L or maximal 100 nmol/L concentration of ISO), β_1-AR with 100 nmol/L ISO in the presence of the selective β_2-AR blocker ICI118551 (50 nmol/L) and β_2-AR with 100 nmol/L ISO in the presence of the selective β_1-AR blocker CGP20712A (100 nmol/L). Responses to individual receptor stimulation were calculated from FRET ratio traces

as a % of maximal response induced by IBMX (100 µmol/L) plus forskolin (10 µmol/L). Means ± SE. *$p < 0.05$ by mixed ANOVA followed by Wald's chi-squared test.

3.2.1 β_1-adrenergic receptor-mediated cAMP responses

The β_1-AR maximal stimulation induced fast increasing cAMP production, which was clearly detectable in the RyR2 microdomain. In healthy cardiomyocytes, the cAMP response reached up to 50%, as expected by receptor saturation with 100 nmol/L ISO. The β_1-AR effect, though, appeared attenuated in the diseased cardiomyocytes (45% ± 5.3%), suggesting receptor desensitization due to cardiac disease progression (*Lohse et al., 2003; Nikolaev et al., 2010; Perera at el., 2015*). In gene therapy with PDE4B3, the cAMP responses were even more decreased (34% ± 3.2%), indicating the successful overexpression of the main cAMP hydrolyzing enzyme in mouse myocardium, PDE4B3 (*Conti et al., 2003*). In contrast to the previous findings, PDE2A3 overexpression led to an impressively increased β_1-mediated cAMP response (62% ± 6.1%) which can indicate the receptor "resensitization" (**Figure 13**).

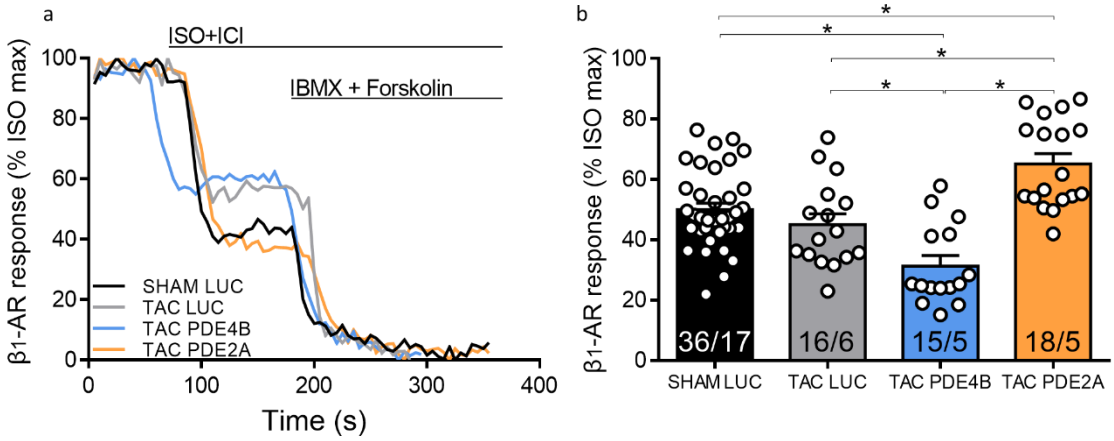

Figure 13. cAMP responses after maximal β_1-adrenergic (β_1-AR) receptor stimulation in Sham LUC, TAC LUC, TAC PDE4B and TAC PDE2A ventricular cardiomyocytes. (a) Representative FRET ratio traces recorded from cells in response to β_1-AR stimulation with 100 nmol/L ISO in the presence of 50 nmol/L ICI118551 (ISO+ICI), followed by the subsequently applied non-selective phosphodiesterase inhibitor IBMX (100 µmol/L) plus the direct adenylyl cyclase activator forskolin (10 µmol/L) to obtain the maximal possible FRET response. (b) Quantification of β_1-AR responses in Sham LUC, TAC LUC, TAC PDE4B and TAC PDE2A cardiomyocytes after maximal stimulation with 100 nmol/L ISO. Means ± SE. *$p < 0.05$ by mixed ANOVA followed by Wald's chi-squared test.

3.2.2 PDE-mediated hydrolysis of cAMP after β-AR submaximal stimulation

By degrading cAMP and generating subcellular compartments, PDEs define how the signaling cascades exert their physiological functions within the cell. In pathological conditions such as heart failure (HF), though, cyclic nucleotide pathways undergo profound alterations affecting significantly PDE expression and localization to distinct microdomains (*Abi-Gerges et al., 2009; Berisha et al., 2019; Pavlaki et al., 2021; Perera et al., 2015; Sprenger et al., 2015*).

To determine the extent that pathological alterations in hypertrophy can have in PDE expression and localization in the RyR2 microdomain, freshly isolated Sham LUC, TAC LUC, TAC PDE4B and TAC PDE2A ventricular cardiomyocytes expressing the E1-JNC biosensor were employed for live cell imaging upon β-AR submaximal stimulation and selective PDE inhibition of the main hydrolyzing enzymes of the myocardium, PDE2, PDE3 and PDE4 (*Bender and Beavo, 2006; Mika et al., 2012*).

According to the FRET protocol for submaximal β-AR experiments, the cells were initially stimulated with 3 nmol/mL ISO for cAMP production. Then, for further cAMP increase, selective inhibitors at determined concentrations were applied for PDE2 (BAY60-7550 100 nmol/L), PDE3 (cilostamide 10 µmol/L) and PDE4 (rolipram 10 µmol/L) inhibition. PDE inhibitor responses were calculated as the % maximal PDE inhibition with the subsequently applied non-selective inhibitor IBMX (100µmol/L). Forskolin (10 µmol/L) was applied at the end of each experiment to obtain the maximal possible FRET response.

The submaximal β-AR stimulation revealed that the main hydrolysing enzyme in the RyR2 microdomain is PDE3, followed by PDE4 and PDE2. This pattern was roughly maintained eight weeks after TAC, with PDE4 presenting slightly increased activity in disease and gene therapy with PDE4B. By PDE2A overexpression, the hydrolysing pattern upon submaximal β-AR stimulation clearly indicated PDE4 as the main cAMP-degrading enzyme followed by PDE2 and PDE3 (**Figure 14**).

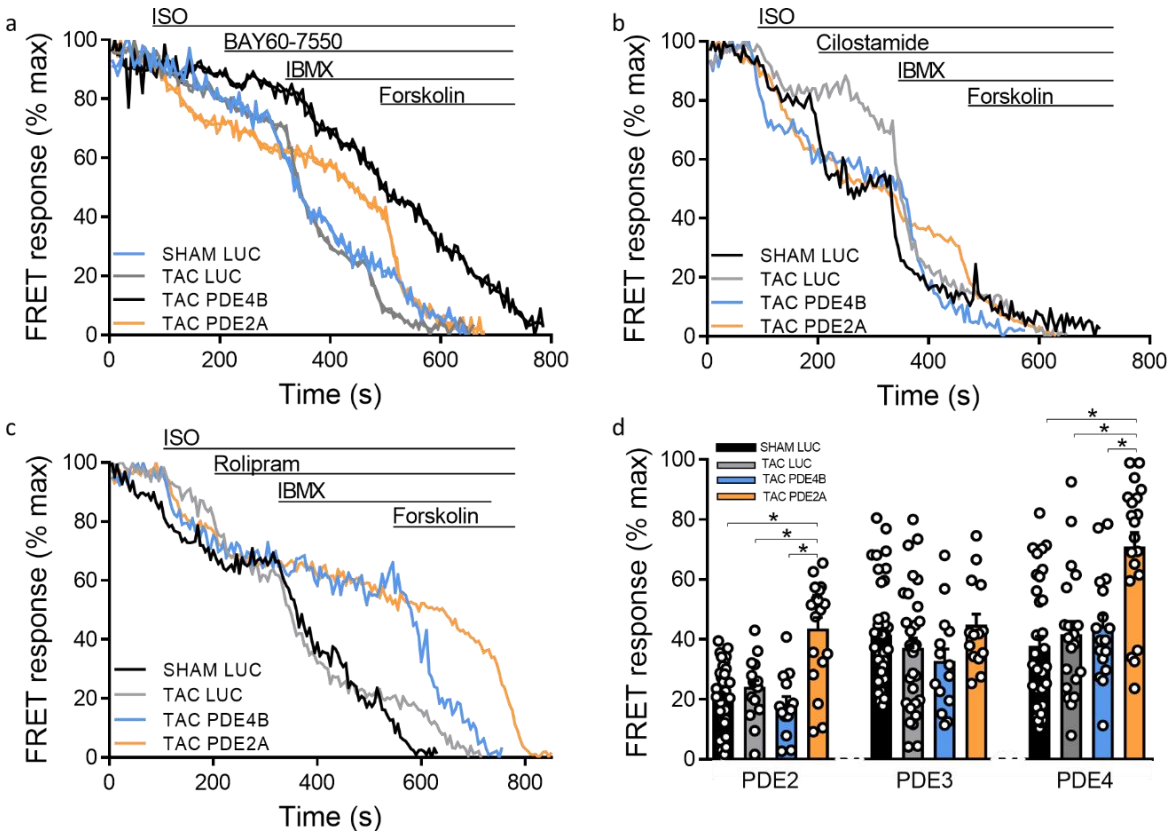

Figure 14. cAMP responses to selective PDE2, PDE3 and PDE4 inhibition after submaximal β-adrenergic (β-AR) receptor stimulation in Sham LUC, TAC LUC, TAC PDE4B and TAC

PDE2A ventricular cardiomyocytes. Representative FRET ratio traces recorded from cells in response to submaximal β-AR stimulation with 3 nmol/L ISO, followed by (a) 100 nmol/L of the PDE2 inhibitor BAY60-7550, (b) 10 μmol/L of the PDE3 inhibitor cilostamide, and (c) 10μmol/L of the PDE4 inhibitor rolipram. PDE inhibitor responses were calculated as the % maximal PDE inhibition with the subsequently applied non-selective PDE inhibitor IBMX (100 μmol/L). Forskolin (10 μmol/L) was applied at the end of each experiment to obtain the maximal possible FRET response. (d) Quantification of PDE inhibitor responses in Sham LUC, TAC LUC, TAC PDE4B and TAC PDE2A cardiomyocytes after submaximal stimulation with 3 nmol/L ISO. Means ± SE. *$p < 0.05$ by mixed ANOVA followed by Wald's chi-squared test.

3.2.3 PDE-mediated hydrolysis of cAMP after β-AR maximal stimulation

According to the FRET protocol for maximal β-AR experiments, freshly isolated Sham LUC, TAC LUC, TAC PDE4B and TAC PDE2A ventricular cardiomyocytes expressing the E1-JNC biosensor were employed for live cell imaging upon β-AR maximal stimulation and selective PDE inhibition of PDE2, PDE3 and PDE4.

Similarly, the cells were fist stimulated with 100 nmol/L ISO (receptor saturation) for maximal cAMP production. Then, the selective inhibitors at the same concentrations were applied for PDE2 (BAY60-7550 100 nmol/L), PDE3 (cilostamide 10 μmol/L) and PDE4 (rolipram 10 μmol/L) inhibition. The specific inhibitor responses were calculated as the % maximal PDE inhibition with the subsequently applied non-selective inhibitor IBMX (100μmol/L), and forskolin (10 μmol/L) was applied at the end of each experiment to obtain the maximal possible FRET response.

In contrast to the PDE pattern generated by submaximal stimulation, PDE4 was the main enzyme to exert its hydrolytic activity and degrade cAMP in the RyR2 microdomain of healthy cardiomyocytes. The high concentration of ISO (100 nmol/L) induced 55%-60% cAMP production *per se*, while PDE4 specific inhibition with rolipram further increased cAMP levels (~80%), almost to sensor saturation. And this phenomenon was further enhanced by PDE4B overexpression. Moreover, PDE3 did not hydrolyze as much cAMP as PDE4 after β-AR maximal stimulation, while the role of PDE2 in cAMP hydrolysis was minor in this microdomain. The diseased phenotype, however, significantly reduced the PDE3 and PDE4 activity, while boosted the one of PDE2 (**Figure 15**). The gene therapy with either PDE2 or PDE4 restored the respective FRET responses back to normal.

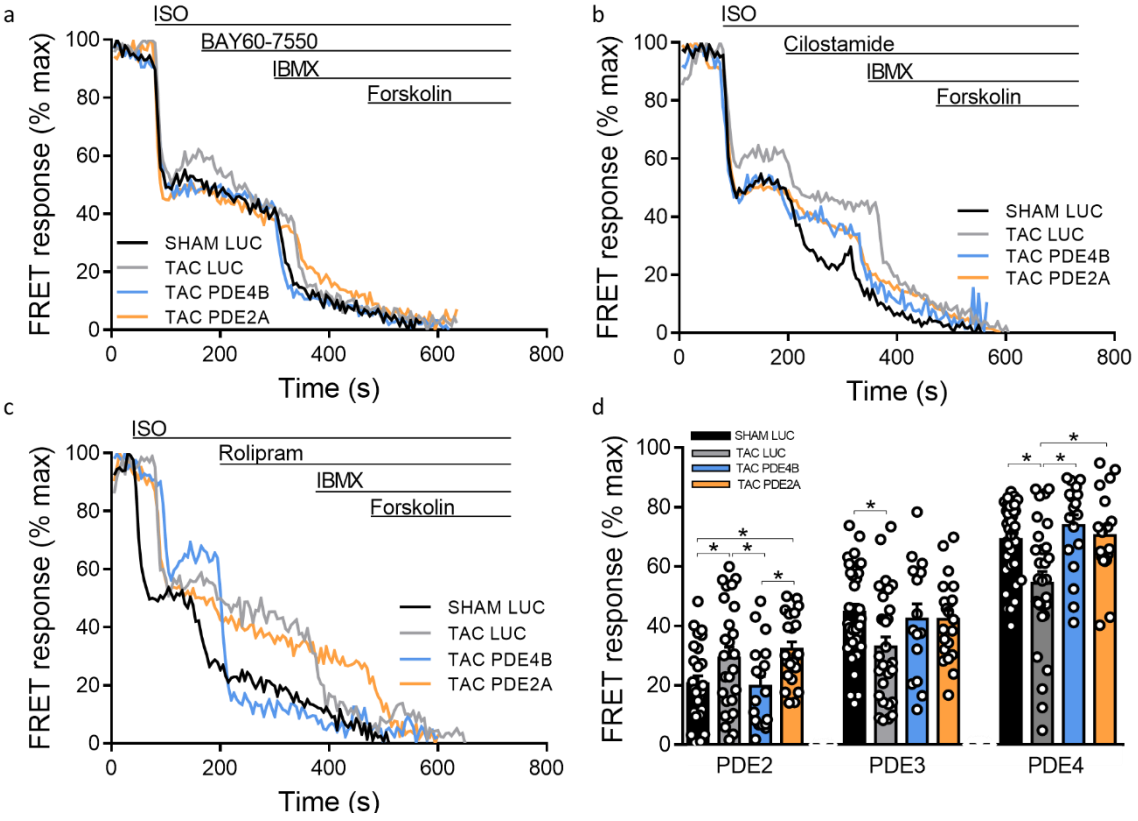

Figure 15. cAMP responses to selective PDE2, PDE3 and PDE4 inhibition after maximal β-adrenergic (β-AR) receptor stimulation in Sham LUC, TAC LUC, TAC PDE4B and TAC PDE2A ventricular cardiomyocytes. Representative FRET ratio traces recorded from cells in response to maximal β-AR stimulation with 100 nmol/L ISO, followed by (a) 100 nmol/L of the PDE2 inhibitor BAY60-7550, (b) 10 µmol/L of the PDE3 inhibitor cilostamide, and (c) 10µmol/L of the PDE4 inhibitor rolipram. PDE inhibitor responses were calculated as the % maximal PDE inhibition with the subsequently applied non-selective PDE inhibitor IBMX (100 µmol/L). Forskolin (10 µmol/L) was applied at the end of each experiment to obtain the maximal possible FRET response. (d) Quantification of PDE inhibitor responses in Sham LUC, TAC LUC, TAC PDE4B and TAC PDE2A cardiomyocytes after maximal stimulation with 100 nmol/L ISO. Means ± SE. *$p < 0.05$ by mixed ANOVA followed by Wald's chi-squared test.

3.2.4 PDE-mediated hydrolysis of cAMP after β_2-AR maximal stimulation

Another important parameter of the study was the PDE pattern generated by β_2-AR maximal stimulation. Again, the FRET protocol required freshly isolated Sham LUC, TAC LUC, TAC PDE4B and TAC PDE2A ventricular cardiomyocytes expressing the E1-JNC biosensor. But prior to live cell imaging, all solutions were prepared in FRET buffer containing 100 nmol/L CGP20712A.

The triggered cAMP signals were diminished under physiological conditions, but significantly increased in diseased cardiomyocytes, suggesting altered receptor expression or local PDE dependent regulation (**Figure 16**). Similar to the submaximal β-AR stimulation, the cAMP was mainly regulated by PDE3, followed by PDE4 and PDE2. Only the PDE2 overexpression seemed to counterbalance the predominant

PDE3 activity by increasing the PDE2-mediated cAMP degradation significantly (**Figure 16d**).

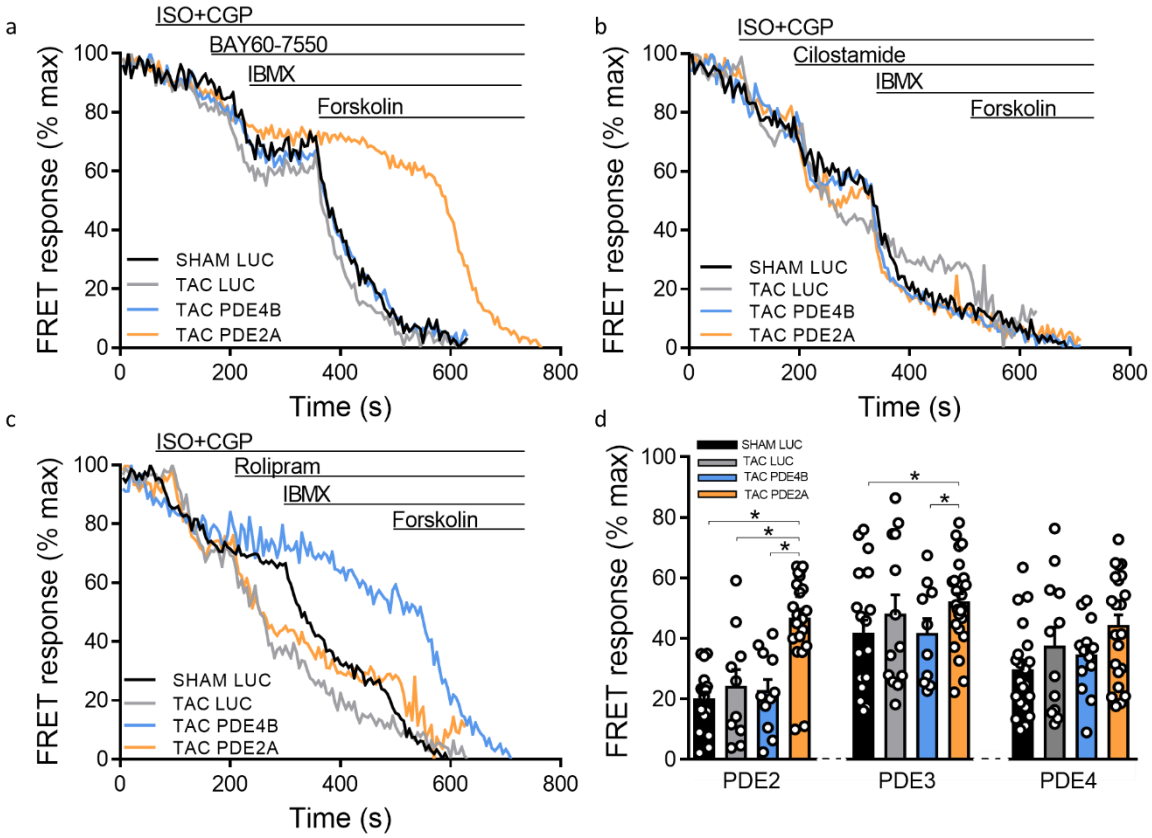

Figure 16. cAMP responses to selective PDE2, PDE3 and PDE4 inhibition after maximal β_2-adrenergic (β_2-AR) receptor stimulation in Sham LUC, TAC LUC, TAC PDE4B and TAC PDE2A ventricular cardiomyocytes. Representative FRET ratio traces recorded from cells in response to maximal β_2-AR stimulation with 100 nmol/L ISO in the presence of 100 nmol/L CGP20712A (ISO+CGP), followed by (a) 100 nmol/L of the PDE2 inhibitor BAY60-7550, (b) 10 µmol/L of the PDE3 inhibitor cilostamide, and (c) 10µmol/L of the PDE4 inhibitor rolipram. PDE inhibitor responses were calculated as the % maximal PDE inhibition with the subsequently applied non-selective PDE inhibitor IBMX (100 µmol/L). Forskolin (10 µmol/L) was applied at the end of each experiment to obtain the maximal possible FRET response. (d) Quantification of PDE inhibitor responses in Sham LUC, TAC LUC, TAC PDE4B and TAC PDE2A cardiomyocytes after maximal stimulation with 100 nmol/L ISO. Means ± SE. Number of cells/hearts are stated at the bottom of each bar. *$p < 0.05$ by mixed ANOVA followed by Wald's chi-squared test.

3.3 Live imaging of cAMP in the plasma membrane (caveolin-rich) microdomain

In the course of this work, it was also important to investigate the pressure-overload-mediated alterations occurring at the caveolin-rich membrane microdomain upon β-AR stimulation (**Figure 17**) and assess the effect of the PDE overexpression.

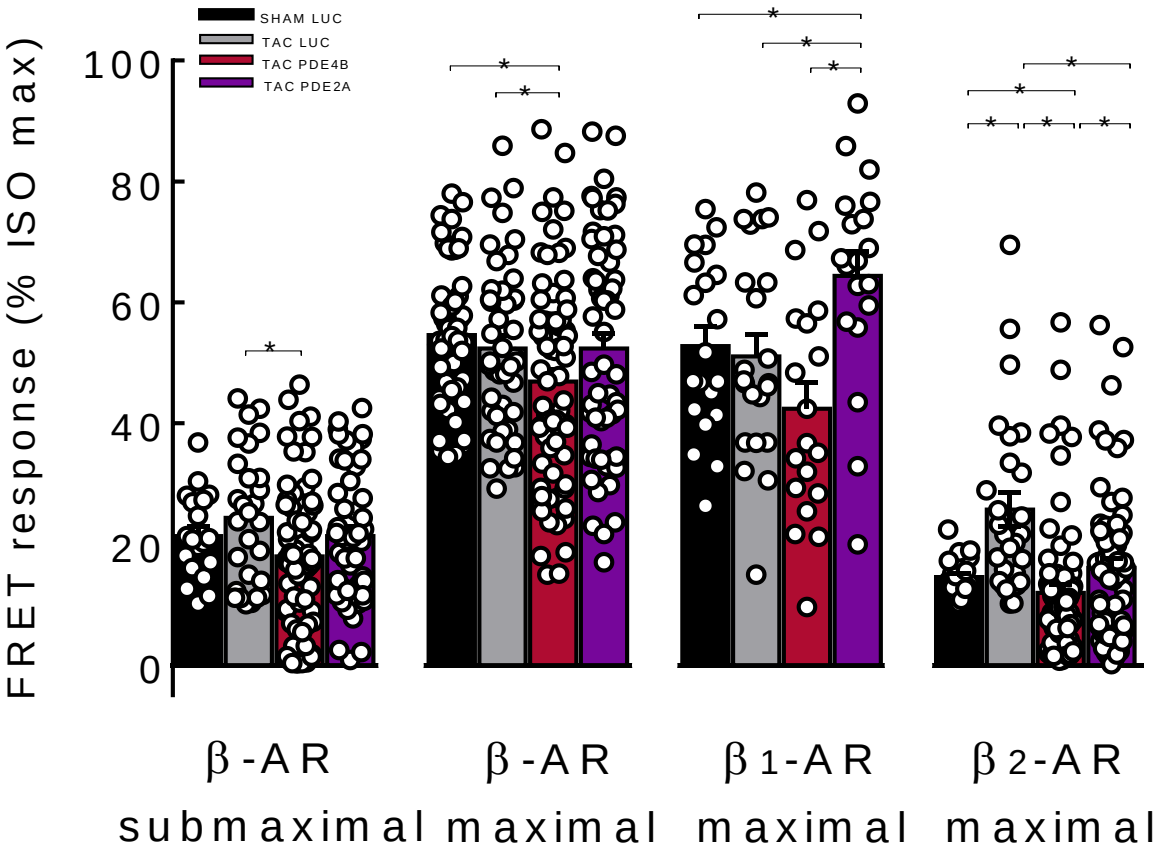

Figure 17. Amplitudes of cAMP response in the sarcolemma (caveolin-rich) microdomain upon stimulation of β-ARs (with submaximal 3nmol/L or maximal 100 nmol/L concentration of ISO), β_1-AR with 100 nmol/L ISO in the presence of the selective β_2-AR blocker ICI118551 (50 nmol/L) and β_2-AR with 100 nmol/L ISO in the presence of the selective β_1-AR blocker CGP20712A (100 nmol/L). Responses to individual receptor stimulation were calculated from FRET ratio traces as a % of maximal response induced by IBMX (100 μmol/L) pus forskolin (10 μmol/L). Means ± SE. *$p < 0.05$ by mixed ANOVA followed by Wald's chi-squared test.

3.3.1 β_1-adrenergic receptor-mediated cAMP responses

The β_1-AR maximal stimulation resulted in strong increase in cAMP production, which was clearly detectable in the caveolin-rich membrane compartment. In healthy cardiomyocytes, the cAMP response reached up to 55%, an effect that appeared marginally attenuated in diseased cardiomyocytes (50% ± 3.2%) and slightly decreased in gene therapy with PDE4B3 (44% ± 4.7%), confirming the successful overexpression of the main hydrolyzing enzyme PDE4B3. In contrast to the other group, the PDE2A3 overexpression led again to an impressively increased β_1-mediated cAMP response (63.2% ± 3.1%) (**Figure 18**).

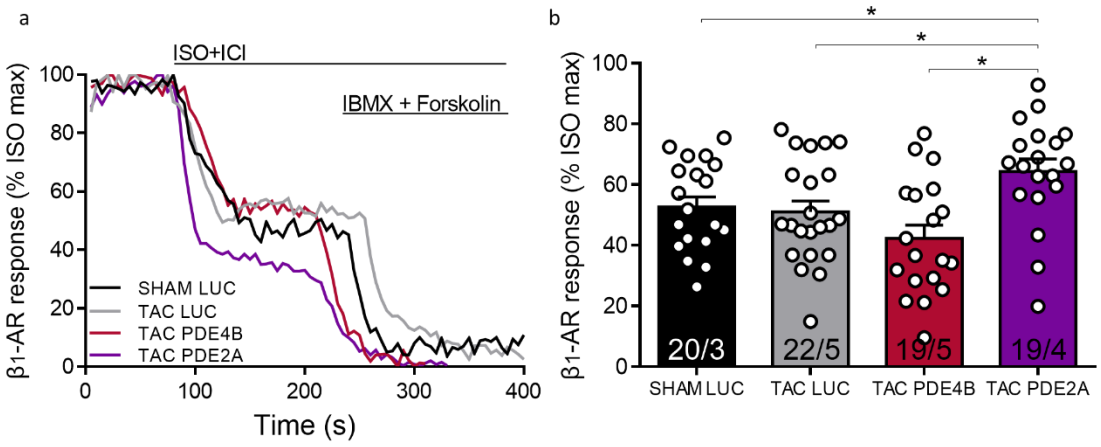

Figure 18. cAMP responses after maximal β_1-adrenergic (β_1-AR) receptor stimulation in Sham LUC, TAC LUC, TAC PDE4B and TAC PDE2A ventricular cardiomyocytes. (a) Representative FRET ratio traces recorded from cells in response to β_1-AR stimulation with 100 nmol/L ISO in the presence of 50 nmol/L ICI118551 (ISO+ICI), followed by the subsequently applied non-selective phosphodiesterase inhibitor IBMX (100 µmol/L) plus the direct adenylyl cyclase activator forskolin (10 µmol/L) to obtain the maximal possible FRET response. (b) Quantification of β_1-AR responses in Sham LUC, TAC LUC, TAC PDE4B and TAC PDE2A cardiomyocytes after maximal stimulation with 100 nmol/L ISO. Means ± SE. *$p < 0.05$ by mixed ANOVA followed by Wald's chi-squared test.

3.3.2 PDE-mediated hydrolysis of cAMP after β-AR submaximal stimulation

To explore the hydrolyzing pattern of the PDEs after β-adrenergic submaximal stimulation, freshly isolated cardiomyocytes were stimulated with 3 nmol/L isoproterenol (ISO), followed by selective PDE inhibitors and the subsequent non-selective inhibitor IBMX. To reach the absolute maximal cAMP response, forskolin was added as the final treatment.

The submaximal β-AR stimulation revealed that the main hydrolysing enzyme in the caveolin-rich membrane microdomain is PDE4, followed by PDE2 and PDE3. This pattern was consistently maintained eight weeks after TAC (**Figure 19**), with exception to the significant decrease of PDE4 during disease. Importantly, PDE4 overexpression

could restore this decline after TAC, whereas PDE2 overexpression did not show this effect.

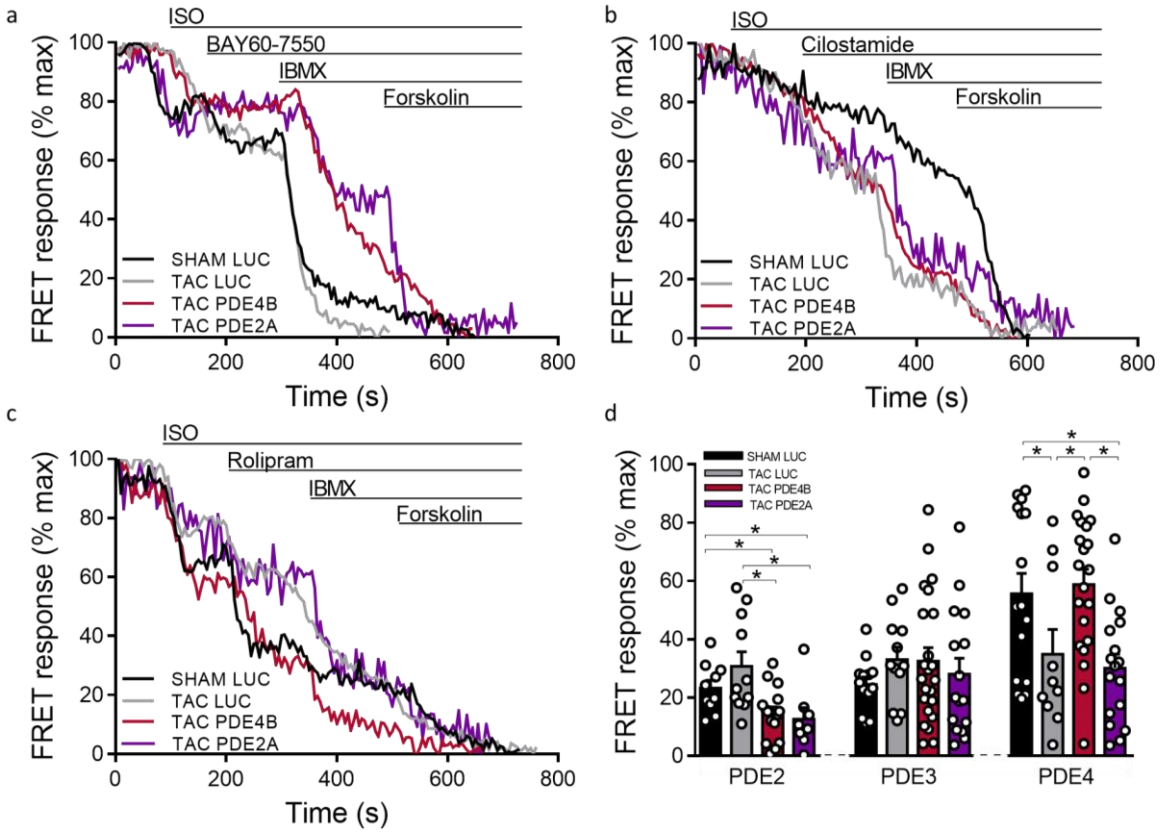

Figure 19. cAMP responses to selective PDE2, PDE3 and PDE4 inhibition after submaximal β-adrenergic (β-AR) receptor stimulation in Sham LUC, TAC LUC, TAC PDE4B and TAC PDE2A ventricular cardiomyocytes. Representative FRET ratio traces recorded from cells in response to submaximal β-AR stimulation with 3 nmol/L ISO, followed by (a) 100 nmol/L of the PDE2 inhibitor BAY60-7550, (b) 10 μmol/L of the PDE3 inhibitor cilostamide, and (c) 10μmol/L of the PDE4 inhibitor rolipram. PDE inhibitor responses were calculated as the % maximal PDE inhibition with the subsequently applied non-selective PDE inhibitor IBMX (100 μmol/L). Forskolin (10 μmol/L) was applied at the end of each experiment to obtain the maximal possible FRET response. (d) Quantification of PDE inhibitor responses in Sham LUC, TAC LUC, TAC PDE4B and TAC PDE2A cardiomyocytes after submaximal stimulation with 3 nmol/L ISO. Means ± SE. *$p < 0.05$ by mixed ANOVA followed by Wald's chi-squared test.

3.3.3 PDE-mediated hydrolysis of cAMP after β-AR maximal stimulation

Similar to the PDE pattern generated by submaximal stimulation, PDE4 was the main enzyme to exert its hydrolytic activity and degrade cAMP in the caveolin-rich membrane microdomain of healthy cardiomyocytes. The high concentration of ISO (100 nmol/L) induced ~60% cAMP production *per se*, while PDE4 specific inhibition with rolipram further increased cAMP levels (~80%), almost to sensor saturation. And this phenomenon was again enhanced by PDE4B overexpression. Moreover, PDE3 did not hydrolyze as much cAMP as PDE4 after β-AR maximal stimulation, while the role of PDE2 in cAMP hydrolysis was minor in this microdomain, and even less after gene therapy (**Figure 20d**). The diseased phenotype, however, reduced the PDE3 and PDE4 activity, while enhanced the one of PDE2 (**Figure 20**). In this microdomain, the gene

therapy with PDE2A and PDE4B seemed to affect more the activities of PDE2 and PDE4.

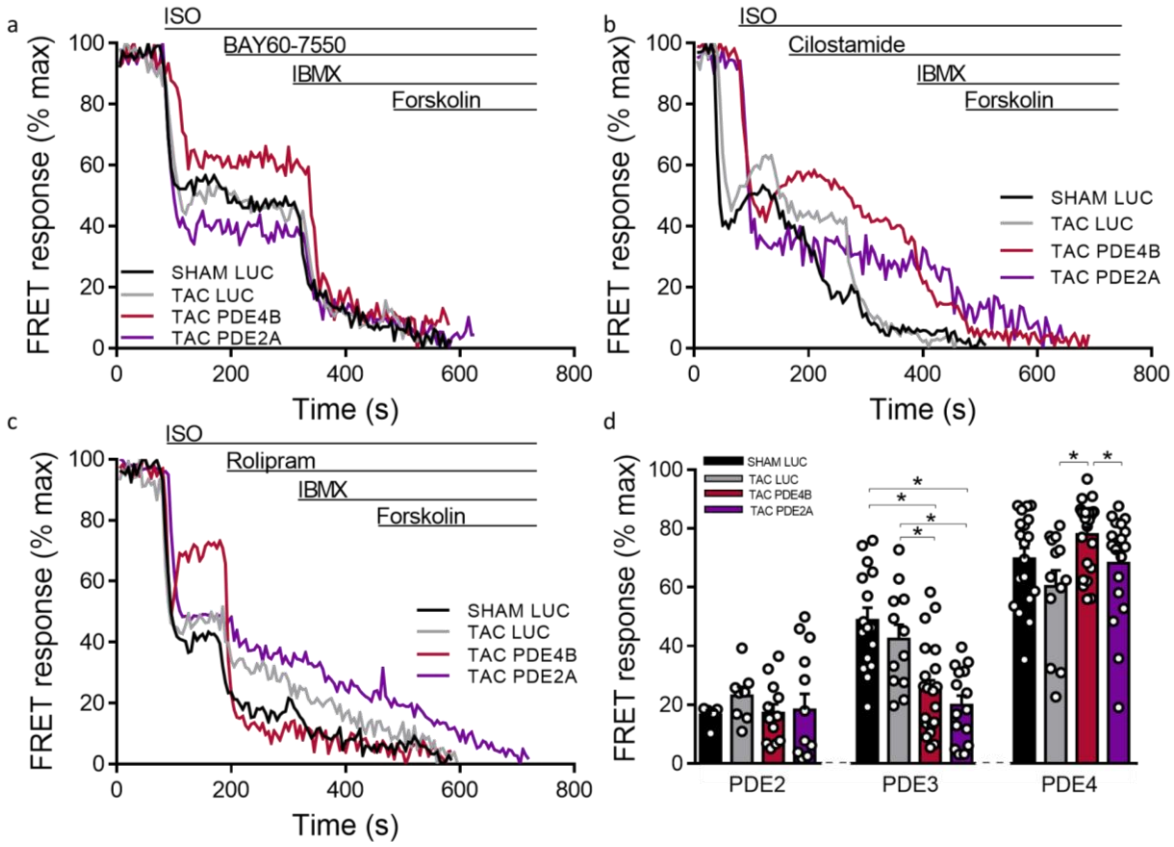

Figure 20. cAMP responses to selective PDE2, PDE3 and PDE4 inhibition after maximal β-adrenergic (β-AR) receptor stimulation in Sham LUC, TAC LUC, TAC PDE4B and TAC PDE2A ventricular cardiomyocytes. Representative FRET ratio traces recorded from cells in response to maximal β-AR stimulation with 100 nmol/L ISO, followed by (a) 100 nmol/L of the PDE2 inhibitor BAY60-7550, (b) 10 μmol/L of the PDE3 inhibitor cilostamide, and (c) 10μmol/L of the PDE4 inhibitor rolipram. PDE inhibitor responses were calculated as the % maximal PDE inhibition with the subsequently applied non-selective PDE inhibitor IBMX (100 μmol/L). Forskolin (10 μmol/L) was applied at the end of each experiment to obtain the maximal possible FRET response. (d) Quantification of PDE inhibitor responses in Sham LUC, TAC LUC, TAC PDE4B and TAC PDE2A cardiomyocytes after maximal stimulation with 100 nmol/L ISO. Means ± SE. *$p < 0.05$ by mixed ANOVA followed by Wald's chi-squared test.

3.3.4 PDE-mediated hydrolysis of cAMP after β_2-AR maximal stimulation

Finally, the pattern generated by β_2-AR maximal stimulation triggered cAMP signals that were low under physiological conditions, but significantly increased in diseased

cardiomyocytes. Similar to the PDE pattern of the RyR2 microdomain, the cAMP was mainly regulated by PDE3, followed by PDE4 and PDE2 (**Figure 21**).

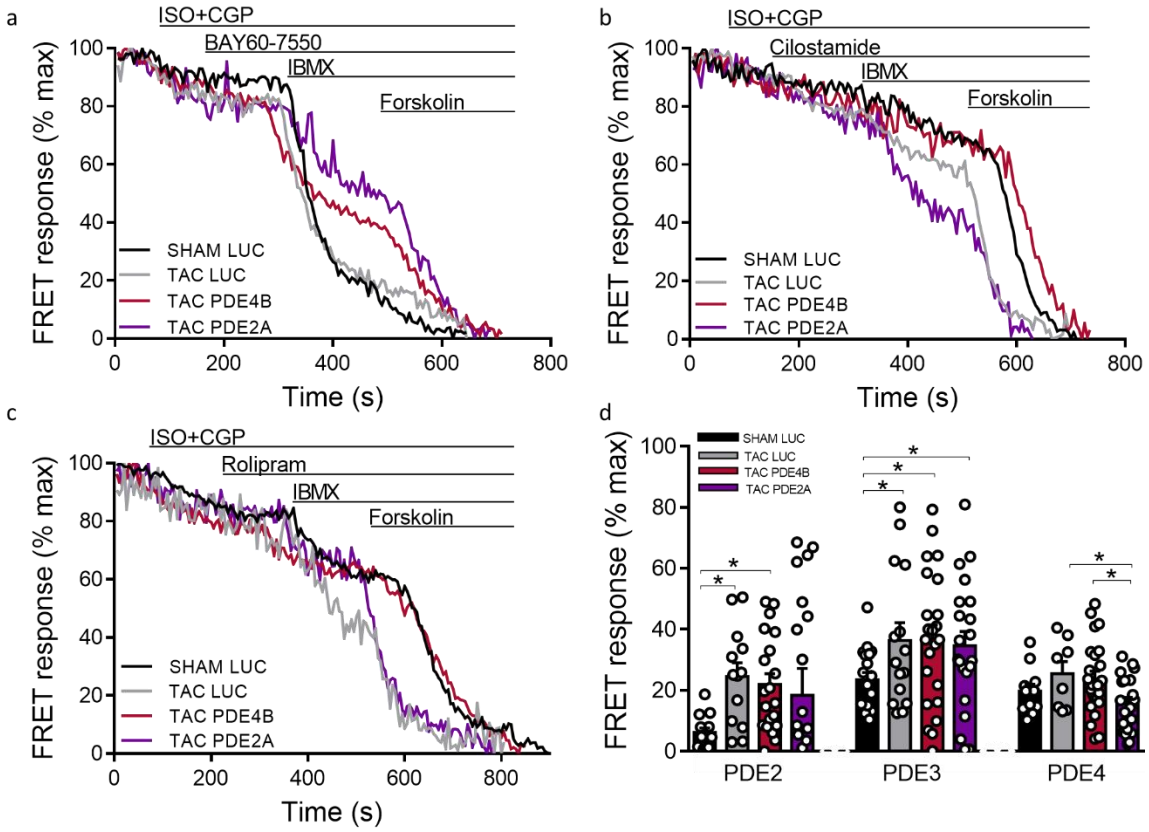

Figure 21. cAMP responses to selective PDE2, PDE3 and PDE4 inhibition after maximal β_2-adrenergic (β_2-AR) receptor stimulation in Sham LUC, TAC LUC, TAC PDE4B and TAC PDE2A ventricular cardiomyocytes. Representative FRET ratio traces recorded from cells in response to maximal β_2-AR stimulation with 100 nmol/L ISO in the presence of 100 nmol/L CGP20712A (ISO+CGP), followed by (a) 100 nmol/L of the PDE2 inhibitor BAY60-7550, (b) 10 µmol/L of the PDE3 inhibitor cilostamide, and (c) 10µmol/L of the PDE4 inhibitor rolipram. PDE inhibitor responses were calculated as the % maximal PDE inhibition with the subsequently applied non-selective PDE inhibitor IBMX (100 µmol/L). Forskolin (10 µmol/L) was applied at the end of each experiment to obtain the maximal possible FRET response. (d) Quantification of PDE inhibitor responses in Sham LUC, TAC LUC, TAC PDE4B and TAC PDE2A cardiomyocytes after maximal stimulation with 100 nmol/L ISO. Means ± SE. *p < 0.05 by mixed ANOVA followed by Wald's chi-squared test.

3.4 Single-cell contractility measurements

In addition to the model characterization and live cell imaging in the specific subcellular compartments after β-stimulation, the extent to which gene therapy was able to preserve contractility in diseased groups and prevent arrhythmia induction due to maladaptive alterations in heart was assessed by the optical sarcomere length measurement method (IonOptix).

Freshly isolated ventricular cardiomyocytes were paced at 1Hz and stimulated with 100 nmol/L ISO. As presented in **Figure 22**, the healthy and TAC PDE2A cardiomyocytes were well protected against arrhythmias, even after maximal β-AR stimulation. Similarly, the TAC PDE4B group occasionally presented a couple of arrhythmias with the incidence being low enough compatible with cardioprotection seen by echocardiographic and histological analysis. On the other hand, the diseased cardiomyocytes showed abnormal contractile function and led to significant arrhythmia incidence compared to other conditions (**Figures 22, 23**).

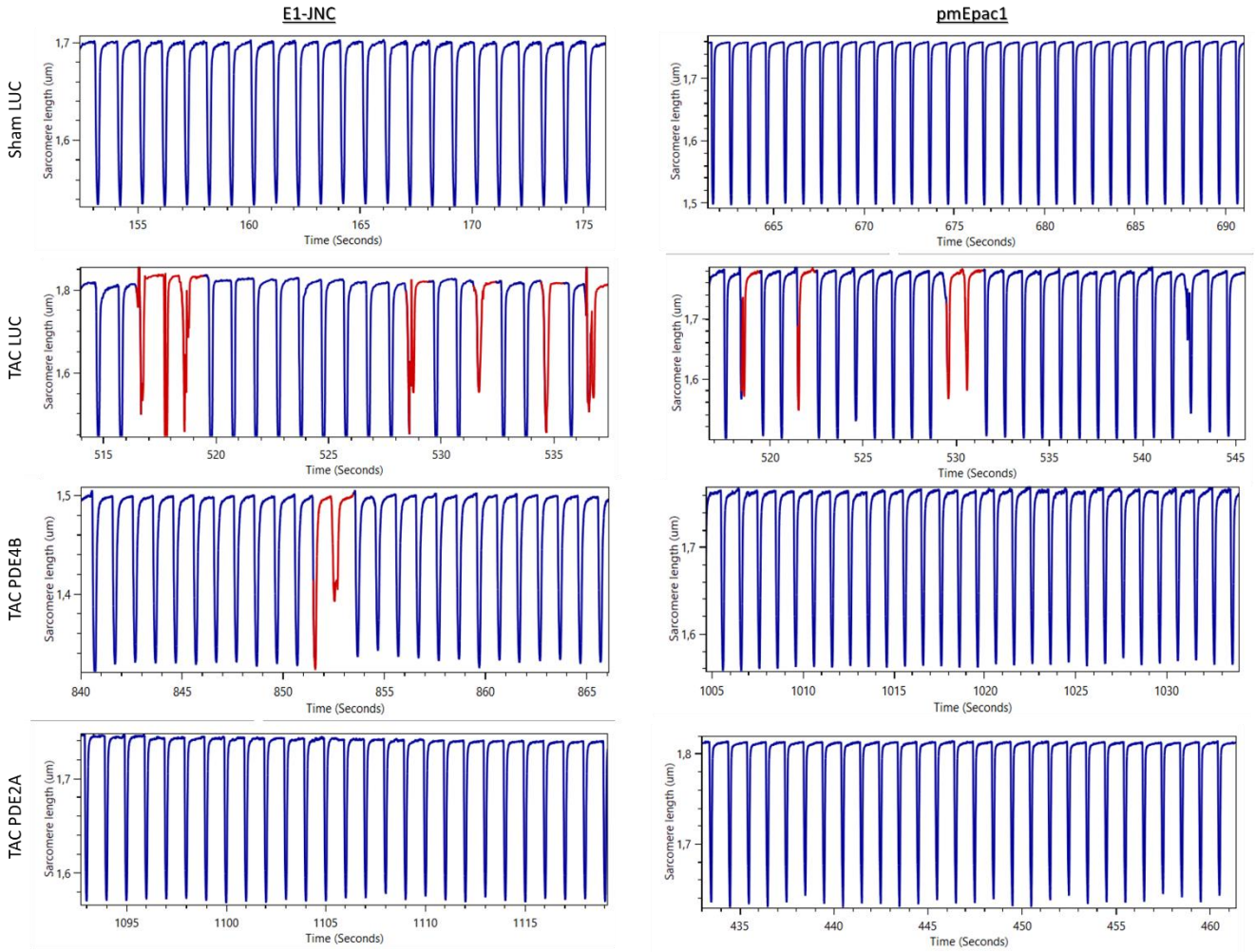

Figure 22. Sarcomere length measurements. Ventricular cardiomyocytes freshly isolated by Sham LUC, TAC LUC, TAC PDE4B and TAC PDE2A hearts were paced at 1Hz and stimulated with 100 nmol/L ISO for arrhythmia detection. n/N= 30-50 cells isolated from at least 3-4 hearts per treatment. * $p < 0.05$.

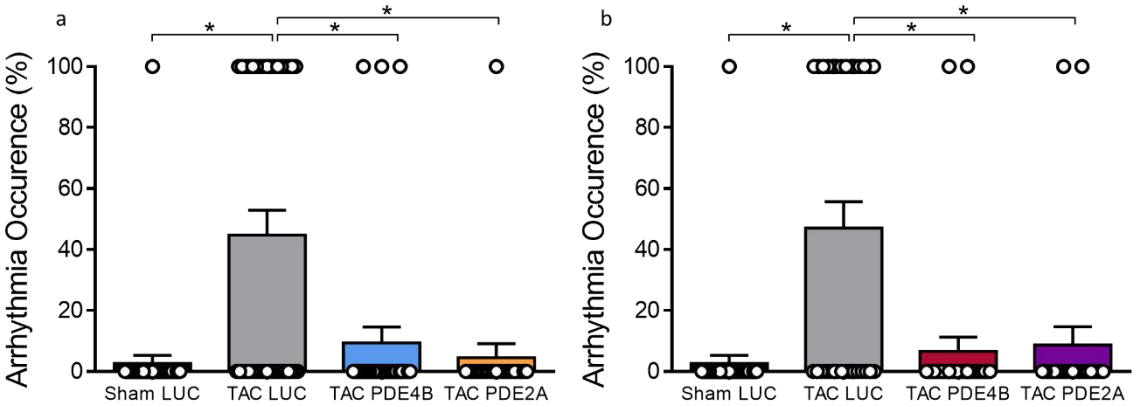

Figure 23. Arrhythmia occurrence of ventricular cardiomyocytes upon maximal β-AR stimulation. (a) E1-JNC cardiomyocytes isolated by Sham LUC, TAC LUC, TAC PDE4B and TAC PDE2A hearts. (b) pmEpac1 cardiomyocytes isolated by Sham LUC, TAC LUC, TAC PDE4B and TAC PDE2A hearts. n/N= 30-50 cells isolated from at least 3-4 hearts per treatment. * $p < 0.05$.

4. Discussion

Historically, PDE inhibitors such as milrinone have been developed to increase cardiac contractility. However, while efficacious for short-term relief in end-stage heart failure patients, they increase cardiac arrhythmias and mortality when used in long-term treatment schemes.

In this work, we tested an opposite hypothesis, i.e., whether overexpression of PDEs can reduce excessive amounts of local cAMP in different cardiomyocyte microdomains and counteract heart failure progression. By cardiomyocyte overexpression of PDE2A and PDE4B in a mouse model of pressure-overload heart failure induced by Transverse Aortic Constriction (TAC), we aimed to restore the altered CN-PDEs interplay in subcellular microdomains and ameliorate HF. For successful transduction and satisfactory cardiac tropism, AAV9 particles (10^{12}) (*Zacchigna et al. 2014*) were injected in the tail vein of transgenic mice expressing FRET-based cAMP biosensors for membrane- and sarcoplasmic reticulum-associated microdomains 3 days after TAC surgery (therapy study). Animals were randomized into four groups, two receiving a control vector AAV9-LUC and other two groups injected with PDE2A and PDE4B AAV9s, respectively. In order to assess the efficacy of the gene transfer approach *in vivo*, echocardiography was performed after TAC at specific time intervals (4 weeks and 8 weeks). Thereafter, the animals were sacrificed for tissue collection and isolation. Biochemical and histological analysis was performed to elucidate the PDE expression and function. Freshly isolated ventricular myocytes were used for live cell imaging by Förster Resonance Energy Transfer (FRET imaging) to evaluate the impact of gene therapy on cAMP dynamics in membrane and sarcoplasmic reticulum associated microdomains. Eight weeks after TAC, mice expressing FRET-based cAMP biosensors were sacrificed for ventricular cardiomyocyte isolation with subsequent cAMP FRET measurements. The effects of PDE2, PDE3 and PDE4 inhibition with BAY-607550, cilostamide and rolipram respectively, upon β-adrenergic prestimulation, were measured under all experimental conditions. Our FRET studies mechanistically dissected the effect of gene therapy on cAMP compartmentation in functionally relevant and disease-altered subcellular microdomains. In addition to FRET studies, single-cell contractility measurements were performed to link microdomain-specific changes upon PDE overexpression to cardiac function.

This strategy provided deep insights into PDE-dependent regulation of cardiomyocyte function and assessed the efficacy of AAV-mediated overexpression of different PDE families on heart failure progression.

4.1 Overexpression of PDE2A3 and PDE4B3 in a TAC mouse model

Since ventricular cardiomyocytes constitute an exemplary type of cells characterized by highly compartmentalized cyclic nucleotide signaling, and hypertrophy-induced changes in local cAMP signaling represent a molecular hallmark of cardiac disease, the current study was designed to assess whether AAV9-mediated overexpression of

PDE2A3 and PDE4B3 could prevent maladaptive alterations in the heart and restore cAMP dynamics and compartmentation under pressure overload-induced hypertrophy.

Transverse aortic constriction (TAC) was employed to experimentally reproduce heart failure with reduced ejection fraction (HFrEF) in transgenic mice (*Houser et al., 2012*). Despite the moderate values (~60mmHg) in pressure gradient, the TG mice developed the phenotype of pressure-overload-induced cardiac hypertrophy that yields in hypertrophied hearts, increased wall thickness (**Table 2**), extended fibrosis, and typical reduction in contractile function. And, as long as the biosensor expression did not seem to induce any functional or structural anomalies, the C57BL/6N background of the transgenic mice accounted for the rapid progression of HF within eight weeks after TAC, a hypothesis further validated by the equally strong phenotype developed in their wild type littermates.

The echocardiographic analysis revealed that the overexpression of PDE4B in female mice partially protected against hypertrophy and ameliorated the contractile loss (**Tables 2, 3 and 4**), a finding that is consistent with a gene therapy approach in a small animal model for HF (*Karam et al., 2020*). Although the TAC PDE4B3 hearts were heavier than the control ones, the LVPWd values remained relatively similar to those in healthy mice and so did the ejection fraction and fractional shortening ones. This is slightly different from the reported data in male C57BL/6J mice where the same gene therapy approach with PDE4B3 ameliorated cardiac hypertrophy but did not restore contractile function eight weeks after TAC. Female C57BL/6N mice studied here show even better protection from HF by PDE4B3. The PDE2A3 overexpression, however, neither prevented increases in heart weight and wall thickness nor did it improve physiological parameters showing more similarities with failing hearts.

Hence, the histological evaluation of the TAC gene therapy models revealed either protection or not against hypertrophy (**Figure 4a, 4c**), fibrosis – hallmark of pathological remodeling (*Zhao et al., 2016*) (**Figure 4a, 4b**) and change in cell size (**Figure 4c, 4d**). Again, only PDE4B3 overexpression exerted its cardioprotective action against hypertrophy (**Figure 4c, 4d**) and collagen deposition (**Figure 4a, 4b**) and proved that the up-regulation of this PDE can make a difference against different HF models (*Karam et al., 2020*). Always consistent with its *in vivo* evaluation, the TAC PDE2A3 group presented similar findings as those observed in the diseased phenotype with increased diameter in ventricular cardiomyocytes and extended fibrosis in the heart cross-sections.

These results were finally corroborated by the immunoblot analysis which showed multi-fold increase of the targeted PDEs at protein level (**Figure 7a, 7c**) - indicative of the successful PDE overexpression in the respective groups, and reduced PDE3 (*Abis-Gerges et al., 2009; Mika et al., 2019; Molina et al., 2014*), PDE4B (*Abis-Gerges et al., 2009; Karam et al., 2020; Mika et al., 2019; Molina et al., 2014*) and PDE4D (*Lohse et al., 2005*) protein expression in failing heart tissues. The gene therapy restored the protein levels in TAC hearts and compensated the enzyme loss detected in disease.

4.2 Live cell imaging of β-AR/cAMP signals in caveolin rich membrane and RyR2 microdomains

As already stated, the heart function is predominantly under the control of the β-adrenergic receptor (β-AR) system upon catecholamine stimulation (*Lohse et al., 2003*), which mediates its excitatory effects ($\beta_1 >> \beta_2$) by increasing cAMP production (*Bers 2008; Zagotta et al., 2003*) via G_s-protein recruitment and subsequent adenylyl cyclase activation (*Xiang and Kobilka, 2003*). Both β_1- and β_2-adrenergic receptors participate in cAMP formation, with β_1-AR subtype being broadly distributed on the membrane and triggering considerably augmented cAMP responses in the cell, while β_2-AR being locally confined in the T-tubules and generating small to moderate compartmentalized signals (*Nikolaev et al., 2006; Nikolaev et al., 2010*). Therefore, it was important to determine and distinguish the β-AR-mediated contribution to cAMP responses in both RyR2 and caveolin-rich membrane microdomains.

4.2.1 Submaximal β-AR/cAMP signals in caveolin-rich membrane and RyR2 microdomains

Upon submaximal β-AR stimulation, the responses remained generally lower than those generated by maximal β_1-AR and β-AR stimulation (**Figures 12, 17**), but were definitely stronger than β_2-AR ones. In caveolin-rich membrane microdomain (**Figure 17**) particularly, the TAC PDE4B group initiated significantly smaller cAMP responses compared to the diseased and TAC PDE2A cardiomyocytes, due to the overexpression of the main hydrolyzing enzyme, PDE4B3 (*Conti et al., 2003*). Although the applied ISO concentration was low (3 nmol/mL), it was sufficient to unmask the effect of the enzyme overexpression via immediate cAMP degradation. In the RyR2 microdomain (**Figure 12)**, the differences observed among the groups were far more pronounced after submaximal stimulation of the β-ARs due to the capacity of the biosensor to target cAMP generated exclusively around the cation channels and the potential contribution of functional β_1-ARs localized in the sarcoplasmic reticulum (*Wang et al., 2021*).

4.2.2 Maximal β_1-AR/cAMP and β-AR/cAMP signals in caveolin-rich membrane and RyR2 microdomains

Two interesting findings were revealed regarding β_1-AR- and β-AR maximal-mediated signaling in the caveolin-rich membrane and RyR2 microdomains; the remarkable reduction in cAMP levels of the TAC PDE4B group, which signals the successful overexpression of the enzyme and verifies that PDE4B3 is the main PDE involved in cAMP degradation in mouse heart (*Conti et al., 2003*); and the impressively increased cAMP responses of the TAC PDE2A group (at least in comparison to Sham LUC group), which also signals the successful overexpression of PDE2A3 and highlights its important role in the sarcolemma (*Castro et al., 2006; Guellich et al., 2014; Leroy et al., 2008; Mongillo et al., 2006; Vettel et al., 2017)* and subsequently to preserved β_1-AR signaling (*Nikolaev et al., 2010*), especially after early (*Berisha et al., 2019; Perera et al., 2015*) cardiac remodeling.

Indeed, careful observation of the β-AR maximal stimulation revealed steadily high cAMP responses (>50%) with exception the TAC PDE4B cardiomyocytes, which hydrolyzed more cAMP compared to responses initiated in the other groups due to

constitutively higher enzyme levels of PDE4 and the consequently negative, PKA-mediated feedback (*MacKenzie et al., 2002*). Similar patterns were monitored in both caveolin-rich membrane and the RyR2 microdomains, where the maximal β-AR signalling strongly enhanced cAMP production by saturating the receptors.

4.2.3 β_2-AR/cAMP signals in caveolin-rich membrane and RyR2 microdomain

Despite the strong cAMP signals upon selective β_1-AR stimulation and non-selective maximal β-AR stimulation using pmEpac1 (**Figures 17, 18, 19**) and E1-JNC (**Figures 12, 13, 15**) biosensors respectively, the β_2-AR signaling yielded very small responses (**Figures 12, 17**).

In spite of detectable cAMP signals in rat cardiomyocytes (*Nikolaev et al., 2010*), relatively small β_2-AR responses were detected in the caveolin-rich membrane microdomains of healthy Sham LUC cardiomyocytes and in TAC PDE2A and TAC PDE4B groups (**Figure 17**). On the other hand, significantly amplified signals were generated in the diseased cardiomyocytes, as the presented β_2-AR/cAMP pattern corresponds well with what was previously found for this microdomain (*Perera et al., 2015; Rudokas et al., 2021*), and shows that β_2-ARs compensated the loss of β_1-AR-mediated cAMP signals due to cardiac remodelling, although the receptor density was rather maintained in disease.

These small β_2-AR-induced responses were also monitored at the RyR2 (**Figure 12**) microdomain, and might be associated with either low expression of the receptor (*Myagmar et al., 2017*) or tight PDE-mediated regulation of cAMP, mostly by PDE4 (*Lohse et al., 2005*), that hinders its diffusion across/within the dyadic cleft (*Berisha et al., 2019*). Equally small β_2-AR/cAMP responses were monitored in the TAC PDE4B group due to PDE4 abundance, but the signal pattern changed significantly in the diseased and TAC PDE2A cardiomyocytes. The responses in the RyR2 microdomain for the latter two groups were significantly amplified and resulted in increased cAMP levels, because of the dramatic downregulation of PDE4 activity there (*Lohse et al., 2005*) that could not be counterbalanced by the increased activity of the redistributed PDE2 and PDE3 enzymes (*Perera et al, 2015*). As for the particularly pronounced difference observed by overexpression of PDE2A3 in comparison to sarcolemmal, this could be attributed also to the specific nature of the E1-JNC biosensor to visualize cAMP in the RyR2s and the enzymatic redistribution occurring post-TAC (*Perera et al., 2015).*

4.3 Live imaging of PDE inhibitor induced cAMP signals in the RyR2 microdomain

Transgenic mice expressing the cAMP specific E1-JNC biosensor (*Berisha et al., 2019*) were backcrossed with C57BL/6N and, then, subjected to transverse aortic constriction and gene transfer with AAV9s for the generation of the TAC gene therapy models.

4.3.1 Live cell imaging of PDE-mediated cAMP hydrolysis

Live imaging was employed to shed more light on the disturbed balance among the crucial factors contributing to the microdomain formation, and assess whether cardiac targeted gene transfer could reverse the maladaptive changes in the diseased phenotype.

FRET analysis after submaximal β-AR stimulation shed light in cAMP compartmentation by demonstrating major PDE3 and less PDE4 contribution to total cAMP hydrolysis in the RyR2 microdomain. This finding was also consistent upon β_2-AR stimulation, which mimics the basal PDE pattern (*Börner et al., 2011*) and might indicate that the main hydrolyzing enzyme, PDE4, is not yet fully activated by PKA due to low cAMP levels. On the other hand, the PDE2- and PDE4-related signals appeared amplified in submaximally stimulated TAC PDE2A cardiomyocytes, while the PDE2- and PDE3-related signals presented similarly high increases upon β_2-AR selective stimulation.

Nevertheless, after being shown that cardiac remodeling by excessive cAMP production inevitably affects the subcellular organization, the experimental protocol was adapted to reproduce *in vitro* the saturation of β-ARs with high concentrations of isoproterenol, i.e., 100 nmol/L. Indeed, maximal β-AR stimulation rendered PDE4 as the major phosphohydrolase of cAMP, while PDE3 had a moderate contribution among all groups (*Berisha et al., 2019; Mika et al., 2013; Mongillo et al., 2004; Nikolaev et al. 2006*). An interesting finding was observed in the diseased (TAC LUC) cardiomyocytes, in which both PDE3 and PDE4 activities appeared downregulated after cardiac remodeling. Although the inhibition with 10 μmol/mL rolipram increased cAMP signals close to sensor saturation, particularly when PDE4B was overexpressed, failing cardiomyocytes could not initiate similar responses.

The above presented PDE pattern unveils, under certain conditions, that the well-established notion of cAMP being under the exclusive control of PDE4D3 hydrolytic activity in the RyR2 microdomain might not be quite true. The PDE4B overexpression obviously outweighed and exclusively controlled the cAMP hydrolysis around the channels, but it also seemed to substantially participate in cAMP compartmentation in the RyR2 microdomain when PDE4D3 was downregulated (*Lohse et al., 2005*), and a potential explanation is the physical proximity of RyR2 (controlled mainly by PDE4D3) with LTCCs, where PDE4B is the main regulator of signal compartmentation (*Kraft et al., 2019; Leroy et al., 2011*). Although not entirely elucidated, the PDE4B and PDE4D could intertwine between LTCCs and RyR2 channels for cAMP catabolism and compartmentation (*Kraft et al., 2019*).

The role of PDE2 in RyR2 microdomain appears rather restricted in healthy cardiomyocytes upon maximal β-AR stimulation, while its hypertrophy-induced amplified signals in TAC hearts (**Figures 8a, 14d, 15d, 16d**) may compensate the dramatic loss of PDE3 and PDE4 activity in disease (**Figures 15d, 20d)** (*Abi-Gerges et al., 2009; Karam et al. 2020; Mehel et al., 2013*) upon microdomain switch/redistribution (*Perera et al., 2015*), and counterbalance the unfavorable effects of dysfunctional β-AR signaling (*Vettel et al., 2017*). Its overexpression significantly increased the FRET signals after selective PDE2 and PDE4 inhibition upon

submaximal stimulation, and after selective PDE2 and PDE3 inhibition upon β_2-AR stimulation (*Perera et al., 2015*), respectively.

4.4 Live imaging of PDE inhibitor induced cAMP signals in the sarcolemma (caveolin-rich) microdomain

Transgenic mice expressing the cAMP specific pmEpac1 (*Perera et al., 2015*) were backcrossed with C57BL/6N and, then, subjected to transverse aortic constriction and gene transfer with AAV9s for the generation of the TAC gene therapy model.

4.4.1 Live cell imaging of PDE-mediated cAMP hydrolysis

FRET microscopy in the caveolin-rich plasma membrane revealed different PDE patterns upon β-AR submaximal and maximal stimulation compared to those in the RyR2 microdomain. The main hydrolyzing enzyme in sarcolemma was clearly PDE4, followed by PDE3 after saturating or PDE2 after subsaturating ISO concentrations (**Figures 19, 20 and 21**).

This finding, consistent with previous results (*Perera et al., 2015*), confirmed the functional involvement of PDE4 in this subcellular compartment and explained why PDE4B3 had been overexpressed to ameliorate maladaptive alterations during disease. Both PDE4B and PDE4D regulate cAMP signaling events in the caveolin-rich membrane microdomain (*Kraft, 2019; Leroy et al., 2011*), but the impact of PDE4B was known only in neonatal mouse cardiomyocytes (*Mika et al., 2014*). The fact that this finding could be verified in adult cardiomyocytes alone (*Kraft, 2019*) and be further corroborated upon PDE4B3 overexpression is highly remarkable, given that T-tubules are absent in neonatal cardiomyocytes (*Ibrahim et al., 2011*).

PDE4 is reportedly the predominant phosphohydrolase for cAMP catabolism in murine cardiomyocytes (*Leroy et al., 2008*), its activity dependents on PKA phosphorylation via feedback loop after cAMP degradation (*MacKenzie et al., 2002*), and its major isoforms mainly regulate the subcellular organization. The most important one is PDE4B that mediates the β-AR induced PKA-phosphorylation of the LTCC channels in the plasma membrane of adult murine cardiomyocytes (*Leroy et al., 2011*), while the other one, PDE4D, is linked to the RyR2 and SERCA2a complexes. Although not directly involved in cardiac contractility, heart rate or blood pressure (*Zhao et al., 2015*), PDE4 enzymes tightly regulate PKA phosphorylation and modify the localized signaling into tight compartments (*Fertig and Bailllie, 2018*).

Pharmacologically, PDE4 inhibition has beneficial effects on cardiomyocyte function (*Lehnart and Marks, 2006*); however, many unfavorable cardiac effects occurred from sustained inhibition of this enzyme, increasing the incidence of mortality (*Packer et al., 1991*). Moreover, in pathological cardiac hypertrophy induced by sympathetic overdrive, there was dramatic reduction in enzyme expression (~ 50% for PDE4B) (*Abi-Gerges et al., 2009; Karam et al. 2020*) and subsequently increased susceptibility to arrhythmias and heart failure (*Bobin et al., 2016; Lehnart et al., 2005; Leroy et al., 2011; Molina et al, 2012*). Cardiac-targeted overexpression of PDE4B3 (*Karam et al., 2020*) in diseased animal and human cell models presented for the first time

cardioprotective effects against sympathetic overdrive without depressing basal function.

Indeed, by reproducing the excessive cAMP production due to sympathetic overdrive *in vitro,* the saturating concentrations of isoproterenol, i.e., 100 nmol/L unmasked the contribution of PDE4 as the major phosphohydrolase of cAMP, while PDE3 was moderate among all groups (*Mika et al., 2013; Mongillo et al., 2004; Nikolaev et al. 2006*). The diseased TAC LUC cardiomyocytes demonstrated decreased PDE3-related and PDE4-related cAMP responses despite inhibition with 10 μmol/L cilostamide or rolipram, respectively, while PDE2 appeared upregulated (*Mehel et al., 2013*) (**Figure 20d**) in failing cardiomyocytes or after PDE2A3 overexpression.

The involvement of PDE2A in cAMP hydrolysis at the caveolin-rich membrane microdomain was minimal, but its overexpression seemed to restore the PDE pattern found in healthy cardiomyocytes and to prevent the PDE2/PDE3 redistribution detected in disease (*Perera et al., 2015*). The role of PDE2 in failing cardiomyocytes (TAC LUC) may be a compensatory mechanism against the dramatic loss of PDE3 and PDE4 activity in disease (**Figures 15d, 20d)** (*Abi-Gerges et al., 2009; Karam et al. 2020; Mehel et al., 2013*) or against the side effects of dysfunctional β-AR signaling (*Vettel et al., 2017*).

4.5 Sarcomere length measurements for arrhythmia detection

As already stated, the heart function is predominantly under the control of the β-adrenergic receptor (β-AR) system upon catecholamine stimulation (*Lohse et al., 2003*), which mediates its excitatory effects ($\beta_1 >> \beta_2$) by increasing cAMP production (*Bers 2008; Zagotta et al., 2003*) via G_s-protein recruitment and subsequent adenylyl cyclase activation (*Xiang and Kobilka, 2003*). The imbalance induced by sympathetic overdrive not only affects cAMP compartmentation, but disrupts the natural course of Ca^{2+} cycling in the myocardium, especially by sustained β_1-AR-mediated Ca^{2+}overload and hyperphosphorylated RyR2s (*Lohse et al., 2005*). Very recently, calcium spark analysis in an animal model for HF demonstrated that the generally cardioprotective β_2-AR signaling (*Communal et al., 1999; Zhu et al., 2001*) exclusively potentiates premature ventricular beats in failing hearts and *in vitro* arrhythmias around RyR2 channels, probably due to insufficient cAMP degradation (*Berisha et al., 2019*) by its downregulated PDE4 enzyme (*Lohse et al., 2005*).

To combine the data acquired from FRET measurements in TAC LUC, TAC PDE2A and TAC PDE4B cardiomyocytes with Ca^{2+} homeostasis, we performed single-cell sarcomere length measurements, in which TAC PDE2A and TAC PDE4B cardiomyocytes appeared completely resistant to arrhythmias (**Figures 22, 23**).

The failing cardiomyocytes presented an increased susceptibility to ventricular arrhythmias after β-AR stimulation with 100 nmol/L ISO, with almost one out of two diseased cells manifesting premature ventricular beats (**Figures 22, 23**). The excessive cAMP concentrations accounted for the increased incidence of arrhythmias observed in *vitro,* probably because of a series of interconnected phenomena. Following the main events occurring during EC-coupling (*Bers, 2002*), we could assume that the decreased

PDE4B levels (*Karam et al., 2020*) could no longer control the physiological phosphorylation of LTCCs (*Leroy et al., 2011*), the membrane potential got perturbed and further destabilized normal CICR, which led to uncoordinated opening of the RyR2s (leaky RyR2s) by the concurrent downregulation of PDE4D3 (*Lohse et al., 2005*), and, eventually, the resultant SR Ca^{2+} overload performed as a substrate for ventricular arrhythmia initiation upon β-AR stimulation with saturating ISO concentration.

The overexpression of PDE2A3 clearly abrogated arrhythmias after maximal β-AR stimulation, a finding which could be potentially explained by the important role of PDE2 in heartbeat initiation. According to this theory, PDE2 intertwines with cell membrane ion channels ("membrane clock) (*DiFrancesco, 2010*) and Ca^{2+} cycling ("Ca^{2+} clock") (*Lakatta et al., 2010*), and mediates the Ca^{2+} clock regulation in atrial myocytes (*Lakatta et al., 2010; Vettel et al., 2017*). It is likely that such type of a beneficial regulation of calcium channel function may occur also in ventricular myocytes to prevent arrhythmias. The abundance of protein detected in cardiomyocytes overexpressing PDE2A3 outweighed the maladaptive alterations induced by TAC and protected against arrhythmia initiation *in vitro*.

Similarly, PDE4B3 overexpression protected against ventricular arrhythmias, as the incidence after β-AR stimulation appeared really low (**Figures 22, 23**). This finding could be probably attributed to the PKA-mediated phosphorylation and activation of the long PDE4 isoforms, PDE4B3 being one of them (*Ghigo et al., 2012; Leroy et al., 2008; Mika et al., 2014*), which degrade the pathologically high cAMP levels that might lead to leaky RyR2 (*Karam et al., 2020*). As outlined above, this PDE isoform seems to be able to tightly regulate local cAMP signaling at the RyR2, making it a good candidate for protection against diastolic calcium leak and ventricular arrhythmias. Again, the protein abundance detected in cardiomyocytes overexpressing PDE4B3 was capable of buffering the side effects of excessive sympathetic drive induced by TAC by restoring the activity of the main PDE across the dyadic cleft.

4.6 Potential limitations

A general limitation PDE2A3 and PDE4B3 overexpression in transgenic mice is the isoform spill over within subcellular compartments, where the protein of interest may not be physiologically localized. Furthermore, the overexpressed PDE2A3 and PDE4B3 isoforms were chosen based on their hydrolytic activity in mouse heart (*Conti et al., 2003; Vettel et al., 2017*) and their results may not fully correspond to those required for human cardiac disease, i.e., PDE3A (*Hambleton et al., 2005*). Moreover, the gene therapy approach could have been also usefully utilized in a prevention study for HF (AAV9 gene transfer before TAC), especially for PDE2A3 where the therapy study (AAV9 gene transfer after TAC) could not prevent maladaptive alterations at subcellular level or cardiac remodeling. Finally, the therapy study should have been compared to a diseased (TAC) group of transgenic mice receiving β-blockers (*Harding et al., 2001*) for eight weeks post-surgery (equal to the duration of the gene therapy protocol) for evaluation of its efficacy and development of better therapeutic schemes.

5. Conclusions

In conclusion, cardiac-targeted gene therapy with phosphodiesterases PDE2A3 and PDE4B3 had mild but beneficial effects against pressure overload-induced hypertrophy and arrhythmias.

As the major enzyme involved in cAMP compartmentation in murine heart, PDE4B3 overexpression partially protected against hypertrophy and loss of contractile function, significantly contributed in cAMP hydrolysis and compartmentation and substantially minimized arrhythmia initiation after β-AR stimulation, without leading to unfavorable effects seen by excessive protein expression.
PDE2A3 overexpression, on the other hand, neither protected against hypertrophy nor preserved contractile function after TAC, but unequivocally abrogated arrhythmias mediated by β-AR signaling *in vitro* and restored β-AR/PDE pattern in the sarcolemma in contrast to beneficial effects seen by chronic PDE2 inhibition *(Zoccarato et al., 2015)*.

6. Future Perspectives

It has been revealed that the target of the cardiotonic drug milrinone, i.e., PDE3A, is also decreased in hypertrophy and HF (*Abi-Gerges et al., 2009*). Apart from regulating PLB phosphorylation and thus SERCA2a activity in humans and mice (*Ahmad et al., 2015; Beca et al., 2013*), PDE3A1 also acts as a negative regulator of cardiomyocyte apoptosis, by controlling the expression of the transcriptional repressor and pro-apoptotic factor, ICER (inducible cAMP early repressor) (*Yan et al., 2007*). Inhibition of this mechanism in mice with cardiac-specific overexpression of PDE3A1 was associated with protection during ischemia-reperfusion (*Oikawa et al., 2013*). Recently, elegantly performed studies at the onset of cardiac hypertrophy were able to show that both PDE2A and PDE3A undergo a disease-driven redistribution between various subcellular microdomains such as β-AR-associated membrane compartments and the SR (*Perera et al., 2015; Sprenger et al., 2015*), a mechanism by which changes in cAMP compartmentation can drastically impact on contractile function, but also facilitate the development of better HF therapeutics. In this regard, it would be rather interesting to assess the effect of potential PDE3A overexpression against hypertrophy and loss of contractility in heart failure models and to, eventually, distinguishing which isoform could offer the highest cardioprotection for future clinical practice. This gene therapy approach could be also usefully utilised in bigger animal models of HF (dogs or pigs) for appropriate extrapolation of results and even be compared to currently available β-blockers and assessed as an effective alternative or complementary therapeutic strategy. Finally, the concept of up-regulating or overexpressing target proteins or enzymes should not be restricted exclusively to gene therapy approaches, but rather become broader, even if this means to resort to conventional drug-induced solutions, such as the example of PDE4 activators that reduce chronically elevated cAMP levels and prevent cyst formation in animal and human cell models of autosomal dominant polycystic kidney disease (*Omar et al., 2019).*

7. Bibliography

Abi-Gerges A., Richter W., Lefebvre F., Matéo P., Varin A., Heymes C., Samuel J.L., Lugnier C., Conti M., Fischmeister R., Vandecasteele G. (2009). Decreased expression and activity of cAMP phosphodiesterases in cardiac hypertrophy and its impact on ß-adrenergic cAMP signals. Circ. Res., 105:784-792.

Acin-Perez R., Gatti D.L., Bai Y., Manfredi G. (2011). Protein phosphorylation and prevention of cytochrome oxidase inhibition by ATP: Coupled mechanisms of energy metabolism regulation. Cell Metab., 13, 712–719.

Adams S.R., Harootunian A.T., Buechler Y.J., Taylor S.S., Tsien R.Y. (1991). Fluorescence ratio imaging of cyclic AMP in single cells. Nature, 349, 694-697.

Afzal F., Aronsen J.M., Moltzau L.R., Sjaastad I., Levy F.O., Skomedal T., Osnes J.B., Qvigstad E. (2011). Differential regulation of beta2 -adrenoceptor-mediated inotropic and lusitropic response by PDE3 and PDE4 in failing and non-failing rat cardiac ventricle. Br. J. Pharmacol., 162:54-71.

Agarwal S.R., Clancy C.E., Harvey R.D. (2016). Mechanisms Restricting Diffusion of Intracellular cAMP. Sci. Rep. 6, 19577.

Agarwal S. R., MacDougall D. A., Tyser R., Pugh S. D., Calaghan S. C., Harvey R. D. (2011). Effects of cholesterol depletion on compartmentalized cAMP responses in adult cardiac myocytes. J. Mol. Cell Cardiol., 50:500–509.

Agarwal S.R., Gratwohl J., Cozad M., Yang P.C., Clancy C.E., Harvey R.D. (2018). Compartmentalized cAMP Signaling Associated with Lipid Raft and Non-raft Membrane Domains in Adult Ventricular Myocytes. Front. Pharmacol., 9, 332.

Agarwal S.R., Ostrom R.S., Harvey R.D. (2017). Membrane Microdomains and cAMP Compartmentation in Cardiac Myocytes. In Microdomains in the Cardiovascular System; Nikolaev, V.O., Zaccolo, M., Eds.; Springer: Cham, Switzerland, pp. 17–35.
Agarwal S.R., Yang P.C., Rice M. et al (2014). Role of membrane microdomains in compartmentation of cAMP signaling. PLoS One, 9:e95835.

Ahmad F., Shen W., Vandeput F., Szabo-Fresnais N., Krall J., Degerman E., Goetz F., Klussmann E., Movsesian M., Manganiello V.C. (2015). Regulation of sarcoplasmic reticulum Ca2+ ATPase 2 (SERCA2) activity by phosphodiesterase 3A (PDE3A) in human myocardium: Phosphorylation-dependent interaction of PDE3A1 with SERCA2. J. Biol. Chem., 290:6763-6776.

Ahmad F., Murata T., Shimizu K., Degerman E., Maurice D., Manganiello V.C. (2015). Cyclic nucleotide phosphodiesterases: important signaling modulators and therapeutic targets. Oral diseases, 21(1), e25-e50.

Allen J.A., Halverson-Tamboli R.A., Rasenick M.M. (2007). Lipid raft microdomains and neurotransmitter signalling. Nat. Rev. Neurosci., 8:128–140.

Altarejos J.Y., Montminy M. (2011). Creb and the crtc co-activators: Sensors for hormonal and metabolic signals. Nat. Rev. Mol. Cell Biol., 12:141-151.

Akar F.G., Hajjar R.J. (2014). Gene therapies for arrhythmias in heart failure. Eur. J. Physiol., 466: 1211-1217.

Anwar A., Schlüter K.D., Heger J., Piper H.M., Euler G. (2008). Enhanced SERCA2A expression improves contractile performance of ventricular cardiomyocytes of rat under adrenergic stimulation. Eur. J. Physiol., 457: 485-491.

Anwar A., Taimor G., Korkusuz H., Schreckenberg R., Berndt T., Abdallah Y., Piper H.M., Schluter K.D. (2005). PKC-independent signal transduction pathways increase SERCA2 expression in adult rat cardiomyocytes. J. Mol. Cell. Cardiol., 39: 911-919.

Baker D.L., Hashimoto K., Grupp I.L., Ji Y., Reed T., Loukianov E., Grupp G., Bhagwhat A., Hoit B., Walsh R., Marban E., Periasamy M. (1998). Targeted overexpression of the sarcoplasmic reticulum Ca^{2+} -ATPase increases cardiac contractility in transgenic mouse hearts. Circ. Res., 83: 1205-1214.

Baillie G.S., Adams D.R., Bhari N., Houslay T.M., Vadrevu S., Meng D., Li X., Dunlop A., Milligan G., Bolger G.B., Klussmann E., Houslay M.D. (2007). Mapping binding sites for the PDE4D5 cAMP-specific phosphodiesterase to the N-and C-domains of β-arrestin using spot-immobilized peptide arrays. Biochemical Journal, 404(1), 71-80.

Baillie G.S., Houslay M.D. (2005). Arrestin times for compartmentalised cAMP signalling and phosphodiesterase-4 enzymes. Curr. Opin. Cell Biol., 17(2), 129-134.

Baillie G.S., Sood A., McPhee I., Gall I., Perry S.J., Lefkowitz R.J., Houslay M.D. (2003). β-Arrestin-mediated PDE4 cAMP phosphodiesterase recruitment regulates β-adrenoceptor switching from Gs to Gi. Proc. Natl. Acad. Sci. U. S. A. (3), 940-945.

Baliga R. S., Preedy M. E., Dukinfield M. S., Chu S. M., Aubdool A. A., Bubb K. J., Moyes A.J., Tones M.A., Hobbs A. J. (2018). Phosphodiesterase 2 inhibition preferentially promotes NO/guanylyl cyclase/cGMP signaling to reverse the development of heart failure. Proc. Natl. Acad. Sci. U. S. A., 115(31), E7428-E7437.

Balijepalli R.C., Foell J.D., Hall D.D., Hell J.W., Kamp T.J. (2006). Localization of cardiac L-type Ca2+ channels to a caveolar macromolecular signaling complex is required for β2-adrenergic regulation. Proc. Natl. Acad. Sci. USA, 103, 7500–7505.

Balijepalli R.C., Kamp T.J. (2008). Caveolae, ion channels and cardiac arrhythmias. Prog. Biophys. Mol. Biol., 98, 149–160.

Beca S., Ahmad F., Shen W., Liu J., Makary S., Polidovitch N., Sun J., Hockman S., Chung Y.W., Murphy E., Manganiello V.C., Backx P.H. (2013). PDE3A regulates basal myocardial contractility through interacting with SERCA2a-signaling complexes in mouse heart. Circ. Res., 112:289-297.

Beca S., Helli P.B., Simpson J.A., Zhao D., Farman G.P., Jones P.P., Tian X., Wilson L.S., Ahmad F., Chen W.S.R., Movsesian M.A., Manganiello V.C., Maurice D.H., Conti M., Backx P.H. (2011). Phosphodiesterase 4D regulates baseline sarcoplasmic reticulum Ca2+ release and cardiac contractility, independently of L-type Ca2+ current. Circ. Res., 109(9), 1024-1030.

Bender A.T., Beavo J.A. (2006). Cyclic nucleotide phosphodiesterases: from molecular regulation to clinical use. Pharmacol. Rev., 58:488-520.

Benkusky N.A., Weber C.S., Scherman J.A., Farrell E.F., Hacker T.A., John M.C., Powers P.A., Valdivia H.H. (2007). Intact beta-adrenergic response and unmodified progression toward heart failure in Literature 94 mice with genetic ablation of a major protein kinase a phosphorylation site in the cardiac ryanodine receptor. Circ. Res., 101:819-829.

Bers D.M. (2002). Cardiac excitation-contraction coupling. Nature, 415(6868): 198-205.

Bers D.M. (2008). Calcium cycling and signaling in cardiac myocytes. Annu. Rev. Physiol., 70:23-49.

Bers D.M., Xiang Y.K., Zaccolo M. (2019). Whole-Cell cAMP and PKA Activity are Epiphenomena, Nanodomain Signaling Matters. Physiology, 34, 240–249.

Berisha F., Götz K.R., Wegener J. W., Jungen C., Pape U., Kraft A.E., Warnke S., Lindner D., Westermann D., Blakenberg S., Meyer C., Hasenfuß G., Lehnart S. E., Nikolaev V.O. (2019). Direct monitoring of cAMP at the cardiac ryanodine receptor using a novel targeted fluorescence biosensor mouse. bioRxiv, 623934.

Bethani I., Skånland S. S., Dikic I., Acker-Palmer A. (2010). Spatial organization of transmembrane receptor signalling. The EMBO journal, 29(16), 2677-2688.

Bhat M.B., Zhao J., Takeshima H., Ma J. (1997). Functional calcium release channel formed by the carboxyl-terminal portion of ryanodine receptor. Biophys. J., 73(3), 1329-1336.

Biel M., Zong X., Ludwig A., Sautter A., Hofmann F. (1999). Structure and function of cyclic nucleotide-gated channels. Rev. Physiol. Biochem. Pharmacol., 135:151-171.
Blaese R. M. (1993). Development of gene therapy for immunodeficiency: adenosine deaminase deficiency. Pediatr. Res., 33(4), S49-S55.

Blaese R.M., Culver K.W., Miller A.D., Carter C.S., Fleisher T., Clerici M., Shearer G., Chang L., Chiang Y., Tolstoshev P., Greenblatt J.J., Rosenberg S.A., Klein H., Berger M., Mullen C.A., Ramsey W.J., Muul l., Morgan R.A., Anderson

W.F. (1995). T lymphocyte-directed gene therapy for ADA− SCID: initial trial results after 4 years. Science, 270(5235), 475-480.

Bodor J., Bopp, T., Vaeth M., Klein M., Serfling E., Hünig T., Becker C., Schild H., Schmitt E. (2012). Cyclic AMP underpins suppression by regulatory T cells. Eur. J. Immunol., 42(6), 1375-1384.

Brandes R., Bers D.M. (1997). Intracellular Ca^{2+} increases the mitochondrial nadh concentration during elevated work in intact cardiac muscle. Circ. Res., 80:82-87.

Brescia M., Zaccolo M. (2016). Modulation of compartmentalised cyclic nucleotide signalling via local inhibition of phosphodiesterase activity. Int. J. Mol. Sci., 17.

Bridges C.R., Gopal K., Holt D.E., Yarnall C., Cole S., Anderson R.B., Yin X., Nelson A., Kozyak B.W., Wang Z., Lesniewski J., Su L.T., Thesier D.M., Sundar H., Stedman H.H. (2005). Efficient myocyte gene delivery with complete cardiac surgical isolation in situ. J. Thorac. Cardiovasc. Surg., 130: 1364.

Brinks H., Rohde D., Voelkers M., Qiu G., Pleger S.T., Herzog N., Rabinowitz J., Ruhparwar A., Silvestry S., Lerchenmuller C., Mather P.J., Eckhart A.D., Katus H.A., Carrel T., Koch W.J., Most P. (2011). S100A1 genetically targeted therapy reverses dysfunction of human failing cardiomyocytes. J. Am. Coll. Cardiol., 58:966–973.

Bristow M.R., Ginsburg R., Minobe W., Cubicciotti R.S., Sageman W.S., Lurie K., Billingham M.E., Harrison D.C., Stinson E.B. (1982). Decreased catecholamine sensitivity and beta-adrenergic-receptor density in failing human hearts. N. Engl. J. Med., 307:205-211.

Brown D.A. (2006). Lipid rafts, detergent-resistant membranes, and raft targeting signals. Physiology, 21:430–439.

Brudvik K.W., Tasken K. (2012). Modulation of T cell immune functions by the prostaglandin E_2- cAMP pathway in chronic inflammatory states. Br. J. Pharmacol., 166, 411-419.

Brunton L.L., Hayes J.S., Mayer S.E. (1981). Functional compartmentation of cyclic AMP and protein kinase in heart. Adv. Cycl. Nucleotide Res., 14, 391–397.

Bobin P., Varin A., Lefebvre F., Fischmeister R., Vandecasteele G., Leroy J. (2016). Calmodulin kinase II inhibition limits the pro-arrhythmic Ca2+ waves induced by cAMP-phosphodiesterase inhibitors. Cardiovasc. Res., 110:151-161.

Borner S., Schwede F., Schlipp A., Berisha F., Calebiro D., Lohse M.J., Nikolaev V.O. (2011). Fret measurements of intracellular cAMP concentrations and cAMP analogue permeability in intact cells. Nat. Protoc., 6:427-438.

Brodde O.E. (1993). Beta-adrenoceptors in cardiac disease. Pharmacol. Ther., 60:405-430.

Buxton I.L., Brunton L.L. (1983). Compartments of cyclic amp and protein kinase in mammalian cardiomyocytes. J. Biol. Chem., 258:10233-10239.

Byrne C.D., Olufadi R., Bruce K.D., Cagampang F.R., Ahmed M.H. (2009). Metabolic disturbances in non-alcoholic fatty liver disease. Clin. Sci. (Lond), 116: 539-564.

Calebiro D., Nikolaev V.O., Gagliani M.C., de Filippis T., Dees C., Tacchetti C., Persani L., Lohse M.J. (2009). Persistent camp-signals triggered by internalized g-protein-coupled receptors. PLoS Biol., 7:e1000172.

Camors E., Valdivia H.H. (2014). CaMKII regulation of cardiac ryanodine receptors and inositol triphosphate receptors. Front. Pharmacol., 5:101.

Carnegie G.K., Means C.K., Scott J.D. (2009). A-kinase anchoring proteins: From protein complexes to physiology and disease. IUBMB Life, 61, 394–406.

Castro L.R., Schittl J., Fischmeister R. (2010). Feedback control through cGMP-dependent protein kinase contributes to differential regulation and compartmentation of cGMP in rat cardiac myocytes. Circ Res., 107:1232-1240.

Castro L.R., Verde I., Cooper D.M.F., Fischmeister R. (2006). Cyclic guanosine monophosphate compartmentation in rat cardiac myocytes. Circulation. 113:2221-2228.

Cavalli A., Eghbali M., Minosyan T. Y., Stefani E., Philipson K. D. (2007). Localization of sarcolemmal proteins to lipid rafts in the myocardium. Cell calcium, 42(3), 313-322.

Cavazzana-Calvo M., Hacein-Bey S., de Saint Basile G., Gross F., Yvon E., Nusbaum P., Selz F., Hue C., Certain S., Casanova J. L., Bousso P., Le Deist F., Fischer A. (2000). Gene therapy of human severe combined immunodeficiency (SCID)-X1 disease. Science, 288(5466), 669-672.

Cheepala S., Hulot J.S., Morgan J.A., Sassi Y., Zhang W., Naren A.P., Schuetz J.D. (2013). Cyclic nucleotide compartmentalization: Contributions of phosphodiesterases and ATP-binding cassette transporters. Annu. Rev. Pharmacol. Toxicol., 53, 231–253.

Chen Y., Escoubet B., Prunier F., Amour J., Simonides W.S., Vivien B., Lenoir C., Heimburger M., Choqueux C., Gellen B., Riou B., Michel J.B., Franz W.M., Mercadier J.J. (2004). Constitutive cardiac overexpression of sarcoplasmic/endoplasmic reticulum Ca^{2+}-ATPase delays myocardial failure after myocardial infarction in rats at a cost of increased acute arrhythmias. Circulation, 109: 1898-1903.

Choi Y.H., Park S., Hockman S., Zmuda-Trzebiatowska E., Svennelid F., Haluzik M., Gavrilova O., Ahmad F., Pepin L., Napolitano M., Taira M., Sundler F., Stenson Holst L., Degerman E., Manganiello V.C. (2006). Alterations in regulation of energy homeostasis in cyclic nucleotide phosphodiesterase 3B–null mice. J. Clin. Investig., 116, 3240–3251.

Chopra N., Kannankeril P.J., Yang T., Hlaing T., Holinstat I., Ettensohn K., Pfeifer K., Akin B., Jones L.R., Franzini-Armstrong C., Knollmann B.C. (2007). Modest reductions of cardiac calsequestrin increase sarcoplasmic reticulum Ca^{2+} leak

independent of luminal Ca^{2+} and trigger ventricular arrhythmias in mice. Circ. Res., 101(6): 617-626.

Chung Y.W., Lagranha C., Chen Y., Sun J., Tong G., Hockman S.C., Ahmad F., Esfahani S.G., Bae D.H., Polidovitch N., Wu J., Rhee D.K., Lee B.S., Gucek M., Daniels M.P., Brantner C.A., Backx P.H., Murphy E., Manganiello V.C. (2015). Targeted disruption of PDE3B, but not PDE3A, protects murine heart from ischemia/reperfusion injury. Proc. Natl. Acad. Sci. USA, 112, E2253–E2262.

Cittadini A., Cuocolo A., Merola B., Fazio S., Sabatini D., Nicolai E., Colao A., Longobardi S., Lombardi G., Sacca L. (1994). Impaired cardiac performance in GH-deficient adults and its improvement after GH replacement. Am. J. Physiol., 267: E219-E225.

Communal C, Singh K, Sawyer DB and Colucci WS. (1999). Opposing effects of beta (1)- and beta (2)-adrenergic receptors on cardiac myocyte apoptosis: role of a pertussis toxin-sensitive G protein. Circulation.100:2210-2.

Concept Draw. Hazard Pictograms (https://www.conceptdraw.com/How-To-Guide/hazard-pictograms), Apr. 05 2021.

Conti M., Beavo J. (2007). Biochemistry and physiology of cyclic nucleotide phosphodiesterases: Essential components in cyclic nucleotide signaling. Annu. Rev. Biochem., 76:481-511.

Conti M., Mika D., Richter W. (2014). Cyclic AMP compartments and signaling specificity: Role of cyclic nucleotide phosphodiesterases. J. Gen. Physiol., 143, 29–38.

Conti M., Richter W., Mehats C., Livera G., Park J. Y., Jin C. (2003). Cyclic AMP-specific PDE4 phosphodiesterases as critical components of cyclic AMP signaling. J. Biol. Chem., 278(8), 5493-5496.

Corbin J.D., Sugden P.H., Lincoln T.M., Keely S.L. (1977). Compartmentalization of adenosine 30 : 50 -monophosphate and adenosine 30 : 50 -monophosphate-dependent protein kinase in heart tissue. J. Biol. Chem., 252, 3854–3861.

Clusin W.T. (2003). Calcium and Cardiac Arrhythmias: DADs, EADs and alternans. Crit. Rev. Clin. Lab. Sci., 40(3): 337-375.

Cutler M.J., Wan X., Laurita K.R., Hajjar R.J., Rosenbaum D.S. (2009). Targeted SERCA2a gene expression identifies molecular mechanism and therapeutic target for arrhythmogenic cardiac alternans. Circ Arrhythm. Electrophysiol., 2: 686-694.

Cutler M.J., Wan X., Plummer B.N., Liu H., Deschenes I., Laurita K.R., Hajjar R.J., Rosenbaum D.S. (2013). Targeted sarcoplasmic reticulum Ca^{2+} -ATPase 2a gene delivery to restore electrical stability in the failing heart. Circulation, 126: 2095-2104.

Daaka Y., Luttrell L. M., Lefkowitz R. J. (1997). Switching of the coupling of the β 2-adrenergic receptor to different G proteins by protein kinase A. Nature, 390(6655), 88-91.

Dally S., Corvazier E., Bredoux R., Bobe R., Enouf J. (2010). Multiple and diverse co-expression, location and regulation of additional SERCA2 and SERCA3 isoforms in non-failing and failing human heart. J. Mol. Cell. Cardiol., 48: 633-644.

Davia K., Bernobich E., Ranu H.K., del Monte F., Terracciano C.M., MacLeod K.T., Adamson D.L., Chaundhri B., Hajjar R.J., Harding S.E. (2001). SERCA2a overexpression decreases the incidence of aftercontractions in adult rabbit ventricular myocytes. J. Mol. Cell Cardiol., 33: 1005-1015.

Defer N., Best-Belpomme M., Hanoune J. (2000). Tissue specificity and physiological relevance of various isoforms of adenylyl cyclase. Am. J. Physiol. Renal Physiol., 279:F400–416.

Degerman E., Ahmad F., Chung Y.W., Guirguis E., Omar B., Stenson L., Manganiello V.C. (2011). From PDE3B to the regulation of energy homeostasis. Curr. Opin. Pharmacol., 11, 676–682.

Degerman E., Belfrage P., Manganiello V.C. (1997). Structure, localization, and regulation of cGMP-inhibited phosphodiesterase (PDE3). J. Biol. Chem., 272, 6823–6826.

Del Monte F., Hajjar R.J. (2003). Targeting calcium cycling proteins in heart failure through gene transfer. J. Physiol., 546(1): 49-61.

Del Monte F., Harding S.E., Dec G.W., Gwathmey J.K., Hajjar R.J. (2002). Targeting phospholamban by gene transfer in human heart failure. Circulation, 105:904–907.

Del Monte F., Harding S.E., Schmidt U., Matsui T., Kang Z.B., Dec G.W., Gwathmey J.K., Rosenzweig A., Hajjar R.J. (1999). Restoration of contractile function in isolated cardiomyocytes from failing human hearts by gene transfer of SERCA2a. Circulation, 100: 2308-2311.

Del Monte F., Lebeche D., Guerrero J.L., Tsuji T., Doye A.A., Gwathmey J.K., Hajjar R.J. (2004). Abrogation of ventricular arrhythmias in a model of ischemia and reperfusion by targeting myocardial calcium cycling. Proc. Natl. Acad. Sci. U. S. A., 101(15): 5622-5627.

Del Monte F., Williams E., Lebeche D., Schmidt U., Rosenzweig A., Gwathmey J.K., Lewandowski E.D., Hajjar R.J. (2001). Improvement in survival and cardiac metabolism after gene transfer of sarcoplasmic reticulum Ca^{2+} -ATPase in a rat model of heart failure. Circulation, 104: 1424-1429.

de Rooij J., Zwartkruis F.J., Verheijen M.H., Cool R.H., Nijman S.M., Wittinghofer A., Bos J.L. (1998). Epac is a rap1 guanine-nucleotide-exchange factor directly activated by cyclic amp. Nature, 396:474-477.

Di Benedetto G., Zoccarato A., Lissandron V., Terrin A., Li X., Houslay M.D., Baillie G.S., Zaccolo M. (2008). Protein kinase A type I and type II define distinct intracellular signaling compartments. Circ. Res., 103, 836–844.

Dickinson N.T., Haslam R.J. (1997). Activation of cGMP-stimulated phosphodiesterase by nitroprusside limits cAMP accumulation in human platelets: Effects on platelet aggregation. Biochem. J., 323, 371–377.

Ding B., Abe J., Wei H., Huang Q., Walsh R.A., Molina C.A., Zhao A., Sadoshima J., Blaxall B.C., Berk B.C., Yan C. (2005). Functional role of phosphodiesterase 3 in cardiomyocyte apoptosis: Implication in heart failure. Circulation, 111:2469-2476.

Ding B., Abe J.I., Wei H., Xu H., Che W., Aizawa T., Liu W., Molina C.A., Sadoshima J., Blaxall B.C., Berk B.C., Yan C. (2005). A positive feedback loop of phosphodiesterase 3 (PDE3) and inducible cAMP early repressor (ICER) leads to cardiomyocyte apoptosis. Proc. Natl. Acad. Sci. USA, 102, 14771–14776.

DiPilato L. M., Cheng X., Zhang J. (2004). Fluorescent indicators of cAMP and Epac activation reveal differential dynamics of cAMP signaling within discrete subcellular compartments. Proc. Natl. Acad. Sci. U. S. A., 101(47), 16513-16518.

Dodge-Kafka K.L., Langeberg L., Scott J.D. (2006). Compartmentation of cyclic nucleotide signaling in the heart: the role of A-kinase anchoring proteins. Circ. Res., 98:993-1001.

Dodge K.L., Khouangsathiene S., Kapiloff M.S., Mouton R., Hill E.V., Houslay M.D., Langeberg L.K., Scott J.D. (2001). mAKAP assembles a protein kinase a/pde4 phosphodiesterase camp signaling module. Embo j., 20:1921-1930.

Driessen H.E., Bourgonje V.J.A., van Veen T.A.B., Vos M.A. (2014). New antiarrhythmic targets to control intracellular calcium handling. Netherlands Heart J., 22(5): 198-213.

Eisner D. A., Caldwell J. L., Kistamás K., Trafford A. W. (2017). Calcium and excitation-contraction coupling in the heart. Circ. Res., 121(2), 181-195.

Espinasse I., Iourgenko V., Richer C., Heimburger M., Defer N., Bourin M.C., Samson F., Pussard E., Giudicelli J.F., Michel J.B., Hanoune J., Mercadier J.J. (1999). Decreased type VI adenylyl cyclase mRNA concentration and Mg^{2+}-dependent adenylyl cyclase activities and unchanged type V adenylyl cyclase mRNA concentration and Mn^{2+}-dependent adenylyl cyclase activities in the left ventricle of rats with myocardial infarction and longstanding heart failure. Cardiovasc. Res., 42:87–98.

Fabiato A. (1983). Calcium-induced release of calcium from the cardiac sarcoplasmic reticulum. Am. J. Physiol. Cell Physiol., 245(1), C1-C14.

Fan G. C., Yuan Q., Kranias E. G. (2008). Regulatory roles of junctin in sarcoplasmic reticulum calcium cycling and myocardial function. Trends Cardiovasc. Med., 18(1), 1-5.

Farrell E.F., Antaramian A., Rueda A., Gomez A.M., Valdivia H.H. (2003). Sorcin inhibits calcium release and modulates excitation-contraction coupling in the heart. J. Biol. Chem., 278:34660- 34666.

Feldman D.S., Carnes C.A., Abraham W.T., Bristow M.R. (2005). Mechanisms of disease: beta-adrenergic receptors--alterations in signal transduction and pharmacogenomics in heart failure. Nat. Clin. Pract. Cardiovasc. Med., 2:475–483.

Fertig B. A., Baillie G. S. (2018). PDE4-mediated cAMP signalling. J. Cardiovasc. Dev. Dis., 5(1), 8.

Fischmeister R., Castro L.R.V., Abi-Gerges A., Rochais F., Jurevicius J., Leroy J., Vandecasteele G. (2006). Compartmentation of cyclic nucleotide signaling in the heart: The role of cyclic nucleotide phosphodiesterases. Circ. Res., 99:816-828.

Flesch M., Schwinger R.H.G., Schnabel P., Schiffer F., van Gelder I., Bavendiek U., Südkamp M., Kuhn-Regnier F., Böhm M. (1996). Sarcoplasmic reticulum Ca^{2+} -ATPase and phospholamban mRNA and protein levels in end-stage heart failure due to ischemic or dilated cardiomyopathy. J. Mol. Med., 74: 321-332.

Förster T. (1948). Zwischenmolekulare energiewanderung und fluoreszenz. Annalen der physik, 437(1-2), 55-75.

Francis S. H., Blount M. A., Corbin J. D. (2011). Mammalian cyclic nucleotide phosphodiesterases: molecular mechanisms and physiological functions. Physiol. Reviews, 91(2), 651-690.

Frey N., Katus H.A., Olson E.N., Hill J.A. (2004). Hypertrophy of the heart: A new therapeutic target? Circulation, 109:1580-1589.

Frey N., Olson E.N. (2003). Cardiac hypertrophy: The good, the bad, and the ugly. Annu. Rev. Physiol., 65:45-79.

Friedmann T., Roblin R. (1972). Gene therapy for human genetic disease?. Science, 175(4025), 949-955.

Froese A., Breher S.S., Waldeyer C., Schindler R.F., Nikolaev V.O., Rinné S., Vauti F. (2012). Popeye domain containing proteins are essential for stress-mediated modulation of cardiac pacemaking in mice. J. Clin. Investig., 122.

Froese A., Nikolaev V.O. (2015). Imaging alterations of cardiomyocyte cAMP microdomains in disease. Front. Pharmacol., 6, 172.

Gamanuma M., Yuasa K., Sasaki T., Sakurai N., Kotera J., Omori K. (2003). Comparison of enzymatic characterization and gene organization of cyclic nucleotide phosphodiesterase 8 family in humans. Cell Signal. Technol., 15, 565–574.

Gao M.H., Lai N.C., Roth D.M., Zhou J., Zhu J., Anzai T., Dalton N., Hammond H.K. (1999). Adenylylcyclase increases responsiveness to catecholamine stimulation in transgenic mice. Circulation, 99:1618–1622.

Gao M.H., Tang T., Guo T., Miyanohara A., Yajima T., Pestonjamasp K., Feramisco J.R., Hammond H.K. (2008). Adenylyl cyclase type VI increases Akt activity and phospholamban phosphorylation in cardiac myocytes. J. Biol. Chem., 283:33527–33535.

Gao M.H., Tang T., Miyanohara A., Feramisco J.R., Hammond H.K. (2010). Beta-(1)-Adrenergic receptor vs adenylyl cyclase 6 expression in cardiac myocytes: differences in transgene localization and intracellular signaling. Cell. Signal., 22:584–589.

Georget M., Mateo P., Vandecasteele G., Jurevicius J., Lipskaia L., Defer N., Hanoune J., Hoerter J., Fischmeister R. (2002). Augmentation of cardiac contractility with no change in L-type Ca2+ current in transgenic mice with a cardiac-directed expression of the human adenylyl cyclase type 8 (AC8). Faseb J., 16:1636–1638.

Georget M., Mateo P., Vandecasteele G., Lipskaia L., Defer N., Hanoune J., Hoerter J., Lugnier C., Fischmeister R. (2003). Cyclic AMP compartmentation due to increased cAMP-phosphodiesterase activity in transgenic mice with a cardiac-directed expression of the human adenylyl cyclase type 8 (AC8). Faseb J., 17:1380–1391.

Ghigo A., Perino A., Mehel H., Zahradnikova A.J., Morello F., Leroy J., Nikolaev V.O., Damilano F., Cimino J., De Luca E., Richter W., Westenbroek R., Catterall W.A., Zhang J., Yan C., Conti M., Gomez A.M., Vandecasteele G., Hirsch E., Fischmeister R. (2012). PI3KY Protects against catecholamine-induced ventricular arrhythmia through PKA-mediated regulation of distinct phosphodiesterases. Circulation. 126:2073-2083.

Ghigo A., Pirozzi F., Li M., Hirsch E. (2017). Chatting Second Messengers: PIP3 and cAMP. In Microdomains in the Cardiovascular System; Nikolaev, V.O., Zaccolo, M., Eds.; Springer: Cham, Switzerland, pp. 85–95.

Giordano F.J., He H., McDonough P., Meyer M., Sayen R.M., Dillman W.H., (1997). Adenovirus-mediated gene transfer reconstitutes depressed sarcoplasmic reticulum Ca^{2+}-ATPase levels and shortens prolonged cardiac myocyte Ca^{2+} transients. Circulation, 96: 400-403.

Go A.S., Mozaffarian D., Roger V.L., Benjamin E.J., Berry J.D., Borden W.B., Bravata D.M., Dai S., Ford E.S., Fox C.S., Franco S., Fullerton H.J., Gillespie C., Hailpern S.M., Heit J.A., Howard V.J., Huffman M.D., Kissela B.M., Kittner S.J., Lackland D.T., Lichtman J.H., Lisabeth L.D., Magid D., Marcus G.M., Marelli A., Matchar D.B., McGuire D.K., Mohler E.R., Moy C.S., Mussolino M.E., Nichol G., Paynter N.P., Schreiner P.J., Sorlie P.D., Stein J., Turan T.N., Virani S.S., Wong N.D., Woo D., Turner M.B. (2013). Executive summary: heart disease and stroke statistics--2013 update: a report from the American Heart Association. Circulation. 127:143-152.

Götz K.R., Nikolaev V.O. (2013). Advances and techniques to measure cGMP in intact cardiomyocytes. Methods Mol. Biol.,1020:121-129.

Götz, K., Sprenger, JU., Perera, R.K., Steinbrecher, J.H., Lehnart, S.E., Kuhn, M., Gorelik, J., Balligand, J .L., and Nikolaev, V.O. (2014). Transgenic Mice for Real Time Visualization of cGMP in Intact Adult Cardiomyocytes. Circ. Res., 114, 1235-1245.

Gorelik J., Yang L.Q., Zhang Y., Lab M., Korchev Y., Harding S.E. (2006). A novel z-groove index characterizing myocardial surface structure. Cardiovasc. Res., 72:422-429.

Greene A.I., Lalli M.J., Ji Y., Babu G.J., Grupp I., Sussman M., Periasamy M. (2000). Overexpression of SERCA2b in the heart leads to an increase in sarcoplasmic reticulum calcium transport function and increased cardiac contractility. J. Biol. Chem., 275: 24722-24727.

Guellich A., Mehel H., Fischmeister R. (2014). Cyclic AMP synthesis and hydrolysis in the normal and failing heart. Pflügers Arch., 466:1163-1175.

Guo X., Chapman D., Dhalla N.S. (2003). Partial prevention of changes in SR gene expression in congestive heart failure due to myocardial infarction by enalapril or losartan. Mol. Cell Biol. Biochem., 254: 163-172.

Gwathmey J.K., Copelas L., MacKinnon R., Schoen F.J., Feldman M.D., Grossman W., Morgan J.P. (1987). Abnormal intracellular calcium handling in myocardium from patients with end-stage heart failure. Circ. Res., 61:70–76.

Gwathmey J.K., Yerevanian A.I., Hajjar R.J. (2011). Cardiac gene therapy with SERCA2a: from bench to bedside. J. Mol. Cell. Cardiol., 50: 803-812.

Gyorke S., Terentyev D. (2008). Modulation of ryanodine receptor by luminal calcium and accessory proteins in health and cardiac disease. Cardiovasc. Res., 77:245-255.

Hacein-Bey-Abina S., Von Kalle C., Schmidt M., McCormack M. P., Wulffraat N., Leboulch P. A., Lim A., Osborne C.S., Pawliuk R., Morillon E., Sorensen R., Forster A. Fraser P., Cohen J.I., De Saint Basile G., Alexander I., Wintergerst U., Frebourg T., Aurias A., Stoppa-Lyonet D., Romana S., Radford-Weiss I., Gross F., Valensi F., Delabesse E., Macintyre E., Sigaux F., Soulier J., Leiva L.E., Wissler M., Prinz C., Rabbitts T.H., Le Deist F., Fischer A., Cavazzana-Calvo M. (2003). LMO2-associated clonal T cell proliferation in two patients after gene therapy for SCID-X1. Science, 302(5644), 415-419.

Hadri L., Bobe R., Kawase Y., Ladage D., Ishikawa K., Atassi F., Lebeche D., Kranias E.G., Leopold J.A., Lompre A.M., Lipskaia L., Hajjar R.J. (2010). SERCA2a gene transfer enhances eNOS expression and activity in endothelial cells. Mol. Ther., 18:1284–1292.

Haj Slimane Z., Bedioune I., Lechêne P., Varin A., Lefebvre F., Mateo P., Domergue-Dupont V., Dewenter M., Richter W., Conti M., El-Armouche A., Zhang J., Fischmeister R., Vandecasteele G. (2014). Control of cytoplasmic and nuclear protein kinase A activity by phosphodiesterases and phosphatases in cardiac myocytes. Cardiovasc. Res., 102:97-106.

Hajjar R.J., Zsebo K., Deckelbaum L., Thompson C., Rudy J., Yaroshinsky A., Ly H., Kawase Y., Wagner K., Borow K., Jaski B., London B., Greenberg B., Pauly D.F., Patten R., Starling R., Mancini D., Jessup M. (2008). Design of a Phase 1/2 trial of intracoronary administration of AAV1/SERCA2a in patients with heart failure. J. Cardiac Fail., 14(5): 355-367.

Hambleton R., Krall J., Tikishvili E., Honeggar M., Ahmad F., Manganiello V. C., Movsesian M. A. (2005). Isoforms of cyclic nucleotide phosphodiesterase PDE3 and their contribution to cAMP hydrolytic activity in subcellular fractions of human myocardium. J. Biol. Chem., 280(47), 39168-39174.

Hambleton M., Hahn H., Pleger S.T., Kuhn M.C., Klevitsky R., Carr A.N., Kimball T.F., Hewett T.E., Dorn G.W. 2nd, Koch W.J., Molkentin J.D. (2006). Pharmacological- and gene therapy-based inhibition of protein kinase Calpha/beta enhances cardiac contractility and attenuates heart failure. Circulation, 114:574–582.

Hanoune J., Defer N. (2001). Regulation and role of adenylyl cyclase isoforms. Annu. Rev. Pharmacol. Toxicol., 41:145–174.

Hansma P.K., Drake B., Marti O., Gould S.A., Prater C.B. (1989). The scanning ion-conductance microscope. Science, 243, 641–643.

Harding V.B., Jones L.R., Lefkowitz R.J., Koch W.J., Rockman H.A. (2001). Cardiac β ARK1 inhibition prolongs survival and augments β blocker therapy in a mouse model of severe heart failure. Proc. Natl. Acad. Sci. USA. 98:5809-5814.

Harvey R.D., Calaghan S.C. (2012). Caveolae create local signalling domains through their distinct protein content, lipid profile and morphology. J. Mol. Cell. Cardiol., 52, 366–375.

Hasenfuss G., Teerlink J.R. (2011). Cardiac inotropes: current agents and future directions. Eur. Heart J., 32:1838–1845.

Hayes J.S., Brunton, L.L. (1982). Functional compartments in cyclic nucleotide action. J. Cycl. Nucleotide Res., 8, 1–16.

Hayes J.S., Brunton L.L., Brown J.H., Reese J.B., Mayer S.E. (1979). Hormonally specific expression of cardiac protein kinase activity. Proc. Natl. Acad. Sci. USA, 76, 1570–1574.

Hayes J.S., Brunton L.L., Mayer S.E. (1980). Selective activation of particulate cAMP-dependent protein kinase by isoproterenol and prostaglandin E1. J. Biol. Chem, 255, 5113–5119.

He H., Giordano F.J., Hilal-Dandan R., Choi D.J., Rockman H.A., McDonough P.M., Bluhm W.F., Meyer M., Sayen M.R., Swanson E., Dillmann W.H. (1997). Overexpression of the rat sarcoplasmic reticulum Ca^{2+} ATPase gene in the heart of transgenic mice accelerates calcium transients and cardiac relaxation. J. Clin. Invest., 100: 380-389.

Head B.P., Patel H.H., Roth D.M., Lai N.C., Niesman I.R., Farquhar, M.G., Insel P.A. (2005). G-protein-coupled receptor signaling components localize in both sarcolemmal and intracellular caveolin-3-associated microdomains in adult cardiac myocytes. J. Biol. Chem., 280, 31036–31044.

Head B.P., Patel H.H., Roth D.M. Murray F., Swaney J.S., Niesman I.R., Farquhar M.G., Insel P.A. (2006). Microtubules and actin microfilaments regulate

lipid raft/caveolae localization of adenylyl cyclase signaling components. J. Biol. Chem., 281: 26391–26399.

Hein P., Rochais F., Hoffmann C., Dorsch S., Nikolaev V.O., Engelhardt S., Berlot C.H., Lohse M.J., Bunemann M. (2006). Gs activation is time-limiting in initiating receptor-mediated signaling. J. Biol. Chem. 281, 33345-33351.

Hellstern S., Pegoraro S., Karim C.B., Lustig A., Thomas D.D., Moroder L., Engel J. (2001). Sarcolipin, the shorter homologue of phospholamban, forms oligomeric structures in detergent micelles and in liposomes. J. Biol. Chem., 276(33): 30845-30852.

Hoffman B.F., Rosen M.R. (1981). Cellular mechanisms of cardiac arrhythmias. Circ. Res., 49(1): 1-15.

Holz G.G. (2004). Epac: A new cAMP-binding protein in support of glucagon-like peptide-1 receptor-mediated signal transduction in the pancreatic beta-cell. Diabetes 53, 5-13.

Honda A., Adams S.R., Sawyer C.L., Lev-Ram V., Tsien R.Y., Dostmann W.R. (2001). Spatiotemporal dynamics of guanosine 30 , 50 -cyclic monophosphate revealed by a genetically encoded, fluorescent indicator. Proc. Natl. Acad. Sci. USA, 98, 2437–2442.

Houser S.R., Margulies K.B., Murphy A.M., Spinale F.G., Francis G.S., Prabhu S.D., Rockman H.A., Kass D.A., Molkentin J.D., Sussman M.A., Koch W.J. (2012). Animal models of heart failure: A scientific statement from the American Heart Association. Circ. Res., 111:131-150.

Houslay M.D. (2010). Underpinning compartmentalised cAMP signalling through targeted cAMP breakdown. Trends Biochem. Sci., 35, 91–100.

Houslay M.D., Adams D.R. (2003). PDE4 cAMP phosphodiesterases: modular enzymes that orchestrate signalling cross-talk, desensitization and compartmentalization. Biochem. J., 370(1), 1-18.

Houslay M. D., Baillie G. S. (2003). The role of ERK2 docking and phosphorylation of PDE4 cAMP phosphodiesterase isoforms in mediating cross-talk between the cAMP and ERK signalling pathways. Biochem. Soc. Trans., 31(6), 1186-1190.

Houslay M.D., Baillie G.S., Maurice D.H. (2007). cAMP-Specific phosphodiesterase-4 enzymes in the cardiovascular system: a molecular toolbox for generating compartmentalized cAMP signaling. Circ. Res., 100(7), 950-966.

Houslay K. F., Christian F., MacLeod R., Adams D. R., Houslay M. D., Baillie G. S. (2017). Identification of a multifunctional docking site on the catalytic unit of phosphodiesterase-4 (PDE4) that is utilised by multiple interaction partners. Biochem. J., 474(4), 597-609.

Hu C.L., Chandra R., Ge H., Pain J., Yan L., Babu G., Depre C., Iwatsubo K., Ishikawa Y., Sadoshima J., Vatner S.F., Vatner D.E. (2009). Adenylyl cyclase type

5 protein expression during cardiac development and stress. Am. J. Physiol. Heart Circ. Physiol., 297:H1776–1782.

Hu S.T., Tang Y., Shen Y.F., Ao H.H., Bai J., Wang Y.L., Yang Y.J. (2011). Protective effect of oxymatrine on chronic rat heart failure. J. Physiol. Sci., 61: 363-372.

Hu P., Zhang D., Swenson L., Chakrabarti G., Abel E.D., Litwin S.E. (2003). Minimally invasive aortic banding in mice: Effects of altered cardiomyocyte insulin signaling during pressure overload. Am. J. Physiol. Heart Circ. Physiol., 285:H1261-1269.

Hughes E., Edwards R., Middleton D.A. (2010). Heparin-derived oligosaccharides interact with the phospholamban cytoplasmic domain and stimulate SERCA function. Biochem. Biophys. Res. Commun., 401: 370-375.

Huke S., Bers D.M. (2008). Ryanodine receptor phosphorylation at serine 2030, 2808 and 2814 in rat cardiomyocytes. Biochem. Biophys. Res. Commun., 376:80-85.

Hulot J. S., Ishikawa K., Hajjar R. J. (2016). Gene therapy for the treatment of heart failure: promise postponed. Eur. Heart J., 37(21), 1651-1658.

Hung L.M., Chen J.K., Huang S.S., Lee R.S., Su M.J. (2000). Cardioprotective effect of resveratrol, a natural antioxidant derived from grapes. Cardiovasc. Res., 47: 549-555.

Iancu R. V., Ramamurthy G., Warrier,S., Nikolaev V. O., Lohse,M. J., Jones S. W., Harvey R. D. (2008). Cytoplasmic cAMP concentrations in intact cardiac myocytes. Am. J. Physiol. Cell Physiol., 295(2), C414-C422.

Inesi G., Prasad M.A., Pilankatta R. (2007). The Ca^{2+} ATPase of cardiac sarcoplasmic reticulum: Physiological role and relevance to diseases. Biochem. Biophys. Res., 369: 182-187.

Insel P.A., Head B.P., Ostrom R.S., Patel H.H., Swaney J.S., Tang C.M., Roth D.M. (2005). Caveolae and lipid rafts: G protein-coupled receptor signaling microdomains in cardiac myocytes. Ann. N. Y. Acad. Sci., 1047, 166–172.

Ito K., Yan X., Feng X., Manning W.J., Dillmann W.H., Lorell B.H. (2001). Transgenic expression of sarcoplasmic reticulum Ca^{2+} ATPase modifies the transition from hypertrophy to early heart failure. Circ. Res., 89: 422-429.

Jacobson K., Mouritsen O.G., Anderson R.G.W. (2007). Lipid rafts: at a crossroad between cell biology and physics. Nat. Cell. Biol., 9:7–14.

Janse M.J., Wit A.L. (1989). Electrophysiological mechanisms of ventricular arrhythmias resulting from myocardial ischemia and infarction. Physiol. Rev., 69: 1049-1169.

Jaski B.E., Jessup M.L., Mancini D.M., Cappola T.P., Pauly D.F., Greenberg B., Borow K., Dittrich H., Zsebo K.M., Hajjar R.J. (2009). Calcium Upregulation by Percutaneous Administration of gene therapy in Cardiac Disease (CUPID Trial), a First-in-Human Phase 1/2 Clinical Trial. J. Cardiac Fail., 15(3): 171-181.

Jessup M., Greenberg B., Mancini D., Cappola T., Pauly D.F., Jaski B., Yaroshinsky A., Zsebo K.M., Dittrich H., Hajjar R.J. (2011). Calcium Upregulation by Percutaneous Administration of Gene Therapy in Cardiac Disease (CUPID): a phase 2 trial of intracoronary gene therapy of sarcoplasmic reticulum Ca2+-ATPase in patients with advanced heart failure. Circulation, 124:304–313.

John S.W., Veress A.T., Honrath U., Chong C.K., Peng L., Smithies O., Sonnenberg H. (1996). Blood pressure and fluid-electrolyte balance in mice with reduced or absent anp. Am J Physiol., 271:R109-114 33.

Juilfs D.M., Soderling S., Burns F., Beavo J.A. (1999). Cyclic GMP as substrate and regulator of cyclic nucleotide phosphodiesterases (PDEs). Reviews Physiol. Biochem. Pharmacol., 135, 67-104.

Jurevicius J., Fischmeister R. (1996). cAMP compartmentation is responsible for a local activation of cardiac Ca2+ channels by ß-adrenergic agonists. Proc. Natl. Acad. Sci. USA. 93:295-299.

Kairouz V., Lipskaia L., Hajjar R. J., Chemaly E. R. (2012). Molecular targets in heart failure gene therapy: current controversies and translational perspectives. Ann. N. Y. Acad. Sci., 1254, 42.

Kamp T.J., Hell J.W. (2000). Regulation of cardiac L-type calcium channels by protein kinase A and protein kinase C. Circ. Res., 87, 1095–1102.

Kandel E.R. (2001). The molecular biology of memory storage: a dialogue between genes and synapses. Science, 294, 1030-1038.

Kao Y.H., Cheng C.C., Chen Y.C., Chung C.C., Lee T.I., Chen S.A., Chen Y.J. (2011). Hydralazine-induced promoter demethylation enhances sarcoplasmic reticulum Ca^{2+}-ATPase and calcium homeostasis in cardiac myocytes. Lab. Invest., 91: 1291-1297.

Karam S., Margaria J. P., Bourcier A., Mika D., Varin A., Bedioune I., Lindner M., Bouadjel K., Dessillons M., Gaudin F., Lefebvre F., Mateo P., Mechene P. Gomez S., Domergue V. Robert P., Coquard C., Algalarrondo V., Samuel J.L., Michel J.B., Charpentier F. Ghigo A., Hirsch E., Fischmeister R., Leroy J., Vandecasteele G. (2020). Cardiac overexpression of PDE4B blunts β-adrenergic response and maladaptive remodeling in heart failure. Circulation, 142(2), 161-174.

Kass-Eisler A., Falck-Pedersen E., Alvira M., Rivera J., Buttrick P.M., Wittenberg B.A., Cipriani L., Leinwand L.A. (1993). Quantitative determination of adenovirus-mediated gene delivery to rat cardiac myocytes in vitro and in vivo. Proc. Natl. Acad. Sci U S A, 90:11498-11502.

Kawase Y., Hajjar R.J. (2008). The cardiac sarcoplasmic/endoplasmic reticulum calcium ATPase: a potent target for cardiovascular diseases. Nature Clin. Pract. Cardiovasc. Med., 5: 554-565.

Kawase Y., Ladage D., Hajjar R.J. (2011). Rescuing the failing heart by targeted gene transfer. J. Am. Coll. Cardiol., 57:1169–1180.

Kawase Y., Ly H.Q., Prunier F., Lebeche D., Shi Y., Jin H., Handri L., Yoneyama R., Hoshimo K., Takewa Y., Sakata S., Peluso R., Zsebo K., Gwathmey J.K.,

Tardif J.C., Tanguay J.F., Hajjar R.J. (2008). Reversal of cardiac dysfunction after long-term expression of SERCA2a by gene transfer in a preclinical model of heart failure. J. Am. Coll. Cardiol., 51: 1112-1119.

Keating M.T., Sanguinetti M.C. (2001). Molecular and cellular mechanisms of cardiac arrhythmias. Cell, 104: 569-580.

Keeler CE. (1947). Gene therapy, J Hered, 38, 294-298.

Keely S. L. (1977). Activation of cAMP-dependent protein kinase without a corresponding increase in phosphorylase activity. Res. Commun. Chem. Pathol. Pharmacol., 18(2), 283-290.

Keravis T., Lugnier C. (2012). Cyclic nucleotide phosphodiesterase (PDE) isozymes as targets of the intracellular signalling network: Benefits of PDE inhibitors in various diseases and perspectives for future therapeutic developments. Br. J. Pharmacol., 165, 1288–1305.

Kerfant B.G., Zhao D., Lorenzen-Schmidt I., Wilson L.S., Cai S., Chen S.W., maurice D.H., Backx P.H. (2007). PI3Kγ is required for PDE4, not PDE3, activity in subcellular microdomains containing the sarcoplasmic reticular calcium ATPase in cardiomyocytes. Circ. Res., 101(4), 400-408.

Khan H., Metra M., Blair J.E., Vogel M., Harinstein M.E., Filippatos G.S., Sabbah H.N., Porchet H., Valentini G., Gheorghiade M. (2009). Istaroxime, a first in class new chemical entity exhibiting SERCA-2 activation and Na-K-ATPase inhibition: a new promising treatment for acute heart failure syndromes? Heart Fail. Rev., 14: 277-287.

Kho C., Lee A., Jeong D., Oh J.G., Chaanine A.H., Kizana E., Park W.J., Hajjar R.J. (2011). SUMO1-dependent modulation of SERCA2a in heart failure. Nature, 477:601–605.

Kim S.J., Abdellatif M., Koul S., Crystal G.J. (2008). Chronic treatment with insulin-like growth factor I enhances myocyte contraction by upregulation of Akt-SERCA2a signaling pathway. Am. J. Physiol. Heart Circ. Physiol., 295: H130-H135.

Klarenbeek J.B., Goedhart J., Hink M.A., Gadella T.W., Jalink K. (2011). A mTurquoise-based cAMP sensor for both FLIM and ratiometric read-out has improved dynamic range. PLoS One. 6: e19170.

Klarenbeek J., Goedhart J., van Batenburg A., Groenewald D., Jalink K. (2015). Fourth-generation epac-based FRET sensors for cAMP feature exceptional brightness, photostability and dynamic range: Characterization of dedicated sensors for FLIM, for ratiometry and with high affinity. PLoS ONE, 10.

Kraft A.E. (2019). Phosphodiesterases 4B and 4D Differentially Regulate cAMP Signaling in Calcium Handling Microdomains of Adult Mouse Cardiomyocytes. UHH, PhD Dissertation.

Koitabashi N., Arai M., Tomaru K., Takizawa T., Watanabe A., Niwano K., Yokoyama T., Wuytack F., Periasamy M., Nagai R., Kurabayashi M. (2005). Carvedilol effectively blocks oxidative stress-mediated downregulation of

sarcoplasmic reticulum Ca^{2+}-ATPase 2 gene transcription through modification of Sp1 binding. Biochem. Biophys. Res. Commun., 328: 116-124.

Korchev Y.E., Bashford C.L., Milovanovic M., Vodyanoy I., Lab M.J. (1997). Scanning ion conductance microscopy of living cells. Biophys. J., 73, 653–658.

Kostic M.M., Erdogan S., Rena G., Borchert G., Hoch B., Bartel S., Scotland G., Huston E., Houslay M.D., Krause E.G. (1997). Altered expression of PDE1 and PDE4 cyclic nucleotide phosphodiesterase isoforms in 7-oxo-prostacyclin-preconditioned rat heart. J. Mol. Cell. Cardiol., 29(11), 3135-3146.

Kuschel M., Zhou Y.Y., Spurgeon H.A., Bartel S., Karczewski P., Zhang S.J., Krause E.G., Lakatta E.G., Xiao R.P. (1999). β_2-adrenergic cAMP signaling is uncoupled from phosphorylation of cytoplasmic proteins in canine heart. Circulation, 99(18), 2458-2465.

Kubo H., Margulies K.B., Piacentino 3rd V., Gaughan J.P., Houser S.R. (2001). Patients with end-stage congestive heart failure treated with beta-adrenergic receptor antagonists have improved ventricular myocyte calcium regulatory protein abundance. Circulation, 104: 1012-1018.

Kuhn M. (2003). Structure, regulation, and function of mammalian membrane guanylyl cyclase receptors, with a focus on guanylyl cyclase-a. Circ. Res., 93:700-709.

Kushnir A., Marks A.R. (2010). The ryanodine receptor in cardiac physiology and disease. Adv. Pharmacol., 59:1-30.

Laemmli U. K. (1970). Cleavage of structural proteins during the assembly of the head of bacteriophage T4. Nature, 227(5259), 680-685.

Landry Y., Gies J.P. (2008). Drugs and their molecular targets: An updated overview. Fundam. Clin. Pharmacol., 22, 1–18.

Larsson H.P. (2010). How is the heart rate regulated in the sinoatrial node? Another piece to the puzzle. J. Gen. Physiol., 88, 96–107.

Laurita K.R., Rosenbaum D.S. (2007). Mechanisms and potential therapeutic targets for ventricular arrhythmias associated with impaired cardiac calcium cycling. J. Mol. Cell. Cardiol., 44: 31-43.

Lee D.I., Zhu G., Sasaki T., Cho G.S., Hamdani N., Holewinski R., Jo S.H., Danner T., Zhang M., Rainer P.P., Bedja D., Kirk J.A., Ranek M.J., Dostmann W.R., Kwon C., Margulies K.B., Van Eyk J.E., Paulus W.J., Takimoto E., Kass D.A. (2015). Phosphodiesterase 9A controls nitric-oxide-independent cGMP and hypertrophic heart disease. Nature, 519:472-476.

Leech C.A., Chepurny O.G., Holz G.G. (2010). Epac2-dependent rap1 activation and the control of islet insulin secretion by glucagon-like peptide-1. Vitam. Horm. 84, 279-302.

Lefkowitz R.J. Shenoy S.K. (2005). Transduction of receptor signals by beta-arrestins. Science, 308, 512-517.

Lehnart S.E. (2007). Novel targets for treating heart and muscle disease: Stabilizing ryanodine receptors and preventing intracellular calcium leak. Curr. Opin. Pharmacol., 7:225-232.

Lehnart S.E., Marks A.R. (2006). Phosphodiesterase 4D and heart failure: a cautionary tale. Expert Opin. Ther. Targets, 10(5), 677-688.

Lehnart S.E., Mongillo M., Bellinger A., Lindegger N., Chen B.X., Hsueh W., Reiken S., Wronska A., Drew L.J., Ward C.W., Lederer W.J., Kass R.S., Morley G., Marks A.R. (2008). Leaky Ca 2+ release channel/ryanodine receptor 2 causes seizures and sudden cardiac death in mice. J. Clin. Investig., 118(6), 2230-2245.

Lehnart S.E., Terrenoire C., Reiken S., Wehrens X.H., Song L.S., Tillman E.J., Mancarella S., Coromilas J., Lederer W.J., Kass R.J., Marks A.R. (2006). Stabilization of cardiac ryanodine receptor prevents intracellular calcium leak and arrhythmias. Proc. Natl. Acad. Sci. U. S. A., 103(20), 7906-7910.

Lehnart S.E., Wehrens X.H., Reiken S., Warrier S., Belevych A.E., Harvey R.D., Richter W., Jin S.L., Conti M., Marks A.R. (2005). Phosphodiesterase 4d deficiency in the ryanodine-receptor complex promotes heart failure and arrhythmias. Cell, 123:25-35.

Leroy J., Abi-Gerges A., Nikolaev V.O., Richter W., Lechêne P., Mazet J.L., Conti M., Fischmeister R., Vandecasteele G. (2008). Spatiotemporal dynamics of ß-adrenergic cAMP signals and L-type Ca^{2+} channel regulation in adult rat ventricular myocytes: Role of phosphodiesterases. Circ. Res., 102:1091-1100.

Leroy J., Richter W., Mika D., Castro L.R.V., Abi-Gerges A., Xie M., Scheitrum C., Lefebvre F., Schittl J., Westenbroek R., Catterall W.A., Charpentier F., Conti M., Fischmeister R., Vandecasteele G. (2011). Phosphodiesterase 4B in the cardiac L-type Ca2+ channel complex regulates Ca2+ current and protects against ventricular arrhythmias. J. Clin. Invest., 121:2651-2661.

Levin S.D., Taft D.W., Brandt C.S., Bucher C., Howard E.D., Chadwick E.M., Johnston J., Hammond A., Bontadelli K., Ardourel D., Hebb L., Wolf A., Bukowski T.R., Rixon M.W., Kuijper J.L., Ostrander C.D., West J.W., Bilsborough J., Fox B., Gao Z., Xu W., Ramsdell F., Blazar B.R., Lewis K.E. (2011). Vstm3 is a member of the CD28 family and an important modulator of T-cell function. Eur. J. Immunol., 41:902–915.

Lipskaia L., Defer N., Esposito G., Hajar I., Garel M.C., Rockman H.A., Hanoune J. (2000). Enhanced cardiac function in transgenic mice expressing a Ca^{2+}-stimulated adenylyl cyclase. Circ. Res., 86:795–801.

Lipskaia L., Chemaly E.R., Hadri L., Lompre A.M., Hajjar R.J. (2010) Sarcoplasmic reticulum Ca^{2+} ATPase as a therapeutic target for heart failure**.** Expert Opin. Biol. Ther., 10:29–41.

Lipskaia L., Ly H., Kawase Y., Hajjar R.J., Lompre A.M. (2007). Treatment of heart failure by calcium cycling gene therapy. Future Cardiol., 3:413–423.

Lipskaia L., Mougenot N., Jacquet A., Atassi F., Hajjar R.J., Hatem S.N., Limon I. (2011). Compartmentalization of cAMP increase at the level of sarcoplasmic

reticulum results in dilated and hypertrophic cardiomyopathy in aged transgenic mice. Eur. Heart J., 32(suppl 1):999.

Lohse M.J., Engelhardt S., Eschenhagen T. (2003). What is the role of ß-adrenergic signaling in heart failure? Circ. Res., 93:896-906.

Lompré A.M., Anger M., Levitsky D. (1994). Sarco (endo) plasmic reticulum calcium pumps in the cardiovascular system: function and gene expression. J. Mol. Cell. Cardiol., 26(9), 1109-1121.

Lompre A.M., Hajjar R.J., Harding S.E., Kranias E.G., Lohse M.J., Marks A.R. (2010). Ca^{2+} cycling and new therapeutic approaches for heart failure. Circulation, 121: 822-830.

Lorenz K., Schmitt J.P., Schmitteckert E.M., Lohse M.J. (2009). A new type of ERK1/2 autophosphorylation causes cardiac hypertrophy. Nat. Med., 15, 75–83.

Louch W.E., Sheehan K.A., Wolska B.M. (2011). Methods in cardiomyocyte isolation, culture, and gene transfer. J. Mol. Cell. Cardiol., 51:288-298.

Loukianov E., Ji Y., Grupp I.L., Kirkpatrick D.L., Baker D.L., Loukianova T., Grupp G., Lytton J., Walsh R.A., Periasamy M. (1998). Enhanced myocardial contractility and increased Ca^{2+} transport function in transgenic hearts expressing the fast-twitch skeletal muscle sarcoplasmic reticulum Ca^{2+}-ATPase. Circ. Res., 83: 889-897.

Lugnier C. (2006). Cyclic nucleotide phosphodiesterase (PDE) superfamily: A new target for the development of specific therapeutic agents. Pharmacol. Ther., 109, 366–398.

Lynch M.J., Baillie G.S., Mohamed A., Li X., Maisonneuve C., Klussmann E., van Heeke G., Houslay, M.D. (2005). RNA silencing identifies PDE4D5 as the functionally relevant cAMP phosphodiesterase interacting with βarrestin to control the protein kinase A/AKAP79-mediated switching of the β2-adrenergic receptor to activation of ERK in HEK293B2 cells. J. Biol. Chem., 280(39), 33178-33189.

Lyon A.R., Bannister M.L., Collins T., Pearce E., Sepehripour A.H., Dubb S.S., Garcia E., O'Gara P., Liang L., Kohlbrenner E., Hajjar R.J., Peters N.S., Poole-Wilson P.A., Macleod K.T., Harding S.E. (2011). SERCA2a gene transfer decreases sarcoplasmic reticulum calcium leak and reduces ventricular arrhythmias in a model of chronic heart failure. Circ. Arrhythm. Electrophysiol., 4: 362-372.

Lyon A.R., Sato M., Hajjar R.J., Samulski R.J., Harding S.E. (2008). Gene therapy: targeting the myocardium. Heart, 94:89–99.

Lytton J., Zarain-Herzberg A., Periasamy M., MacLennan D.H. (1989). Molecular cloning of the mammalian smooth muscle sarco(endo)plasmic reticulum Ca^{2+} -ATPase. J. Biol. Chem., 264: 7059-7065.

MacDonnell S.M., Garcia-Rivas G., Scherman J.A., Kubo H., Chen X., Valdivia H., Houser S.R. (2008). Adrenergic regulation of cardiac contractility does not involve phosphorylation of the cardiac ryanodine receptor at serine 2808. Circ. Res., 102:e65-72.

MacFarland R.T., Zelus B.D., Beavo J.A. (1991). High concentrations of a cGMP-stimulated phosphodiesterase mediate ANP-induced decreases in cAMP and steroidogenesis in adrenal glomerulosa cells. J. Biol. Chem., 266, 136–142.

MacKenzie S.J., Baillie G.S., McPhee I., MacKenzie C., Seamons, R, McSorley T., Millen J., Beard M.B., van Heeke G., Houslay M.D. (2002). Long PDE4 cAMP specific phosphodiesterases are activated by protein kinase A-mediated phosphorylation of a single serine residue in Upstream Conserved Region 1 (UCR1). Br. J. Pharmacol., 136(3), 421-433.

Maczewski M., Mackiewicz U. (2008). Effect of metoprolol and ivabradine on left ventricular remodeling and Ca^{2+} handling in the post-infarction rat heart. Cardiovasc. Res., 79: 42-51.

Madissoon E., Töhönen V., Vesterlund L., Katayama S., Unneberg P., Inzunza J., Hovatta O., Kere J. (2014). Differences in gene expression between mouse and human for dynamically regulated genes in early embryo. PLoS One, 9(8), e102949.

Marshall E. (1999). Gene therapy death prompts review of adenovirus vector. Science, 286(5448), 2244-2245.

Martinez S.E., Wu A.Y., Glavas N.A., Tang X.B., Turley S., Hol W.G., Beavo, J.A. (2002). The two GAF domains in phosphodiesterase 2A have distinct roles in dimerization and in cGMP binding. Proc. Natl. Acad. Sci. USA, 99, 13260–13265.

Martins T.J., Mumby M.C., Beavo J.A. (1982). Purification and characterization of a cyclic GMP-stimulated cyclic nucleotide phosphodiesterase from bovine tissues. J. Biol. Chem., 257, 1973–1979.

Marx S.O., Marks A.R. (2013). Dysfunctional ryanodine receptors in the heart: new insights into complex cardiovascular diseases. J. Mol. Cell. Cardiol., 58, 225-231.

Marx S.O., Reiken S., Hisamatsu Y., Jayaraman T., Burkhoff D., Rosemblit N., Marks A.R. (2000). PKA phosphorylation dissociates fkbp12.6 from the calcium release channel (ryanodine receptor): Defective regulation in failing hearts. Cell, 101:365-376.

Massberg S., Sausbier M., Klatt P., Bauer M., Pfeifer A., Siess W., Fassler R., Ruth P., Krombach F., Hofmann F. (1999). Increased adhesion and aggregation of platelets lacking cyclic guanosine 3',5'- monophosphate kinase i. J. Exp. Med., 189:1255-1264.

McMurray J.J., Adamopoulos S., Anker S.D., Auricchio A., Bohm M., Dickstein K., Falk V., Filippatos G., Fonseca C., Gomez-Sanchez M.A., Jaarsma T., Kober L., Lip G.Y., Maggioni A.P., Parkhomenko A., Pieske B.M., Popescu B.A., Ronnevik P.K., Rutten F.H., Schwitter J., Seferovic P., Stepinska J., Trindade P.T., Voors A.A., Zannad F., Zeiher A. (2012) ESC Guidelines for the diagnosis and treatment of acute and chronic heart failure 2012: The Task Force for the Diagnosis and Treatment of Acute and Chronic Heart Failure 2012 of the European Society of Cardiology. Developed in collaboration with the Heart Failure Association (HFA) of the ESC. Eur. Heart J., 33:1787-1847.

Maurice D.H., Ke H., Ahmad F., Wang Y., Chung J., Manganiello V.C. (2014). Advances in targeting cyclic nucleotide phosphodiesterases. Nat. Rev. Drug Discov., 13, 290–314.

Mehel H., Emons J., Vettel C., Wittköpper K., Seppelt D., Dewenter M., Lutz S., Sossalla S., Maier L.S., Lechêne P., Leroy J., Lefebvre F., Varin A., Eschenhagen T., Nattel S., Dobrev D., Zimmermann W.H., Nikolaev V.O, Vandecasteele G., Fischmeister R., El-Armouche A. (2013). Phoshodiesterase-2 is upregulated in human failing hearts and blunts ß-adrenergic responses in cardiomyocytes. J. Am. Coll. Cardiol., 62:1596-1606.

Meissner G. (2017). The structural basis of ryanodine receptor ion channel function. J. Gen. Physiol., 149(12), 1065-1089.

Melsom C.B., Hussain R.I., Orstavik O., Aronsen J.M., Sjaastad I., Skomedal T., Osnes J.B., Levy F.O., Krobert K.A. (2014). Non-classical regulation of beta1- and beta 2-adrenoceptor-mediated inotropic responses in rat heart ventricle by the G protein Gi. Naunyn Schmiedebergs Arch. Pharmacol., 387:1177-1186.

Mendel G. (1865). Versuche über pflanzen-hybriden. Vorgelegt in den Sitzungen.

Méry P.F., Lohmann S.M., Walter U., Fischmeister R. (1991). Ca^{2+} current is regulated by cyclic GMP-dependent protein kinase in mammalian cardiac myocytes. Proc. Natl. Acad. Sci. USA. 88:1197-1201.

Métrich M., Lucas A., Gastineau M., Samuel J.L., Heymes C., Morel E., Lezoualc'h F. (2008). Epac mediates β-adrenergic receptor–induced cardiomyocyte hypertrophy. Circ. Res., 102, 959–965.

Mi Y.F., Li X.Y., Tang L.J., Lu X.C., Fu Z.Q., Ye W.H. (2009). Improvement in cardiac function after sarcoplasmic reticulum Ca^{2+}-ATPase gene transfer in a beagle heart failure model. Chin. Med. J., 122(12): 1423-1428.

Micheletti R., Palazzo F., Barassi P., Giacalone G., Ferrandi M., Schiavone A., Moro B., Parodi O., Ferrari P., Bianchi G. (2007). Istaroxime, a stimulator of sarcoplasmic reticulum calcium adenosine triphosphatase isoform 2a activity, as a novel therapeutic approach to heart failure. Am. J., Cardiol., 99: 24A-32A.

Miller N. (2012). Glybera and the future of gene therapy in the European Union. Nat. Rev. Drug Discov., 11(5), 419-419.

Miragoli M., Moshkov A., Novak P., Shevchuk A., Nikolaev V.O., El-Hamamsy I., Potter C.M., Wright P., Kadir S.H., Lyon A.R., et al. (2011). Scanning ion conductance microscopy: A convergent high-resolution technology for multi-parametric analysis of living cardiovascular cells. J. R. Soc. Interface, 8, 913–925.

Mika D., Bobin P., Lindner M., Boet A., Hodzic A., Lefebvre F., Lechene P., Sadoune M., Samuel J.L., Algalarrondo V., Rucker-Martin C., Lambert V., Fischmeister R., Vandecasteele G., Leroy J. (2019). Synergic PDE3 and PDE4 control intracellular cAMP and cardiac excitation-contraction coupling in a porcine model. J. Mol. Cell. Cardiol., 133, 57-66.

Mika D., Bobin P., Pomérance M., Lechêne P., Westenbroek R., Catterall W.A., Vandecasteele G., Leroy J., Fischmeister R. (2013). Differential regulation of cardiac

excitation-contraction coupling by cAMP phosphodiesterase subtypes. Cardiovasc. Res., 100:336-346.

Mika D., Leroy J., Vandecasteele G., Fischmeister R. (2012). PDEs create local domains of cAMP signaling. J. Mol. Cell Cardiol., 52:323-329.

Mika D., Richter W., Westenbroek R. E., Catterall W. A., Conti M. (2014). PDE4B mediates local feedback regulation of β1-adrenergic cAMP signaling in a sarcolemmal compartment of cardiac myocytes. J. Cell Sci., 127(5), 1033-1042.

Minamisawa S., Hoshijima M., Chu G., Ward C.A., Frank K., Gu Y., Martone M.E., Wang Y., Ross J. Jr, Kranias E.G., Giles W.R., Chien K.R. (1999). Chronic phospholamban-sarcoplasmic reticulum calcium ATPase interaction is the critical calcium cycling defect in dilated cardiomyopathy. Cell, 99:313–322.

Miura M., Boyden P.A., ter Kreurs H.E.D.J. (1998). [Ca^{2+}] waves during triggered propagated contractions in intact trabeculae. Am. J. Physiol., 274: H266-H276.

Miyamoto M.I., del Monte F., Schmidt U., DiSalvo T.S., Kang Z.B., Matsui T., Guerrero J.L., Gwathmey J.K., Rosenzweig A., Hajjar R.J. (2000). Adenoviral gene transfer of SERCA2a improves left-ventricular function in aortic-banded rats in transition to heart failure. Proc. Natl. Acad. Sci. U. S. A., 97(2): 793-798.

Mohamed B.A., Hartmann N., Tirilomis P., Sekeres K., Li W., Neef S., Richter C., Zeisberg E.M., Kattner L., Didie M., Guan K., Schmitto J.D., Lehnart S.E., Luther S., Voigt N., Seidler T., Sossalla S., Hasenfuß G., Toischer, K. (2018). Sarcoplasmic reticulum calcium leak contributes to arrhythmia but not to heart failure progression. Sci. Transl. Med., 10(458).

Molina C.E., Leroy J., Richter W., Xie M., Scheitrum C., Lee I.O., Maack C., Rucker-Martin C., Donzeau-Gouge P., Verde I., Llach A., Hove-Madsen L., Conti M., Vandecasteele G., Fischmeister R. (2012). Cyclic adenosine monophosphate phosphodiesterase type 4 protects against atrial arrhythmias. J. Am. Coll. Cardiol., 59:2182-2190.

Molina C. E., Johnson D. M., Mehel H., Spätjens R. L., Mika D., Algalarrondo V., Slimane Z.H., Lechene P., Abi-Gerges N., van de Linde H.J., Leroy J., Volders P.G.A., Fischmeister R., Vandecasteele, G. (2014). Interventricular Differences in β-Adrenergic Responses in the Canine Heart: Role of Phosphodiesterases. J. Am. Heart Assoc., 3(3), e000858.

Moltzau L.R., Aronsen J.M., Meier S., Nguyen C.H., Hougen K., Orstavik O., Sjaastad I., Christensen G., Skomedal T., Osnes J.B., Levy F.O., Qvigstad E. (2013). SERCA2 activity is involved in the CNP-mediated functional responses in failing rat myocardium. Br. J. Pharmacol., 170:366-379.

Moltzau L.R., Aronsen J.M., Meier S., Skogestad J., Orstavik O., Lothe G.B., Sjaastad I., Skomedal T., Osnes J.B., Levy F.O., Qvigstad E. (2014). Different compartmentation of responses to brain natriuretic peptide and C-type natriuretic peptide in failing rat ventricle. J. Pharmacol. Exp. Ther., 350:681-690.

Moltzau L.R., Meier S., Aronsen J.M., Afzal F., Sjaastad I., Skomedal T., Osnes J.B., Levy F.O., Qvigstad E. (2014). Differential regulation of C-type natriuretic

peptide-induced cGMP and functional responses by PDE2 and PDE3 in failing myocardium. Naunyn Schmiedebergs Arch. Pharmacol., 387:407-417.

Mongillo M., McSorley T., Evellin S., Sood A., Lissandron V., Terrin A., Huston E., Hannawacker A., Lohse M.J., Pozzan T., Houslay M.D., Zaccolo M. (2004). Fluorescence resonance energy transfer-based analysis of camp dynamics in live neonatal rat cardiac myocytes reveals distinct functions of compartmentalized phosphodiesterases. Circ. Res., 95:67-75.

Mongillo M., Tocchetti C.G., Terrin A., Lissandron V., Cheung Y.F., Dostmann W.R., Pozzan T., Kass D.A., Paolocci N., Houslay M.D., Zaccolo M. (2006). Compartmentalized phosphodiesterase-2 activity blunts ß-adrenergic cardiac inotropy via an NO/cGMP-dependent pathway. Circ. Res., 98:226-234.

Morel E., Marcantoni A., Gastineau M., Birkedal R., Rochais F., Garnier A., Lompre A.M., Vandecasteele G., Lezoualc'h F. (2005). cAMP-binding protein Epac induces cardiomyocyte hypertrophy. Circ. Res., 97, 1296–1304.

Morozov A., Muzzio I.A., Bourtchouladze R., Van-Strien N., Lapidus K., Yin D., Winder D.G., Adams J.P., Sweatt J.D., Kandel E.R. (2003). Rap1 couples cAMP signaling to a distinct pool of p42/44MAPK regulating excitability, synaptic plasticity, learning, and memory. Neuron 39, 309-325.

Mougenot N., Mika D., Czibik G., Marcos E., Abid S., Houssaini A., Vallin B., Guellich A., Mehel H., Sawaki D., Vandecasteele G., Fischmeister R., Hajjar R.J., Dubois-Rande J.L., Limon I., Adnot S., Derumeaux G., Lipskaia L. (2019). Cardiac adenylyl cyclase overexpression precipitates and aggravates age-related myocardial dysfunction. Cardiovasc. Res., 115(12), 1778-1790.

Moussavi-Harami F., Razumova M.V., Racca A.W., Cheng Y., Stempien-Otero A., Regnier M. (2015). 2-Deoxy adenosine triphosphate improves contraction in human end-stage heart failure. J. Mol. Cell. Cardiol., 79:256–26.

Movsesian M. A. (2000). Therapeutic potential of cyclic nucleotide phosphodiesterase inhibitors in heart failure. Expert Opin. Investig. Drugs, 9(5), 963-973.

Movsesian M., Stehlik J., Vandeput F., Bristow M.R. (2009). Phosphodiesterase inhibition in heart failure. Heart Fail Rev., 14:255-263.

Mozaffarian D., Anker S. D., Anand I., Linker D.T., Sullivan M.D., Cleland J.G., Carson P.E., Maggioni A.P., Mann D.L., Pitt B., Poole-Wilson P.A., Levy W.C. (2007). Prediction of mode of death in heart failure. Circulation, 116(4), 392-398.

Müller F.U., Lewin G. Matus M., Neumann J., Riermann B., Wistuba J., Schütz G., Schmitz W. (2003). Impaired cardiac contraction and relaxation and decreased expression of sarcoplasmic Ca^{2+}-ATPase in mice lacking the CREM gene. The FASEB Journal, 17(1): 103-105.

Müller O.J., Lange M., Rattunde H., Lorenzen H.P., Müller M., Frey N., Bittner C., Simonides W., Katus H.A., Franz W.M. (2003). Transgenic rat hearts overexpressing SERCA2a show improved contractility under baseline conditions and pressure overload. Cardiovasc. Res., 59: 380-389.

Mumby M.C., Martins T.J., Chang M.L., Beavo J.A. (1982). Identification of cGMP-stimulated cyclic nucleotide phosphodiesterase in lung tissue with monoclonal antibodies. J. Biol. Chem., 257, 13283–13290.

Nichols C.B., Rossow C.F., Navedo M.F., Westenbroek R.E., Catterall W.A., Santana L.F., McKnight G.S. (2010). Sympathetic stimulation of adult cardiomyocytes requires association of AKAP5 with a subpopulation of L-type calcium channels. Circ. Res., 107(6), 747-756.

Niino Y., Hotta K., Oka K. (2009). Simultaneous live cell imaging using dual FRET sensors with a single excitation light. PLoS ONE, 4.

Nikolaev V.O., Bunemann M., Hein L., Hannawacker A., Lohse M.J. (2004). Novel single chain camp sensors for receptor-induced signal propagation. J. Biol. Chem., 279:37215-37218.

Nikolaev V.O., Bunemann M., Schmitteckert E., Lohse M.J., Engelhardt S. (2006). Cyclic AMP imaging in adult cardiac myocytes reveals far-reaching ß1-adrenergic but locally confined ß2-adrenergic receptor-mediated signaling. Circ. Res. 99:1084-1091.

Nikolaev V.O., Gambaryan S., Lohse M.J. (2006). Fluorescent sensors for rapid monitoring of intracellular cgmp. Nat. Methods, 3:23-25.

Nikolaev V.O., Gambaryan S., Engelhardt S., Walter U., Lohse M.J. (2005). Real-time monitoring of the PDE2 activity of live cells: hormone-stimulated cAMP hydrolysis is faster than hormone-stimulated cAMP synthesis. J. Biol. Chem., 280(3), 1716-1719.

Nikolaev V.O., Lohse M.J. (2006). Monitoring of cAMP synthesis and degradation in living cells. Physiology (Bethesda), 21:86-92.

Nikolaev V.O., Moshkov A., Lyon A.R., Miragoli M., Novak P., Paur H., Lohse M.J., Korchev Y.E., Harding S.E., Gorelik J. (2010). β2-Adrenergic receptor redistribution in heart failure changes cAMP compartmentation. Science. 327:1653-1657.

Nowakowski S.G., Kolwicz S.C., Korte F.S., Luo Z., Robinson-Hamm J.N., Page J.L., Brozovich F., Weiss R.S., Tian R., Murry C.E., Regnier M. (2013). Transgenic overexpression of ribonucleotide reductase improves cardiac performance. Proc. Natl. Acad. Sci. USA, 110:6187–6192.

Oikawa M., Wu M., Lim S., Knight W.E., Miller C.L., Cai Y., Lu Y., Blaxall B.C., Takeishi Y., Abe J.I., Yan C. (2013). Cyclic nucleotide phosphodiesterase 3A1 protects the heart against ischemia-reperfusion injury. J Mol Cell Cardiol., 64:11-19.

Okumura S., Takagi G., Kawabe J., Yang G., Lee M.C., Hong C., Liu J., Vatner D.E., Sadoshima J., Vatner S.F., Ishikawa Y. (2003). Disruption of type 5 adenylyl cyclase gene preserves cardiac function against pressure overload. Proc. Natl. Acad. Sci. USA, 100:9986–9990.

Omar F., Findlay J.E, Carfray G., Allcock R.W., Jiang Z., Moore C., Muir A.L., Lannoy M., Fertig B.A., Mai D., Day J.P., Bolger G., Baillie G.S., Schwiebert E., Klussmann E., Pyne N.J., Ong A.C.M., Bowers K., Adam J.M., Adams D.R., Houslay M.D., Henderson D.J.P. (2019). Small-molecule allosteric 558 activators of

PDE4 long form cyclic AMP phosphodiesterases. Proc. Natl. Acad. Sci. U S A. 559, 116:13320-13329.

Omori K., Kotera J. (2007). Overview of pdes and their regulation. Circ. Res., 100:309-327.

Osadchii O.E. (2007). Myocardial phosphodiesterases and regulation of cardiac contractility in health and cardiac disease. Cardiovasc. Drugs Ther., 21(3), 171-194.

Ostrom R.S., Post S.R., Insel P.A. (2000). Stoichiometry and compartmentation in G protein-coupled receptor signaling: implications for therapeutic interventions involving G(s). J. Pharmacol. Exp. Ther., 294:407–412.

Ostrom R.S., Post S.R., Pa I. (2000). Stoichiometry and compartmentation in G protein-coupled receptor signaling: implications for therapeutic interventions involving G(s). J. Pharmacol. Exp. Ther., 294:407–412.

Ostrom R.S., Violin J.D., Coleman S. Insel P.A. (2000). Selective enhancement of beta-adrenergic receptor signaling by overexpression of adenylyl cyclase type 6: colocalization of receptor and adenylyl cyclase in caveolae of cardiac myocytes. Mol. Pharmacol., 57:1075–1079.

Packer M. (1988). Neurohormonal interactions and adaptations in congestive heart failure. Circulation, 77:721-730.

Packer M., Bristow M.R., Cohn J.N., Colucci W.S., Fowler M.B., Gilbert E.M., Shusterman N.H. (1996) The effect of carvedilol on morbidity and mortality in patients with chronic heart failure. U.S. Carvedilol Heart Failure Study Group. N. Engl. J. Med., 334:1349-1355.

Packer M., Carver J.R., Rodeheffer R.J., Ivanhoe R.J., DiBianco R., Zeldis S.M., Hendrix G.H., Bommer W.J., Elkayam U., Kukin M.L., Mallis G.I., Sollano J.A., Shannon J., Tandon P.K., DeMets D.L., the PROMISE Study Research Group (1991). Effect of oral milrinone on mortality in severe chronic heart failure. The PROMISE Study Research Group. N. Engl. J. Med., 325:1468-1475.

Pani B., Singh B.B. (2009). Lipid rafts/caveolae as microdomains of calcium signalling. Cell Calcium, 45, 625–633.

Pathak A., del Monte F., Zhao W., Schultz J.E., Lorenz J.N., Bodi I., Weiser D., Hahn H., Carr A.N., Syed F., Mavila N., Jha L., Qian J., Marreez Y., Chen G., McGraw D.W., Heist E.K., Guerrero J.L., DePaoli-Roach A.A., Hajjar R.J., Kranias E.G. (2005). Enhancement of cardiac function and suppression of heart failure progression by inhibition of protein phosphatase 1. Circ. Res., 96:756–766.

Patrucco E., Notte A., Barberis L., Selvetella G., Maffei A., Brancaccio M., Marengo S., Russo G., Azzolino O., Rybalkin S.D., Silengo L., Altruda F., Wetzker R., Wymann MP., Lembo G., Hirsch E. (2004). PI3Kγ modulates the cardiac response to chronic pressure overload by distinct kinase-dependent and-independent effects. Cell, 118(3), 375-387.

Pavlaki N., De Jong K. A., Geertz B., Nikolaev V. O., Froese, A. (2021). Cardiac Hypertrophy Changes Compartmentation of cAMP in Non-Raft Membrane Microdomains. Cells, 10(3), 535.

Pavlaki N., Nikolaev V. O. (2018). Imaging of PDE2-and PDE3-mediated cGMP-to-cAMP cross-talk in cardiomyocytes. J. Cardiovasc. Dev. Dis., 5(1), 4.

Pearl J.M., Plank D.M., McLean K.M., Wagner C.J., Duffy J.Y. (2011). Glucocorticoids improve calcium cycling in cardiac myocytes after cardiopulmonary bypass. J. Surg. Res., 167: 279-286.

Pereira L., Métrich M., Fernández-Velasco M., Lucas A., Leroy J., Perrier R., Morel E., Fischmeister R., Richard S, Bénitah J.P., Lezoualc'h F., Gómez A.M. (2007). The cAMP binding protein Epac modulates Ca2+ sparks by Ca2+/calmodulin kinase signalling pathway in rat cardiac myocytes. J. Physiol., 583:685-694.

Perera R.K., Nikolaev V.O. (2013). Compartmentation of cAMP signalling in cardiomyocytes in health and disease. Acta Physiol. (Oxf)., 207:650-662.

Perera R.K., Sprenger J.U., Steinbrecher J.H., Hubscher D., Lehnart S.E., Abesser M., Schuh K., El-Armouche A., Nikolaev V.O. (2015). Microdomain switch of cGMP-regulated phosphodiesterases leads to ANP-induced augmentation of beta-adrenoceptor-stimulated contractility in early cardiac hypertrophy. Circ. Res., 116:1304-1311.

Periasamy M., Huke S. (2001). SERCA pump level is a critical determinant of calcium homeostasis and cardiac contractility. J. Mol. Cell. Cardiol., 33: 1053-1063.

Periasamy M., Kalyanasundaram A. (2007). SERCA pump isoforms: their role in calcium transport and disease. Muscle Nerve, 35: 430-442.

Perino A., Ghigo A., Ferrero E., Morello F., Santulli G., Baillie G.S., Damilano F., Dunlop A.J., Pawson C., Walser R., Levi R., Altruda f., Silengo L., Langeberg L.K., Neubauer G., Heymans S., Lembo G., Wymann M.P., Wetzker R., Houslay M.D., Iaccarino G., Scott J.D., Hirsch E. (2011). Integrating cardiac PIP 3 and cAMP signaling through a PKA anchoring function of p110γ. Mol. Cell, 42, 84–95.

Perry S.J., Baillie G.S., Kohout T.A., McPhee I., Magiera M.M., Ang K.L., Miller W.E., McLean A.J., Conti m., Houslay M.D., Lefkowitz R.J. (2002). Targeting of cyclic AMP degradation to β2-adrenergic receptors by β-arrestins. Science, 298(5594), 834-836.

Pfeffer M.A., Claggett B., Assmann S.F., Boineau R., Anand I.S., Clausell N., Desai A.S., Diaz R., Fleg J.L., Gordeev I., Heitner J.F., Lewis E.F., O'Meara E., Rouleau J.L., Probstfield J.L., Shaburishvili T., Shah S.J., Solomon S.D., Sweitzer N.K., McKinlay S.M., Pitt B. (2015). Regional variation in patients and outcomes in the Treatment of Preserved Cardiac Function Heart Failure with an Aldosterone Antagonist (TOPCAT) trial. Circulation. 131:34-42.

Pierkes M., Gambaryan S., Boknik P., Lohmann S.M., Schmitz W., Potthast R., Holtwick R., Kuhn M. (2002). Increased effects of c-type natriuretic peptide on cardiac ventricular contractility and relaxation in guanylyl cyclase a-deficient mice. Cardiovasc. Res., 53:852-861 30.

Pleger S.T., Shan C., Ksienzyk J., Bekeredjian R., Boekstegers P., Hinkel R., Schinkel S., Leuchs B., Ludwig J., Qiu G., Weber C., Raake P., Koch W.J., Katus

H.A., Muller O.J., Most P. (2011). Cardiac AAV9-S100A1 gene therapy rescues post-ischemic heart failure in a preclinical large animal model. Sci. Transl. Med., 3: 92ra64.

Pogwizd S.M., Bers D.M. (2002). Calcium cycling in heart failure. J. Cardio. Electrophysiol., 13: 88-91.

Ponsioen B., Zhao J., Riedl J., Zwartkruis F., van der Krogt G., Zaccolo M., Moolenaar W.H., Bos J.L., Jalink K. (2004). Detecting camp-induced epac activation by fluorescence resonance energy transfer: Epac as a novel camp indicator. EMBO Rep., 5:1176-1180.

Prunier F., Kawase Y., Gianni D., Scapin C., Danik S.B., Ellinor P.T., Hajjar R.J., del Monte F. (2008). Prevention of ventricular arrhythmias with sarcoplasmic reticulum Ca^{2+} ATPase pump overexpression in a porcine model of ischemia reperfusion. Circulation, 118: 614-624.

Puceat M., Bony C., Jaconi M., Vassort G. (1998). Specific activation of adenylyl cyclase V by a purinergic agonist. FEBS letters, 431:189–194.

Qu Z., Weiss J.N. (2015). Mechanisms of ventricular arrhythmias: from molecular fluctuations to electrical turbulence. Ann. Rev. Physiol., 77: 29-55.

Qvigstad E., Moltzau L.R., Aronsen J.M., Nguyen C.H., Hougen K., Sjaastad I., Levy F.O., Skomedal T., Osnes J.B. (2010). Natriuretic peptides increase beta1-adrenoceptor signalling in failing hearts through phosphodiesterase 3 inhibition. Cardiovasc. Res., 85:763-772.

Raake P.W., Hinkel R., Muller S., Delker S., Kreuzpointner R., Kupatt C., Katus H.A., Kleinschmidt J.A., Boekstegers P., Muller O.J. (2008). Cardio-specific long-term gene expression in a porcine model after selective pressure-regulated retroinfusion of adeno-associated viral (AAV) vectors. Gene Ther., 15:12-17.

Raake P.W., Schlegel P., Ksienzyk J., Reinkober J., Barthelmes J., Schinkel S., Pleger S., Mier W., Haberkorn U., Koch W.J., Katus H.A., Most P., Muller O.J. (2013). AAV6.betaARKct cardiac gene therapy ameliorates cardiac function and normalizes the catecholaminergic axis in a clinically relevant large animal heart failure model. Eur. Heart J., 34:1437-1447.

Rapoport R.M., Draznin M.B., Murad F. (1982). Sodium nitroprusside-induced protein phosphorylation in intact rat aorta is mimicked by 8-bromo cyclic GMP. Proc. Natl. Acad. Sci. U S A, 79:6470-6474.

Razani B., Woodman S. E., Lisanti M. P. (2002). Caveolae: from cell biology to animal physiology. Pharmacol. Reviews, 54(3), 431-467.

Redden J.M., Dodge-Kafka K.L., Kapiloff M.S. (2017). Function to Failure: Compartmentalization of Cardiomyocyte Signaling by A-Kinase-Anchoring Proteins. In Microdomains in the Cardiovascular System; Nikolaev, V.O., Zaccolo, M., Eds.; Springer: Cham, Switzerland, pp. 37–57.

Redfield M.M., Chen H.H., Borlaug B.A., Semigran M.J., Lee K.L., Lewis G., LeWinter M.M., Rouleau J.L., Bull D.A., Mann D.L., Deswal A., Stevenson L.W., Givertz M.M., Ofili E.O., O'Connor C.M., Felker G.M., Goldsmith S.R., Bart B.A., McNulty S.E., Ibarra J.C., Lin G., Oh J.K., Patel M.R., Kim R.J., Tracy R.P.,

Velazquez E.J., Anstrom K.J., Hernandez A.F., Mascette A.M., Braunwald E. (2013). Effect of phosphodiesterase-5 inhibition on exercise capacity and clinical status in heart failure with preserved ejection fraction: a randomized clinical trial. JAMA. 309:1268-1277.

Regitz-Zagrosek V., Hertrampf R., Steffen C., Hildebrandt A., Fleck E. (1994). Myocardial cyclic AMP and norepinephrine content in human heart failure. Eur. Heart J. 1994; 15(Suppl D):7–13.

Richter W., Conti M. (2002). Dimerization of the type 4 cAMP-specific phosphodiesterases is mediated by the upstream conserved regions (ucrs). J. Biol. Chem., 277:40212-40221.

Richter W., Day P., Agrawal R., Bruss M.D., Granier S., Wang Y.L., Rasmussen S.G.F., Horner K., Wang P., Lei T., Patterson A.J., Kobilka B., Conti M. (2008). Signaling from β1-and β2-adrenergic receptors is defined by differential interactions with PDE4. The EMBO journal, 27(2), 384-393.

Richter W., Jin S.L.C., Conti M. (2005). Splice variants of the cyclic nucleotide phosphodiesterase PDE4D are differentially expressed and regulated in rat tissue. Biochem. J., 388:803–811.

Richter W., Xie M., Scheitrum C., Krall J., Movsesian M. A., Conti M. (2011). Conserved expression and functions of PDE4 in rodent and human heart. Basic Res. Cardiol., 106(2), 249-262.

Rochais F., Abi-Gerges A., Horne, K., Lefebvre F., Cooper D. M., Conti M., Fischmeister R., Vandecasteele G. (2006). A specific pattern of phosphodiesterases controls the cAMP signals generated by different Gs-coupled receptors in adult rat ventricular myocytes. Circ. Res., 98(8), 1081-1088.

Rosen M.R. (1988). Mechanisms of arrhythmias. Am. J. Cardiol., 61: 2A-8A.

Rosman G.J., Martins T.J., Sonnenburg W.K., Beavo J.A., Ferguson K., Loughney K. (1997). Isolation and characterization of human cDNAs encoding a cGMP-stimulated 30, 50 -cyclic nucleotide phosphodiesterase. Gene, 191, 89–95.

Rudokas M.W., Post J.P., Sataray-Rodriguez A., Sherpa R.T., Moshal K.S., Agarwal S.R., Harvey R.D. (2021). Compartmentation of beta2 -Adrenergic Receptor Stimulated cAMP Responses by Phosphodiesterases Type 2 and 3 in Cardiac Ventricular Myocytes. Br. J. Pharmacol., 178(7), 1574-1587.

Rupp H., Vetter R. (2000). Sarcoplasmic reticulum function and carnitine palmitoyltrasferase-1 inhibition during progression of heart failure. Br. J. Pharmacol., 131: 1748-1756.

Rybin V.O., Xu X., Lisanti M.P., Steinberg S.F. (2000). Differential targeting of beta -adrenergic receptor subtypes and adenylyl cyclase to cardiomyocyte caveolae. A mechanism to functionally regulate the cAMP signaling pathway. J. Biol. Chem., 275:41447–41457.

Sadek M. S., Cachorro E., El-Armouche A., Kämmerer S. (2020). Therapeutic Implications for PDE2 and cGMP/cAMP Mediated Crosstalk in Cardiovascular Diseases. Int. J. Mol. Sci., 21(20), 7462.

Saiki R.K., Gelfand D.H., Stoffel S., Scharf S.J., Higuchi R., Horn G.T., Mullis K.B., Erlich H.A. (1988). Primer-directed enzymatic amplification of DNA with a thermostable DNA polymerase. Science, 239:487-491.

Sakata S., Lebeche D., Sakata N., Sakata Y., Chemaly E.R., Liang L.F., Takewa Y., jeong D., Park W.J., Kawase Y., Hajjar R.J. (2007). Targeted gene transfer increases contractility and decreases oxygen cost of contractility in normal rat hearts. Am. J. Physiol. Heart Circ. Physiol., 292: H2356-H2363.

Sakata S., Lebeche D., Sakata N., Sakata Y., Chemaly E.R., Liang L.F., Tsuji T., Takewa Y., del Monte F., Peluso R., Zsebo K., Jeong D., Park W.J., Kawase Y., Hajjar R.J. (2007). Restoration of mechanical and energetic function in failing aortic-banded rat hearts by gene transfer of calcium cycling proteins. J. Mol. Cell. Cardiol., 42: 852-861.

Sakata S., Lebeche D., Sakata Y., Sakata N., Chemaly E.R., Liang L.F., Nakajima-Takenaka C., Tsuji T., Konishi N., del Monte F., Hajjar R.J., Takaki M. (2007). Transcoronary gene transfer of SRCA2a increases coronary blood flow and decreases cardiomyocyte size in a Type 2 diabetic rat model. Am. J. Physiol. Heart Circ. Physiol., 292: H1204-H1207.

Sakata S., Lebeche D., Sakata Y., Sakata N., Chemaly E.R., Liang L.F., Padmanabhan P., Konishi N., Takaki M., del Monte F., Hajjar R.J. (2006). Mechanical and metabolic rescue in a Type II diabetes model of cardiomyopathy by targeted gene transfer. Mol. Therap., 13(5): 987-996.

Sassi Y., Abi-Gerges A., Fauconnier J., Mougenot N., Reiken S., Haghighi K., Kranias E.G., Marks A.R., Lacampagne A., Engelhardt S., Hatem S.N., Lompre A.M., Hulot J.S. (2012). Regulation of cAMP homeostasis by the efflux protein MRP4 in cardiac myocytes. FASEB J., 26, 1009–1017.

Sato M., Hida N., Ozawa T., Umezawa Y. (2000). Fluorescent indicators for cyclic GMP based on cyclic GMP-dependent protein kinase I alpha and green fluorescent proteins. Anal. Chem., 72, 5918–5924.

Saucerman J.J., Greenwald E.C., Polanowska-Grabowska R. (2014). Mechanisms of cyclic AMP compartmentation revealed by computational models. J. Gen. Physiol., 143, 39–48.

Schindler R.F.R., Brand T. (2016). The Popeye domain containing protein family-A novel class of cAMP effectors with important functions in multiple tissues. Prog. Biophys. Mol. Biol., 120, 28–36.

Schmidt U., del Monte F., Miyamoto M.I., Matsui t., Gwathmey J.K., Rosenzweig A., Hajjar R.J. (2000). Restoration of diastolic function in senescent rat hearts through adenoviral gene transfer of sarcoplasmic reticulum Ca^{2+}-ATPase. Circulation, 101: 790-796.

Schrade K., Klussmann E. (2017). Pharmacological approaches for delineating functions of AKAP-based signalling complexes and finding therapeutic targets. In Microdomains in the Cardiovascular System; Nikolaev, V.O., Zaccolo, M., Eds.; Springer: Cham, Switzerland, pp. 59–83.

Schroeder V.A., Pearl J.M., Schartz S.M., Shanley T.P., Manning P.B., Nelson D.P. (2003). Combined steroid treatment for congenital heart surgery improves oxygen delivery and reduces postbypass inflammatory mediator expression. Circulation, 107: 2823-2828.

Scoote M., Williams A.J. (2004). Myocardial calcium signaling and arrhythmia pathogenesis. Biochem. Biophys. Res. Communi., 322: 1286-1309.

Seifert R. (2015). cCMP and cUMP: Emerging second messengers. Trends Biochem. Sci., 40, 8–15.

Seifert R., Schneider E.H., Bähre H. (2015). From canonical to non-canonical cyclic nucleotides as second messengers: Pharmacological implications. Pharmacol. Ther., 148, 154–184.

Shah S.J., Wasserstrom J.A. (2012). SERCA2a Gene Therapy for the Prevention of Sudden Cardiac Death A Future Theranostic for Heart Failure? Circulation, 126(17): 2047-2050.

Shakur Y., Holst L.S., Landstrom T.R., Movsesian M., Degerman E., Manganiello V. (2001). Regulation and function of the cyclic nucleotide phosphodiesterase (PDE3) gene family. Prog. Nucleic Acid Res. Mol. Biol., 66, 241–277.

Shan J., Betzenhauser M.J., Kushnir A., Reiken S., Meli A.C., Wronska A., Dura M., Chen B.X., Marks A.R. (2010). Role of chronic ryanodine receptor phosphorylation in heart failure and β-adrenergic receptor blockade in mice. J. Clin. Invest., 120(12), 4375-4387.

Shareef M.A., Anwer L.A., Poizat C. (2014). Cardiac SERCA2A/B: Therapeutic targets for heart failure. Eur. J. Pharmacol., 724: 1-8.

Sikkel M.B., Hayward C., MacLeod K.T., Harding S.E., Lyon A.R. (2014). SERCA2a gene therapy in heart failure: an anti-arrhythmic positive inotrope. Brit. J. Pharmacol., 171: 38-54.

Simmerman H.K., Jones L.R. (1998). Phospholamban: Protein structure, mechanism of action, and role in cardiac function. Physiol Rev., 78:921-947 43.

Simmons M.A., Hartzell H.C. (1988). Role of phosphodiesterase in regulation of calcium current in isolated cardiac myocytes. Mol. Pharmacol., 33, 664–671.

Simon M.M., Greenaway S., White J.K. *et al.* (2013). A comparative phenotypic and genomic analysis of C57BL/6J and C57BL/6N mouse strains. Genome Biol**.** 14**,** R82.

Simpson I.A. Sahn D.J. (1993). Comparative imaging techniques and models. Curr. Op. Cardiol., 8, 1021-1026.

Smith P.K., Krohn R.I., Hermanson G.T., Mallia A.K., Gartner F.H., Provenzano M.D., Fujimoto E.K., Goeke N.M., Olson B.J., Klenk D.C. (1985). Measurement of protein using bicinchoninic acid. Anal. Biochem., 150:76-85.

Soga M., Kamal F.A., Watanabe K., Ma M., Palaniyandi S., Prakash P., Veeraveedu P., Mito S., Kunisaki M., Tachikawa H., Kodama M., Aizawa Y. (2006). Effects of angiotensin II receptor blocker (candesartan) in daunorubicin-induced cardiomyopathic rats. Int. J. Cardiol., 110: 378-385.

Sprenger J. U., Nikolaev V. O. (2013). Biophysical techniques for detection of cAMP and cGMP in living cells. Int. J. Mol. Sci., 14(4), 8025-8046.

Sprenger J.U., Perera R.K., Gotz K.R., Nikolaev, V.O. (2012). FRET microscopy for real-time monitoring of signaling events in live cells using unimolecular biosensors. J. Vis. Exp., e4081.

Sprenger J.U., Perera R.K., Steinbrecher J.H., Lehnart S.E., Maier L.S., Hasenfuss G., Nikolaev V.O. (2015). In vivo model with targeted cAMP biosensor reveals changes in receptor-microdomain communication in cardiac disease. Nat. Commun., 6:6965.

Stark J.C., Haydock S.F., Foo R., Brown M.J., Harding S.E. (2004). Effect of overexpressed adenylyl cyclase VI on beta 1- and beta 2-adrenoceptor responses in adult rat ventricular myocytes. Br. J. Pharmacol., 143:465–476.

Stangherlin A., Gesellchen F., Zoccarato A., Terrin A., Fields L.A., Berrera M., Surdo N.C., Craig M.A., Smith G., Hamilton G., Zaccolo M. (2011). cGMP signals modulate cAMP levels in a compartment-specific manner to regulate catecholamine-dependent signaling in cardiac myocytes. Circ Res.,108:929-939.

Steinberg S. F., Brunton L. L. (2001). Compartmentation of G protein-coupled signaling pathways in cardiac myocytes. Annu. Rev. Pharmacol. Toxicol., 41(1), 751-773.

Subramanian H., Froese A., Jönsson P., Schmidt H., Gorelik J., Nikolaev V. O. (2018). Distinct submembrane localisation compartmentalises cardiac NPR1 and NPR2 signalling to cGMP. Nat. Commun., 9(1), 1-9.

Sulaiman M., Matta M.J., Sunderesan N.R., Gupta M.P., Periasamy M., Gupta M. (2010). Resveratrol, an activator of SIRT1, upregulates sarcoplasmic calcium

ATPase and improves cardiac function in diabetic cardiomyopathy. Am. J. Physiol. Heart Circ. Physiol., 298: H833-H843.

Sulakhe P.V., Vo X.T. (1995). Regulation of phospholamban and troponin-i phosphorylation in the intact rat cardiomyocytes by adrenergic and cholinergic stimuli: Roles of cyclic nucleotides, calcium, protein kinases and phosphatases and depolarization. Mol. Cell Biochem., 149- 150:103-126.

Sun Y.L., Hu S.J., Wang L.H., Hu Y., Zhou J.Y. (2005). Effect of beta-blockers on cardiac function and calcium handling protein in postinfarction heart failure rats. Chest, 128: 1812-1821.

Sun B., Li H., Shakur Y., Hensley J., Hockman S., Kambayashi J., Manganiello V.C., Liu Y. (2007). Role of phosphodiesterase type 3A and 3B in regulating platelet and cardiac function using subtype-selective knockout mice. Cell Signal., 19, 1765–1771.

Swaminathan P.D., Purohit A., Hund T.J., Anderson M.E. (2012). Calmodulin-dependent protein kinase II: linking heart failure and arrhythmias. Circ. Res., 110:1661-1677.

Takimoto E., Champion H.C., Li M., Belardi D., Ren S., Rodriguez E.R., Bedja D., Gabrielson K.L., Wang Y., Kass D.A. (2005). Chronic inhibition of cyclic gmp phosphodiesterase 5a prevents and reverses cardiac hypertrophy. Nat. Med.,11:214-222.

Takimoto E., Kass D.A. (2007). Role of oxidative stress in cardiac hypertrophy and remodeling. Hypertension, 49:241-248.

Talukder M.A.H., Kalyanasundaram A., Zhao X., Zuo L., Bhupathy P., Babu G.J., Cardounel A.J., Periasamy M., Zweier J.L. (2007). Expression of SERCA isoform with faster Ca^{2+} transport properties improves postischemic cardiac function and Ca^{2+} handling and decreases myocardial infarction. Am. J. Physiol. Heart Circ. Physiol., 293: H2418-H2428.

Tang T., Hammond H.K., Firth A., Yang Y., Gao M.H., Yuan J.X., Lai N.C. (2011). Adenylyl cyclase 6 improves calcium uptake and left ventricular function in aged hearts. J. Am. Coll. Cardiol., 57:1846–1855.

Tengholm A., Gylfe E. (2009). Oscillatory control of insulin secretion. Mol. Cell Endocrinol., 297, 58-72.

ter Keurs H.E.D.J., Boyden P.A. (2007). Calcium and arrhythmogenesis. Physiol. Rev., 87: 457-506.

Terrin A., Monterisi S., Stangherlin A., Zoccarato A., Koschinski A., Surdo N. C., Mongillo M., Sawa A. Jordanides N.E., Mountford J.C., Zaccolo M. (2012). PKA and PDE4D3 anchoring to AKAP9 provides distinct regulation of cAMP signals at the centrosome. J. Cell Biol., 198(4), 607-621.

Tepe N.M., Lorenz J.N., Yatani A., Dash R., Kranias E.G., Dorn G.W. 2nd, Liggett S.B. (1999). Altering the receptor-effector ratio by transgenic overexpression of type V adenylyl cyclase: enhanced basal catalytic activity and function without increased cardiomyocyte beta-adrenergic signalling. Biochemistry, 38:16706–16713.

Terracciano C.M., Hajjar R.J., Harding S.E. (2002). Overexpression of SERCA2a accelerates repolarization in rabbit ventricular myocytes. Cell Calcium, 31: 299-305.

Thunemann M., Wen L., Hillenbrand M., Vachaviolos A., Feil S., Ott T., Han X., Fukumura D., Jain R.K., Russwurm M., de Wit C., Feil R. (2013). Transgenic mice for cgmp imaging. Circ. Res., 113:365- 371.

Thompson W.J., Appleman M.M. (1971). Multiple cyclic nucleotide phosphodiesterase activities from rat brain. Biochemistry. 10:311-316.

Timerman A.P., Jayaraman T., Wiederrecht G., Onoue H., Marks A.R., Fleischer S. (1994). The ryanodine receptor from canine heart sarcoplasmic reticulum is associated with a novel fk-506 binding protein. Biochem. Biophys. Res. Commun., 198:701-706.

Timofeyev V., Myers R.E., Kim H.J., Woltz R.L., Sirish P., Heiserman J.P., Li N., Singapuri A., Tang T., Yarov-Yarovoy,V., Yamoah E.N., Hammond H.K., Chiamvimonvat N. (2013). Adenylyl cyclase subtype-specific compartmentalization: Differential regulation of L-type Ca2+ current in ventricular myocytes. Circ. Res., 112, 1567–1576.

Torgersen K.M., Vang T., Abrahamsen H., Yaqub S., Tasken K. (2002). Molecular mechanisms for protein kinase A-mediated modulation of immune function. Cell Signal 14, 1-9.

Towbin H., Staehelin T., Gordon J. (1979). Electrophoretic transfer of proteins from polyacrylamide gels to nitrocellulose sheets: procedure and some applications. Proc. Natl. Acad. Sci. U. S. A., 76(9), 4350-4354.

Trost S.U., Belke D.D., Bluhm W.F., Meyer M., Swanson E., Dillmann W.H. (2002). Overexpression of the sarcoplasmic reticulum Ca^{2+}-ATPase improves myocardial contractility in diabetic cardiomyopathy. Diabetes, 51: 1166-1171.

Tsai E.J., Kass D.A., (2009). Cyclic GMP signaling in cardiovascular pathophysiology and therapeutics. Pharmacol. Ther.122:216-238.

Vandecasteele G., Rochais F., Abi-Gerges A., Fischmeister R. (2006). Functional localization of cAMP signalling in cardiac myocytes. Biochem. Soc. Trans., 34, 484–488.

Vandeput F., Wolda S.L., Krall J., Hambleton R., Uher L., McCaw K.N., Radwanski P.B., Florio V., Movsesian M.A. (2007). Cyclic nucleotide phosphodiesterase PDE1C1 in human cardiac myocytes. J. Biol. Chem., 282, 32749–32757.

Vangheluwe P., Raeymaekers L., Dode L., Wyutack F. (2005). Modulating sarco(endo)plasmic reticulum Ca^{2+}-ATPase 2 (SERCA2) activity: cell biological implications. Cell calcium, 38(3): 291-302.

Vangheluwe P., Sipido K.R., Raeymaekers L., Wuytack F. (2006). New perspectives on the role of SERCA2's Ca^{2+} affinity in cardiac function. Biochim. Biophys. Acta, 1763: 1216-1228.

Vatner S.F., Yan L., Ishikawa Y., Vatner D.E., Sadoshima J. (2009). Adenylyl cyclase type 5 disruption prolongs longevity and protects the heart against stress. Circ. J., 73:195–200.

Venetucci L. A., Trafford A.W., O'Neill S.C., Eisner D.A. (2008). The sarcoplasmic reticulum and arrhythmogenic calcium release. Cardiovasc. Res., 77: 285-292.

Vettel C., Lindner M., Dewenter M., Riedel M., Lämmle S., Mason F., Meinecke S., Brunner F.J., Geerts A., Hoffmann M., Wunder F., Wieland T., Wagner M., Sossalla S., Mehel H., Karam S., Lechêne P., Leroy J., Vandecasteele G., Fischmeister R., El-Armouche A. (2017). Phosphodiesterase 2 controls heart rate and protects against catecholamine-induced arrhythmias. Circ. Res., 120(1): 120-132.

Vinge L.E., Raake P.W., Koch W.J. (2008). Gene therapy in heart failure. Circ. Res., 102:1458–1470.

Waagstein F, Hjalmarson A, Varnauskas E, Wallentin I. (1976) Proceedings: Chronic beta-adrenergic receptor blockade in congestive cardiomyopathy. Br. Heart J., 38:537-538.

Wagner E., Lauterbach M.A., Kohl T., Westphal V., Williams G.S., Steinbrecher J.H., Streich J.H., Korff B., Tuan H.T., Hagen B. et al. (2012). Stimulated emission depletion live-cell super-resolution imaging shows proliferative remodeling of T-tubule membrane structures after myocardial infarction. Circ. Res., 111, 402–414.

Wang Y., Shi Q., Li M., Zhao M., Reddy Gopireddy R., Teoh J.P., Xu B., Zhu C., Ireton K.E., Srinivasan S., Chen S., Gasser P.J., Bossuyt J., Hell J.W., Bers D.M., Xiang Y.K. (2021). Intracellular β_1-Adrenergic Receptors and Organic Cation Transporter 3 Mediate Phospholamban Phosphorylation to Enhance Cardiac Contractility. Circ. Res., 128(2):246-261.

Weber C., Neacsu I., Krautz B., Schlegel P., Sauer S., Raake P., Ritterhoff J., Jungmann A., Remppis A.B., Stangassinger M., Koch W.J., Katus H.A., Muller O.J., Most P., Pleger S.T. (2014). Therapeutic safety of high myocardial expression levels of the molecular inotrope S100A1 in a preclinical heart failure model. Gene Ther., 21:131-138.

Weber S., Zeller M., Guan K., Wunder F., Wagner M., El-Armouche, A. (2017). PDE2 at the crossway between cAMP and cGMP signalling in the heart. Cell. Signal., 38, 76-84.

Wehrens X. H., Lehnart S. E., Huang F., Vest J. A., Reiken S. R., Mohler P. J., Sun J., Guatimosim S., Song L.S., Rosemblit N., D'Armiento J.M., Napolitano C., Memmi M., Priori S.G., Lederer W.J., Marks A. R. (2003). FKBP12. 6 deficiency and defective calcium release channel (ryanodine receptor) function linked to exercise-induced sudden cardiac death. Cell, 113(7), 829-840.

Wehrens X.H.T., Lehnart S.E., Marks A.R. (2005). Intracellular calcium release and cardiac disease. Annu. Rev. Physiol., 67: 69-98.

Wehrens X.H., Lehnart S.E., Reiken S.R., Marks A.R. (2004). Ca^{2+}/calmodulin-dependent protein kinase ii phosphorylation regulates the cardiac ryanodine receptor. Circ. Res., 94:e61-70.

Weiss J.N., Nivala M., Garfinkel A., Qu Z. (2011). Alternans and arrhythmias – From cell to heart. Circ. Res., 108: 98-112.

Weishaar R.E., Kobylarz-Singer D.C., Kaplan H.R. (1987). Subclasses of cyclic AMP phosphodiesterase in cardiac muscle. J. Mol. Cell. Cardiol., 19(10), 1025-1036.

Wen J.F., Cui X., Jin J.Y., Kim S.M., Kim S.Z., Kim S.H., Kim S.H., Lee H.S., Cho K.W. (2004). High and low gain switches for regulation of camp efflux concentration. Circ. Res. 94, 936–943.

Williams T.M., Lisanti M.P. (2004). The caveolin proteins. Genome Biol., 5:214.

Wit A.L., Cranfield P.F. (1974). Effect of verapamil on the SA and AV nodes of the rabbit and the mechanism by which it arrests reentrant atrioventricular nodal tachycardia. Circ. Res., 35: 413-425.

Wit A.L., Cranfield P.F. (1978). Reentrant excitation as a cause of cardiac arrhythmias. Am. J. Physiol., 235: H1.

Wit A.L., Rosen M.R. (1983). Pathophysiologic mechanisms of cardiac arrhythmias. Am. Heart J., 106: 798-811.

Witcher D.R., Kovacs R.J., Schulman H., Cefali D.C., Jones L.R. (1991). Unique phosphorylation site on the cardiac ryanodine receptor regulates calcium channel activity. J. Biol. Chem., 266(17), 11144-11152.

Wittkopper K., Dobrev D., Eschenhagen T., El-Armouche A. (2011). Phosphatase-1 inhibitor-1 in physiological and pathological beta-adrenoceptor signalling. Cardiovasc. Res., 91:392–401.

Wood E.R., Bledsoe R., Chai J., Daka P., Deng H., Ding Y., Harris-Gurley S., Kryn L.H., Nartey E., Nichols J., Nolte R.T., Prabhu N., Rise C., Sheahan T., Shotwell B., Smith D., Tai V., taylor J.D., Tomberlin G., Wang L., Wisely B., You S., Xia B., Dickson H., (2015). The role of phosphodiesterase 12 (PDE12) as a negative regulator of the innate immune response and the discovery of antiviral inhibitors. J. Biol. Chem., 290, 19681–19696.

Wuytack F. Raeymaekers L., Missiaen L. (2002). Molecular physiology of the SERCA and SPCA pumps. Cell Calcium, 32(5-6): 279-305.

Xiang Y., Kobilka B.K. (2003). Myocyte adrenoceptor signaling pathways. Science, 300:1530-1532.

Xiao R. P. (2001). β-Adrenergic signaling in the heart: dual coupling of the β2-adrenergic receptor to Gs and Gi proteins. Science's STKE, 2001(104), re15-re15.

Xu L., Meissner G. (2004). Mechanism of calmodulin inhibition of cardiac sarcoplasmic reticulum ca2+ release channel (ryanodine receptor). Biophys. J., 86:797-804.

Xu X.L., Chen X.J., Ji H., Li P., Bian Y.Y., Yang D., Xu J.D., Bian Z.P., Zhang J.N. (2008). Astragaloside IV improved intracellular calcium handling in hypoxia-reoxygenated cardiomyocytes via the sarcoplasmic reticulum Ca-ATPase. Pharmacology 81: 325-332.

Yamaguchi N., Xu L., Pasek D.A, Evans K.E., Meissner G. (2003). Molecular basis of calmodulin binding to cardiac muscle ca(2+) release channel (ryanodine receptor). J. Biol. Chem., 278:23480- 23486.

Yamamoto T., Manganiello V.C., Vaughan M. (1983). Purification and characterization of cyclic GMP-stimulated cyclic nucleotide phosphodiesterase from calf liver. Effects of divalent cations on activity. J. Biol. Chem., 258, 12526–12533.

Yan C., Miller C.L., Abe J. (2007). Regulation of phosphodiesterase 3 and inducible cAMP early repressor in the heart. Circ. Res., 100:489-501.

Yang Q., Paskind M., Bolger G., Thompson W.J., Repaske D.R., Cutler L.S., Epstein P.M. (1994). A novel cyclic GMP stimulated phosphodiesterase from rat brain. Biochem. Biophys. Res. Commun., 205, 1850–1858.

Yang L., Zhou Z., Tan S., Zhnag Y., Jin P. (2009). Detection of carboxypeptidase H specific T cells in peripheral blood of latent autoimmune diabetic patients with carboxypeptidase antibody positivity by ELISPOT assay. Journal of Central South University. Med. Sci., 34(10), 1011-1016.

Yano M., Yamamoto T., Ikeda Y., Matsuzaki M. (2006). Mechanisms of Disease: ryanodine receptor defects in heart failure and fatal arrhythmia. Nat. Clin. Pract. Cardiovasc. Med., 3(1), 43-52.

Yuan Q., Fan G.C., Dong M., Altschafl B., Diwan A., Ren X., Hahn H.H., Zhao W., Waggoner J.R., Jones L.R., Jones W.K., Bers D.M., Dorn G.W. 2nd, Wang H.S., Valdivia H.H., Chu G., Kranias E.G. (2007). Sarcoplasmic reticulum calcium overloading in junctin deficiency enhances cardiac contractility but increases ventricular automaticity. Circulation, 115(3): 300-309.

Zacchigna S., Zentilin L., Giacca M. (2014). Adeno-associated virus vectors as therapeutic and investigational tools in the cardiovascular system. Circ. Res., 114:1827-1846.

Zaccolo M. (2004). Use of chimeric fluorescent proteins and fluorescence resonance energy transfer to monitor cellular responses. Circ. Res., 94(7), 866-873.

Zaccolo M., Movsesian M.A. (2007). cAMP and cGMP signaling cross-talk: Role of phosphodiesterases and implications for cardiac pathophysiology. Circ. Res., 100:1569-1578.

Zaccolo M., Pozzan T. (2002). Discrete microdomains with high concentration of camp in stimulated rat neonatal cardiac myocytes. Science, 295:1711-1715.

Zagotta W.N., Olivier N.B., Black K.D., Young E.C., Olson R., and Gouaux E. (2003). Structural basis for modulation and agonist specificity of HCN pacemaker channels. Nature 425, 200-205.

Zalk R., Lehnart S.E., Marks A.R. (2007). Modulation of the ryanodine receptor and intracellular calcium. Annu. Rev. Biochem., 76:367-385.

Zarain-Herzberg A., MacLennan D.H., Periasamy M. (1990). Characterization of rabbit cardiac sarco(endo)plasmic reticulum Ca^{2+}-ATPase gene. J. Biol. Chem., 265: 4670-4677.

Zaza A., Rocchetti M. (2015). Calcium store stability as an antiarrhythmic endpoint. Curr. Pharm. Des., 21(8): 1053-1061.

Zeng J., Rudy Y. (1995). Early after depolarizations in cardiac myocytes: mechanism and rate dependence. Biophys. J., 68(3): 949-964.

Zhang H., Makarewich C.A., Kubo H., Wang W., Duran J.M., Li Y., Berretta R.M., Koch W.J., Chen X., Gao E., Valdivia H.H., Houser S.R. (2012). Hyperphosphorylation of the cardiac ryanodine receptor at serine 2808 is not involved in cardiac dysfunction after myocardial infarction. Circ. Res., 110:831-840.

Zhang L., Franzini-Armstrong C., Ramesh V., Jones L.R. (2001). Structural alterations in cardiac calcium release units resulting from overexpression of junctin. J. Mol. Cell. Cardiol., 33:233-247.

Zhang L., Kelley J., Schmeisser G., Kobayashi Y.M., Jones L.R. (1997). Complex formation between junctin, triadin, calsequestrin, and the ryanodine receptor. Proteins of the cardiac junctional sarcoplasmic reticulum membrane. J. Biol. Chem., 272:23389-23397.

Zhao C. Y., Greenstein J. L., Winslow R. L. (2015). Interaction between phosphodiesterases in the regulation of the cardiac β-adrenergic pathway. J. Mol. Cell. Cardiol., 88, 29-38.

Zhao X.L., Gutierrez L.M., Chang C.F., Hosey M.M. (1994). The alpha 1-subunit of skeletal muscle l-type ca channels is the key target for regulation by a-kinase and protein phosphatase-1c. Biochem. Biophys. Res. Commun., 198:166-173 42.

Zhu L., Zhong X., Chen S. W., Banavali N., Liu, Z. (2013). Modeling a ryanodine receptor N-terminal domain connecting the central vestibule and the corner clamp region. J. Biol. Chem., 288(2), 903-914.

Zhu W.Z., Zheng M., Koch W.J., Lefkowitz R.J., Kobilka B.K. and Xiao R.P. (2001). Dual modulation of cell survival and cell death by beta(2)-adrenergic signaling in adult mouse cardiac myocytes. Proc. Natl. Acad. Sci. U S A.98:1607-12.

Zoccarato A., Surdo N.C., Aronsen J.M., Fields L.A., Mancuso L., Dodoni G., Stangherlin A., Livie C., Jiang H., Sin Y.Y., Gesellchen F., Terrin A., Baillie G.S., Nicklin S.A., Graham D., Szabo-Fresnais N., Krall J., Vandeput F., Movsesian M., Furlan L., Corsetti V., Hamilton G.M., Lefkimmiatis K., Sjaastad I., Zaccolo M. (2015). Cardiac hypertrophy is inhibited by a local pool of cAMP regulated by phosphodiesterase 2. Circ. Res., 117:707-719.

Zipes D.P (2003). Mechanisms of clinical arrhythmias. J. Cardiovasc. Electrophysiol., 14(8): 902-912.

8. Appendix

8.1 Chemical categorization according to GHS

Chemical	H Statement	P Statement	Hazard Pictograms
Ammonium Persulfate (APS)	**272, 302, 315, 317, 319, 334, 335**	**210, 28, 301 + 012 + 030, 302 + 352, 305 + 351 + 338**	**02, 07, 08**
Ampuwa water			
BAY60-7550			
β-Mercaptoethanol	**301 + 331, 310, 315, 317, 318, 361fd, 373, 410**	**201, 262, 280, 301 + 310 + 330, 302 + 310 + 352, 305 + 310 + 338 + 351**	**05, 06, 08, 09**
Bovine serum albumin (BSA)			
Bromphenolblue			
2,3-Butandione monoxime (BDM)	**302, 312, 315, 319, 332, 335**	**261, 264, 270, 271, 280, 301 + 312, 302 + 352, 304 + 312, 304 + 340, 305 + 338 + 351, P312, 321, 322, 330, 332 + 313, 337 + 313, 362, 363, 403 + 233, 405, 501**	**07**
$CaCl_2$ x 2 H_2O	**319**	**305 + 351 + 338**	**07**
Cilostamide			
D-(+)-Glucose			
D-(+)-Saccharose			
Developer concentrate	**315, 317, 318, 341, 351, 400**	**273, 280, 305 + 351 + 338, 310, 333 + 313, 501**	**05, 07, 08, 09**
Dimethyl sulfoxide (DMSO)			
DMEM			
EDTA	**332, 373**	**260, 271, 304 + 340, 312, 314, 501**	**07, 08**
Ethanol, Ritipuran >99.8% p.a.	**255, 319**	**210, 233, 305 + 351 + 338**	**02, 07**
Ethanol, 70%	**255, 319**	**210, 233, 305 + 351 + 338**	**02, 07**
Fetal Calf Serum (FCS)			
Fixer concentrate	**290, 315, 318**	**280, 305 + 351 + 338, 310, 390, 501**	**05**
Forskolin	**312**	**280**	**07**
Glycerol			

Glycine			
HCl, 37%	**290, 314, 335**	**280, 303 + 361 + 353, 304 + 340, 305 + 351 + 338, 310**	**05, 07**
HEPES			
Insulin-Transferrin Selenium (ITS) X, 100 x			
3-isobutyl-1-methylxanthine (IBMX)	**302**	**313, 301 + 330 + 331**	**07**
Isoflurane (Forene)	**336**	**261, 271, 303 + 340, 312, 403 + 233, 405, 501**	**07, 08**
KCl			
$KHCO_3$			
KH_2PO_4	**315, 319**	**264, 280, 305 + 351 + 338, 321, 332 + 313, 337 + 313**	**07**
Laminin			
L-glutamine			
Liberase DH	**315, 319, 334**	**261, 264, 280, 285, P302 + 352, 304 + 341, 305 + 351 + 338, 332 + 313, 342 + 311, 362, 501**	**08**
MEM without L-glutamine			
Methanol	**225, 301, 311, 331, 370**	**210.3, 270, 280.7, 303 + 361 + 353, 304 + 340, 308 + 311**	**02, 06, 08**
$MgCl_2$ x 6 H_2O			
$MgSO_4$ x 7 H_2O			
Milk powder			
Na_2HPO_4 x 2 H_2O			
NaCl			
$NaHCO_3$			
NaN_3	**300 + 310 + 330, 373, 410**	**262, 273, 280, 301 + 310 + 330, 302 + 352 + 310, 304 + 340 + 310**	**06, 08, 09**
NaOH	**290, 314**	**233, 280, 303 + 361 + 353, 305 + 351 + 338, 310**	**05**
Phosphate-buffered saline (PBS)			
Penicillin/Streptomycin	**302, 317, 361**	**280, 320 + 352, 308 + 313**	**07, 08**
Phosphatase inhibitor cocktail		**280**	
Pierce BCA Protein assay kit			

Ponceau S solution			
Protease inhibitor cocktail	**319**	**305 + 338**	**07**
Protein marker V peqGold			
Sodium dodecyl sulfate (SDS)	**315, 318, 335**	**261, 280, 302 +P352, 304 + 340 + 312, 305 + 351 + 338 + 310**	**05, 07**
SDS-Solution, 20%	**315, H318**	**305 + 351 + 338**	**05**
Taurine			
Tetramethylethylene diamine (TEMED)	**225, 302 + 332, 314**	**210, 280, 301 + 330 + 331, 303 + 361 + 353, 304 + 340 +3112, 305 + 351 + 338**	**02, 05, 07**
Tris-(hydroxymethyl)-aminomethan (TRIS)			
Triton X-100, 10% solution	**318**	**280, 305 + 351 + 338, 313**	**05**
Tween 20			
Trypsin, 2.5%	**334**	**261, 284, 304 + 340, 342 + 311, 501**	**08**

Table 4. Chemicals categorized according to Globally Harmonized System (GHS) for Hazard Communication.

Figure 24. Hazard Pictograms according to Globally Harmonized System (GHS) for Hazard Communication. Hazard symbols adapted from https://www.conceptdraw.com/How-To-Guide/hazard-pictograms.

Acknowledgements

First and foremost, I would like to express my sincere gratitude to my research supervisor, Professor Viacheslav Nikolaev, for offering me the opportunity to work on novel and unconventional projects as a member of his research group. His genuine interest and dedicated involvement in every step of this PhD made my research work an enjoyable and highly rewarding experience over the past four years.

I am also grateful to my co-supervisor Professor Elke Oetjen for her constructive comments and thoughtful suggestions during the TSM meetings, and Professor Friederike Cuello, Professor Christian Lohr and Professor Chris Meier for their participation in and assistance as members of my thesis committee.

I would also wish to thank one and all from Nikolaev's group, who directly or indirectly, have lent their hand in this venture. My sincere thanks for his active engagement, valuable guidance and unceasing support to Dr. Alexander Froese, who shared with me innovative research projects and also contributed to my professional milestones. My deep appreciation to Dr. Hariharan Subramanian for his plentiful experience in biochemical techniques and genuinely kind help during my PhD. I am also thankful to Dr. Kirstie de Jong for sharing her expertise and performing the echocardiographic analysis for this work.

Special thanks for excellent technical assistance to Ms. Birgit Geertz for transthoracic echocardiography, Ms. Kristin Hartmann for heart histology, and Ms. Sophie Sprenger, Ms. Annabell Kühl, and Ms.Viktoria Hänel for mouse genotyping.

Thank you to old and new friends who kept spirits up and offered creative alternatives when needed.

Most importantly, I wish to thank my family for their unwavering love, support and belief in me.

Affidavit

“Hiermit versichere ich an Eides statt, die vorliegende Dissertation selbst verfasst und keine anderen als die angegebenen Hilfsmittel benutzt zu haben. Die eingerichte schriftliche Fassung enspricht der auf dem elekronischen Seichermedium. Ich versichere, dass diese Dissertation nicht in einem früheren Promotionsverfahren eingereicht wurde.“

Nikoleta Pavlaki

Hamburg, April 2021